2012-05-09

Regulation of Early Pattern Formation in the Sea Urchin Embryo by the Wnt Pathway Components Dishevelled and Axin

Chieh-Fu Peng
University of Miami, chiehfu@bio.miami.edu

UNIVERSITY OF MIAMI

REGULATION OF EARLY PATTERN FORMATION IN THE SEA URCHIN EMBRYO BY THE WNT PATHWAY COMPONENTS DISHEVELLED AND AXIN

By

Chieh-Fu Peng

A DISSERTATION

Submitted to the Faculty
of the University of Miami
in partial fulfillment of the requirements for
the degree of Doctor of Philosophy

Coral Gables, Florida

May 2012

UNIVERSITY OF MIAMI

A dissertation submitted in partial fulfillment of
the requirements for the degree of
Doctor of Philosophy

REGULATION OF EARLY PATTERN FORMATION IN THE SEA URCHIN EMBRYO BY THE WNT PATHWAY COMPONENTS DISHEVELLED AND AXIN

Chieh-Fu Peng

Approved:

_____ Athula H. Wikramanayake, Ph.D. Professor of Biology	_____ Terri A. Scandura, Ph.D. Dean of the Graduate School
_____ Zhongmin Lu, Ph.D. Associate Professor of Biology	_____ Julia Dallman, Ph.D. Assistant Professor of Biology
_____ Akira Chiba, Ph.D. Professor of Biology	_____ Mary Lou King, Ph.D. Professor of Cell Biology, Biochemistry & Molecular Biology, and Molecular & Cellular Pharmacology

PENG, CHIEH-FU (Ph.D., Biology)

Regulation of Early Pattern Formation in the Sea Urchin Embryo by the Wnt Pathway Components Dishevelled and Axin (May 2012)

Abstract of a dissertation at the University of Miami.

Dissertation supervised by Professor Athula H. Wikramanayake
No. of pages in the text. (116)

Data from diverse species within the deuterostomes (mouse, frog, fish, amphioxus, hemichordate, ascidians, sea urchin, sea star) and protostomes (annelids, planarians, nemerteans, mollusks) suggest that Wnt/β-catenin signaling determines posterior identity and thus patterns anterior-posterior body plan formation in most bilaterians. Moreover, nuclear β-catenin marks the gastrulation site in many metazoans including the cnidarians. The activation of Wnt/β-catenin signaling at one pole of these embryos is highly influenced by the animal-vegetal (AV) axis of the oocyte. This primary egg axis is specified during oogenesis, however, the maternal mechanisms that establish AV egg polarity and subsequently mediate asymmetric activation of Wnt/β-catenin signaling are largely unknown. For my dissertation research I used the morphologically simple sea urchin embryo to elucidate the roles of critical evolutionarily conserved components that are pre-localized in the unfertilized egg, and are used to establish the primary body axis during early embryonic development. I studied two scaffolding proteins, Dishevelled (Dsh) and axis inhibition protein (Axin), which serve as key regulators of the Wnt/β-catenin pathway. Dsh and Axin each play crucial roles in patterning the early embryo along the AV axis by regulating endomesoderm specification. Work done on Dsh revealed a novel vegetal cortical domain (VCD) that

is specified during oogenesis, maintained after fertilization, and inherited and partitioned by the most vegetal blastomeres to locally activate endomesoderm specification in the sea urchin embryo. Since the AV axis is found in nearly all metazoan eggs, this finding suggests that the VCD might be an evolutionarily conserved mechanism for the establishment of the AV axis in metazoan ova. Work done on Axin suggests that it plays an evolutionarily conserved role in the negative regulation of the Wnt/β-catenin pathway in sea urchin embryos, similar to the function that Axin plays in the vertebrates. Moreover, while Axin plays a crucial role in patterning the dorsal-ventral axis in vertebrates by maintaining ventral cell fates, my results suggest that Axin is required to prevent the Veg_1 tier ectodermal progeny from becoming endoderm. This result suggests a novel mechanism for Axin in axis patterning in the sea urchin embryo. Furthermore, the data in sea urchins also raises the possibility that the ancestral role of Axin was to pattern the AV axis in basal deuterostomes before being co-opted to pattern the dorsal-ventral axis in vertebrates. In sum, the early patterning of the sea urchin embryos along the AV axis relies on locally concentrated Dsh at the VCD to specify endomesoderm at the vegetal pole, and on Axin to suppress endodermal cell fate in the more animal daughters of Veg_1 tier progeny.

ACKNOWLEDGMENT

First of all, I would like to thank my advisor, Dr. Athula H. Wikramanayake, who gave me this opportunity to perform research in the wonderful field of developmental biology. He also guided and challenged me with patience throughout my academic program, never accepting less then my best efforts. I am forever grateful. I would also like to acknowledge and extend my heartfelt gratitude to my thesis committee, Dr. Mary Lou King, Dr. Julia Dallman, Dr. Zhongmin Lu, and Dr. Akira Chiba for their support, insightful feedbacks on my research and enthusiasm throughout my graduate student career.

A special thanks to my lab colleagues, especially Joana Kobayashi and Ronghui Xu, who started this project and provided the reagents required for my entire research. Without you, the research presented here could not have been done. I would also like to extend my thanks to the past and present members in the lab, Nisha Shalika Kumburegama, Christine Byrum, Lingyu Wang, Shioh Ooka, Naveen Wijesena, Albert Hayward, Erica Flores, and Wei Wu for your support, help and company in the lab. I would also like to take this opportunity to thank the Biology graduate students, especially Robert, Thaddeus, Ron, Gavin and Qing. Life as a graduate student wouldn't be the same without you. Special thanks to Paula, Yoshi, Angelia, Jennifer, Fetchi, Sharon and Megan who treated me as family during the eight years of life abroad.

Finally, I would like to thank my parents and particularly my wife, Lisa, who quit her job as a wonderful social worker back home just to accompany me studying abroad. Words alone cannot express what I owe them for their encouragement, understanding, and whose patient love enabled me to complete my doctoral degree.

TABLE OF CONTENTS

LIST OF FIGURES

Chapter I: General Introduction

How an animal's body plan emerges from a zygote is one of the most fundamental questions in biology. To address this question, it is important to understand what information an embryo relies on to specify embryonic axes and cell fates during early embryogenesis. In most metazoans, early embryonic development is strongly influenced by maternally-derived information that is asymmetrically distributed along a primary axis established in the oocyte during oogenesis. This observation was first made in sea urchin eggs and embryos over a hundred years ago by Theodor Boveri (Boveri, 1901a; 1901b). Using the Mediterranean sea urchin *Paracentrotus lividus*, Boveri demonstrated that there was predictable development of the embryo along a polarity already present in the unfertilized egg (Boveri, 1901a; Boveri, 1901b; Horstadius, 1939). This primary egg axis is now referred to as the animal-vegetal (AV) axis, and numerous studies have shown that the differential developmental potential along the AV axis is determined by the asymmetric localization of developmental information in the form of RNAs, proteins, membrane domains, and organelles (Kloc et al., 2001; King et al., 2005; Tao et al., 2005; Heasman, 2006; Lee et al., 2007; Momose et al., 2008). This information is differentially inherited and used by early blastomeres to activate lineage-specific gene expression that leads to cell fate specification and pattern formation in the embryo.

During development, a critical consequence of early embryonic patterning is the establishment of the site for gastrulation. In most embryos, gastrulation is the first major morphogenetic event, and it leads to the segregation of the germ layers and subsequently the induction of major organs as a result of cell interactions between the primary germ layers. Moreover, it is believed that it was the evolution of gastrulation during animal

evolution that allowed the bilaterians to attain the diversity of body plans and forms we see today (Martindale and Hejnol, 2009). However, the molecular mechanisms that activate gastrulation at one pole of an embryo are still far from clear. One strategy to gain insight into this problem is to identify the maternal determinants that are crucial for this event, and then determine how these key regulatory molecules play a role in the event of germ layer specification.

The primary egg axis: animal-vegetal (AV) axis

Since the pioneering work of Boveri, it has been well established that the eggs of most metazoans have an AV axis, and moreover, it has been shown that early pattern formation is organized along this primary egg axis (Boveri, 1901a; Boveri, 1901b; Lillie, 1909a; Lillie, 1909b; Angerer and Angerer, 2000; Martindale and Hejnol, 2009). The animal pole is defined by the site of polar body extrusion at meiosis, and thus can be used as a reference point for comparing the axial relationships of metazoan embryos. In general, the animal pole-derived blastomeres give rise to the ectoderm and subsequently to epidermis, nervous system and the anterior end of the organism, while the vegetal pole-derived blastomeres give rise to the endomesoderm and to the posterior end of the organism (Martindale and Hejnol, 2009; Petersen and Reddien, 2009). Thus, the anterior-posterior axis is highly influenced by the determinants of AV axis polarity of the unfertilized egg. Furthermore, in some metazoans, especially echinoids and lancelets, the apical-basal polarity of the germinal epithelium harboring the developing oocytes corresponds to AV axis of the egg in these species (Smiley, 1990; Frick and Ruppert, 1996; Frick and Ruppert, 1997). Thus, the orientation of the cell within the gonadal

epithelium gives the oocyte its apical-basal polarity, and this later becomes the anterior-posterior axis of the organism, which indicates that this primary polarity is maternally established. However, the maternal molecular mechanisms that establish and regulate this polarity in most metazoans are largely unknown. I use a well studied and morphologically simple sea urchin embryo to elucidate the role of critical evolutionarily conserved components that are pre-localized in the unfertilized egg in establishing the primary body axis during early embryonic development.

Sea urchin as a model organism

The sea urchin embryo is an excellent system to study the fundamental mechanisms of development. First, the gametes can be artificially fertilized and the development of embryos is synchronous and rapid. These conditions are advantageous for molecular studies. Secondly, the gametes are available almost all year round and a single female can give nearly a million eggs. Third, extensive fate mapping studies have identified the developmental origins of all the major cell types in the embryo up to the larval stages. Fourth, the developmental functions of genes can be assessed by experimental perturbations of gene expression. Moreover, the eggs are between 72 to 100 μm in size depending on the species, and mostly transparent, which is ideal for phenotype analysis using light microscopy and for examining consequences of molecular perturbations using immunofluorescence methods. Furthermore, the genome of the purple sea urchin *Strongylocentrotus purpuratus* has been sequenced (Sodergren et al., 2006), which facilitates high throughput screens for genes of interest. Lastly, because of the fast advancement of molecular and genomic information, the sea urchin served as the model

system where the concept of gene regulatory networks (GRN) was developed (Davidson et al., 2002). With the addition that the sea urchin has been used for over a century for experimental embryology studies, the sea urchin embryo is one of the best systems to study the molecular mechanism underlying the establishment of the AV axis.

During early sea urchin development embryonic patterning occurs in a fixed pattern along the AV axis. Classical studies have established that a maternally regulated, reproducible pattern of cell division partitions the egg cytoplasm among blastomeres that have defined sizes and orientations relative to each other (Angerer and Angerer, 2000)(Figure 1.1). In early stage embryos, the geometric precision of cleavage restricts the range of cell-cell interactions in a normal embryo, which results in the fates of blastomeres at different positions along the AV axis being invariant from embryo to embryo. AV polarity is morphologically evident at the 16-cell stage: From animal (top) to vegetal (bottom) are arrayed tiers of eight mesomeres, four macromeres, and four micromeres. When looking at the fate map of the 16- and 60-cell stages in relation to the corresponding derivatives in a gastrula embryo, the subsequent pattern formation is along the AV axis (Figure 1.2).

The sea urchin embryo is one model system where embryonic polarity has been studied for over a hundred years. In 1901, Theodor Boveri, used the pigmented band surrounding the vegetal pole in the eggs of sea urchin species *Paracentrotus lividus* as an endogenous marker, to demonstrate the relationship between the polarity of the egg and the emergence of the primary germ layers (Figure 1.3) (Boveri, 1901a; Boveri, 1901b). Twenty years later, Sven Horstadius (1920) demonstrated the unequal developmental potential in the sea urchin egg by carrying out a simple experiment. When he bisected

unfertilized eggs meridionally into two equal halves and fertilized each half, both halves developed into smaller but relatively normal pluteus larvae. However, when he bisected unfertilized eggs equatorially into two equal halves and fertilized each half, he noted that the animal half gave rise to a hollow ball of epithelial cells, the *dauerblastula*, while the vegetal half gave rise to a relatively normal pluteus larva with derivatives of endomesoderm and ectoderm (Horstadius, 1939; Horstadius, 1973; Maruyama et al., 1986). This simple experiment demonstrated the unequal developmental potential of an unfertilized sea urchin egg and indicated the presence of determinants for endomesoderm at the vegetal pole.

The molecular mechanisms regulating early patterning of the sea urchin embryo

Although it has been known for over a century that sea urchin eggs have unequal developmental potential along the AV axis, very little was known about the molecular mechanisms that specified this polarity until recently. Recent studies have shown that the most critical molecule that is differentially activated at the vegetal pole of the early embryo is β-catenin, a maternally regulated transcriptional regulatory protein that is key to signaling via the canonical or Wnt/β-catenin signaling pathway (Wikramanayake et al., 1998; Logan et al., 1999). β-catenin enters the nuclei of the micromeres at 16-cell stage and it progressively extends towards the animal pole during cleavage, and transcriptional activation by this protein is essential for endomesoderm specification and pattern formation along the AV axis (Wikramanayake et al., 1998; Logan et al., 1999). Nuclear β-catenin gives the micromeres inductive capacity and thus establishes an embryonic organizing center (Logan et al. 1999). Nuclear β-catenin is also required for the

overlaying macromere progeny to become competent to receive micromere signals (McClay et al., 2000). Then, this critical molecular asymmetry establishes distinct vegetal and non-vegetal domains of transcriptional activity. Thus, the entry of β-catenin into the nuclei at the vegetal pole blastomeres initiates endomesoderm specification and germ layer segregation. Moreover, work done by Logan *et al.* (1999) also showed that β-catenin still localizes to nuclei of blastomeres from embryos dissociated very early in development, suggesting that β-catenin nuclearization is cell-autonomous and can take place in the absence of cell-cell interactions.

The Wnt/β-catenin pathway

Nuclear β-catenin is found to activate endomesoderm genes that specify vegetal cell fates in sea urchins, and nuclear β-catenin is also a feature that is found to mark the site of gastrulation in embryos across several phyla (Croce and McClay, 2006). These include chick, zebrafish, frog, acorn worm, sea squirt, starfish, sea urchin, ribbon worm, and sea anemone (Schneider et al., 1996; Larabell et al., 1997; Logan et al., 1999; Roeser et al., 1999; Imai et al., 2000; Miyawaki et al., 2003; Wikramanayake et al., 2003; Henry et al., 2008; Darras et al., 2011).

β-catenin nuclearization is the main outcome of the Wnt/β-catenin pathway activation, an event regulated by a destruction complex, and this pathway is very well characterized in cells, especially during development. The destruction complex is composed of three major proteins, adenomatous polyposis coli protein (APC), glycogen synthase kinase-3β (GSK-3β), and the axis inhibition protein (Axin). In the absence of Wnt ligands, β-catenin is continuously targeted for degradation by the destruction complex (Figure 1.5a).

In the presence of Wnt ligands, the destruction complex is disassembled, causing β-catenin accumulation in the cytoplasm and this protein eventually translocates into the nucleus and acts as a transcriptional co-activator (Figure 1.5b). The disassembly of the destruction complex is achieved by activation of Dishevelled (Dsh) protein by phosphorylation, which is caused by the Wnt ligand binding to the receptors, LRP and frizzled (Fz) (reviewed in (Gao and Chen, 2009)). Although we know much about the regulation of the Wnt/β-catenin pathway, how this pathway is asymmetrically activated in early embryos is not well understood.

In the sea urchin embryo, a major unanswered question in understanding the localized activation of the endomesodermal gene regulatory network (EGRN) at the vegetal pole is: What is the cell-autonomous maternal mechanism that regulates entry of β-catenin into nuclei of blastomeres at the vegetal pole? One way to look at this question is to look at the stability of the β-catenin molecule. β-catenin is differentially regulated along the AV axis. The turnover rate of β-catenin is very rapid in animal blastomeres but the protein is much more stable in vegetal blastomeres (Weitzel et al., 2004). This observation then raises two questions. First we need to understand what stabilizes β-catenin in the vegetal blastomeres, and second, we need to understand what negatively regulates β-catenin nuclearization in the animal blastomeres. In sea urchins, four of the eleven Wnts (Wnt-6, Wnt-7, Wnt-16, and Wnt-A) found in the sea urchin that are present maternally, and although maternal Wnt 6 has been shown to be required for activation of the Wnt pathway in the macromeres, none of these Wnts display localized expression in the egg or early embryo (Croce et al., 2006; Croce et al., 2011). In addition, none of the five maternally expressed receptors is localized. Those include four frizzled (Fz) and one Lrp;

SpFz, SpFz 4, SpFz 5/8, SpFz 9/10, and SpLrp 6 (Croce et al., 2006; Stamateris et al., 2009; Croce et al., 2011; Lhomond et al., 2012). In sum, none of these factors can account for the localized activation of β-catenin at the vegetal pole. Hence, understanding the maternal mechanisms that activate nuclear β-catenin at the vegetal pole, and the maternal mechanisms that antagonize β-catenin nuclearization at the animal pole will provide critical insight into how the AV axis is specified and patterned in sea urchins.

My dissertation research has focused on how the AV axis is specified and patterned using the sea urchin embryo as the model system. Work done in our lab suggested that Dsh, one of the most upstream cytoplasmic proteins in the Wnt pathway, is required for endomesoderm specification at the vegetal pole (Weitzel et al., 2004). When Dsh function in the Wnt/β-catenin pathway is blocked by overexpressing a dominant negative Dsh construct, endomesoderm specification does not occur and gastrulation is blocked. My research is the first to show that endogenous Dsh protein concentrates at the vegetal cortex in the unfertilized egg and through early embryogenesis. This localization pattern correlates perfectly with the nuclearized β-catenin at the vegetal half-derived cells of the embryo. Moreover, I showed that Dsh protein accumulates at the vegetal cortex in the early stage oocytes. My work on the Dsh protein revealed a novel cyto-architectural domain at the vegetal cortex which serves as a platform for the activation of endomesoderm specification. Additionally, work done by our collaborators showed that, when the vegetal egg cortex is stripped from the egg, endomesoderm specification is lost in the embryo. When the vegetal cortex is transplanted onto the animal pole of a host egg, it induces ectopic endoderm formation, suggesting crucial maternal factors that activate endoderm are localized at the vegetal cortex (Croce et al., 2011). In addition, in work

that was done in collaboration with David McClay at Duke University, we used immunostaining to show that the transplanted piece of the vegetal cortex contains Dsh protein, and this result was published last year in Development (Croce et al., 2011). Lastly, I performed Western blot analysis after two dimensional gel electrophoresis, where the proteins are first separated by charge then by size, to demonstrate that the concentrated Dsh at the vegetal cortex and the micromeres, where the Wnt pathway is locally activated, is comprised of Dsh isoforms distinct from the Dsh isoforms in the bulk cytoplasm. This result demonstrated that *endogenous* Dsh is differentially post-translationally modified in different cellular compartments, and provides insight into the regulation of the Wnt pathway during endomesoderm specification in the sea urchin embryo.

In chapters one and two of my dissertation research, I provide the evidence that selective activation of Dsh in a vegetal cortical domain is required for nuclearizing β-catenin in vegetal pole blastomeres. In chapter three I have focused my attention on how the canonical Wnt pathway is negatively regulated in animal pole blastomeres during early embryogenesis. Previous work has shown that β-catenin nuclearization is suppressed in animal pole blastomeres, but how β-catenin nuclearization is suppressed in the animal pole during early sea urchin development remains unclear. In vertebrate systems, loss of Axin gives a striking phenotype of axis duplication, suggesting that Axin plays a negative regulatory role in axis formation (Jacobs-Cohen et al., 1984; Zeng et al., 1997; Hedgepeth et al., 1999a; Heisenberg et al., 2001; Luo and Lin, 2004). In the last chapter, my studies demonstrate that Axin plays a key regulative role in patterning the AV axis in the early sea urchin embryo. Combining reverse genetics, molecular and cell

biological approaches I show that Axin is both required and sufficient for the regulation of endomesoderm specification. Knockdown of Axin by a translation blocking morpholino antisense oligonucleotides expands endoderm specification, which gives rise to a "vegetalized" phenotype. Conversely, overexpression of Axin blocks endomesoderm formation that gives a classic "animalized" phenotype, which is only comprised of ectodermal cells. Moreover, I found Axin mRNA and a specific form of the protein are both removed from the most vegetal cells where the Wnt pathway is initially activated. These results provided new evidence to show that Axin, a scaffold protein, is a crucial regulatory component that antagonizes canonical Wnt signaling in animal pole blastomeres, hence playing a key role in AV axis patterning in the early embryo.

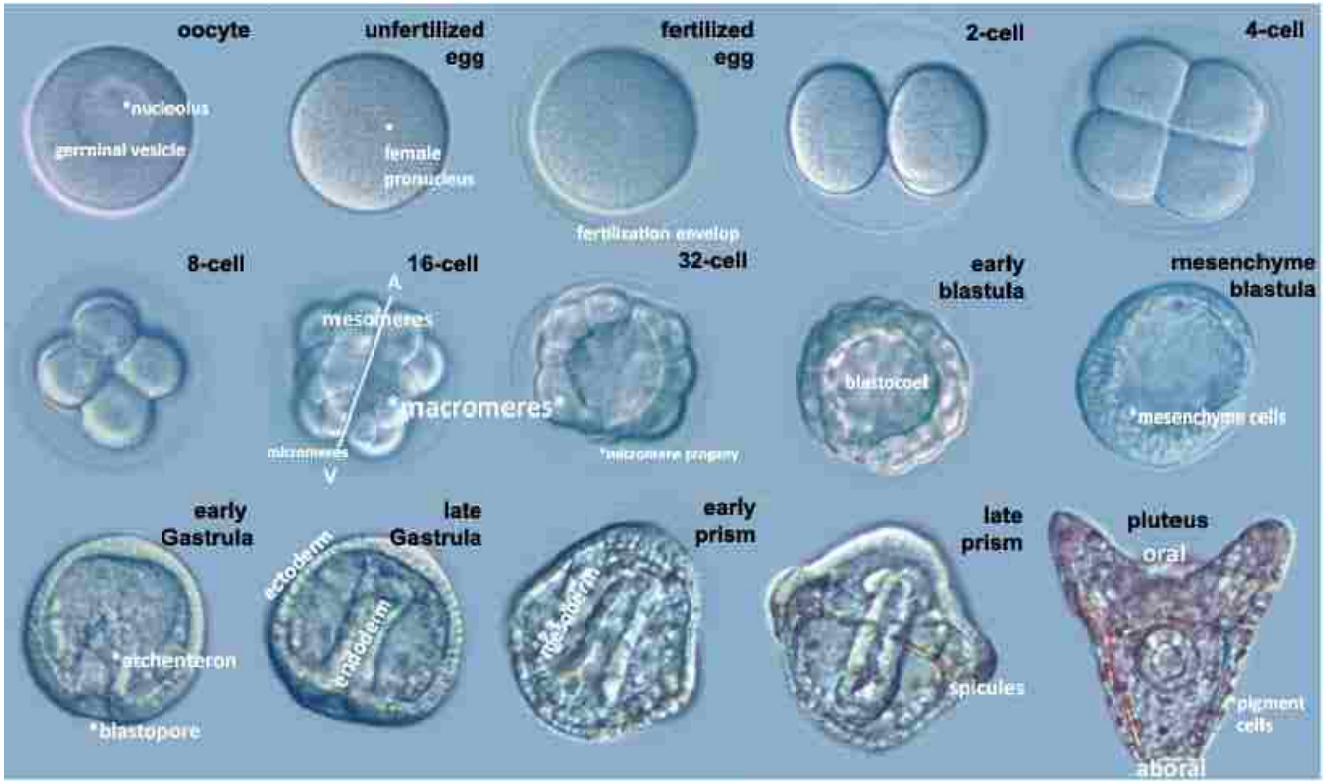

Figure 1.1 Sea urchin embryogenesis. *Lytechinus variegatus*. During early sea urchin development, embryonic patterning occurs in a fixed pattern along the AV axis. Classical studies have established that a maternally regulated, reproducible pattern of cell division partitions the egg cytoplasm among blastomeres that have defined sizes and orientations relative to each other. AV polarity is morphologically evident at the 16-cell stage: From animal (top) to vegetal (bottom) are arrayed tiers of eight mesomeres, four macromeres, and four micromeres. Adapted from www.interscience.wiley.com/developmentaldynamics.

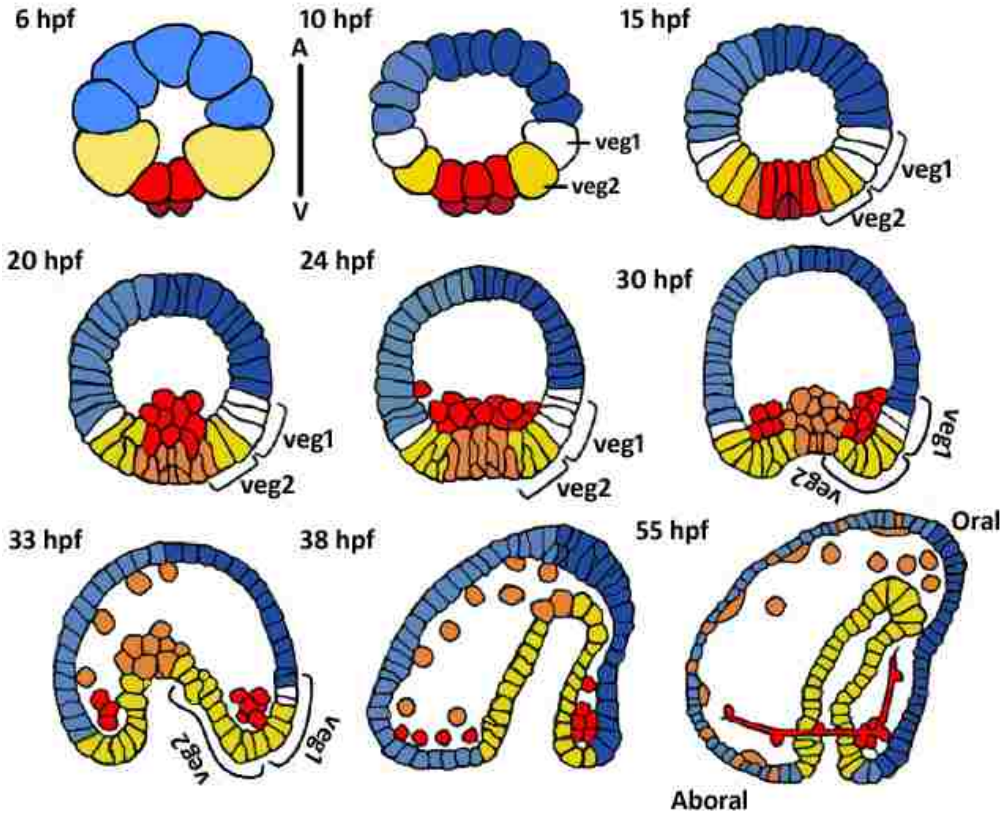

Figure 1.2 Fate map of the *S. purpuratus* sea urchin embryo. Patterning of the sea urchin embryo occurs along the animal-vegetal pole. Lineages of major regions of the sea urchin embryo (*S. purpuratus*) are illustrated in different colors: Skeletogenic mesenchyme lineage (Red), endoderm (Yellow), secondary mesenchyme (Orange), oral ectoderm (dark blue), aboral ectoderm (light blue), unspecified cells (white). **6 and 10 hr,** cleavage stages. **15 hr,** blastula stage. From veg_1 derives ectoderm (mainly) and hindgut endoderm; and from veg_2 nonskeletogenic (secondary) mesenchyme (mesodermal cell types) plus gut endoderm. **20 and 24 hr,** mesenchyme blastula; **30 - 38 hr,** gastrula stages; **55 hr,** prism stage. Figure adapted from (Howard-Ashby et al., 2006).

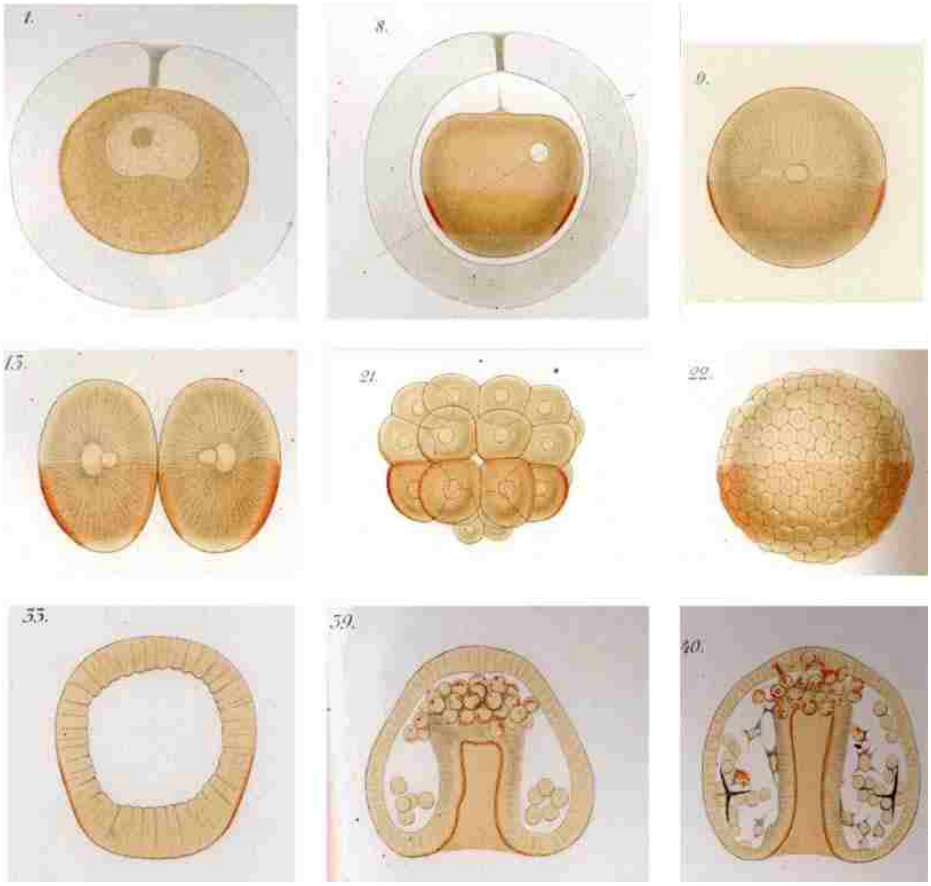

Figure 1.3 The relationship between the pigmented band and germ layer segregation during embryogenesis of *Paracentrotus lividus*. The pigmented band marks the vegetal pole and can be traced to endomesoderm. *1*. Oocyte, jelly canal indicates the animal pole in sea urchins oocyte. *8*. Unfertilized egg. *9*. Zygote. *13*. 2-cell stage. *21*. 32-cell stage. *22*. 120-cell stage. *33*. Hatching blastula. *39 and 40*, Gastrula. Pigment granules can be traced to the gut and mesenchyme cells. All images are orientated with the animal pole on top and vegetal pole towards the bottom. Theodor Boveri's original drawing (Boveri, 1901a).

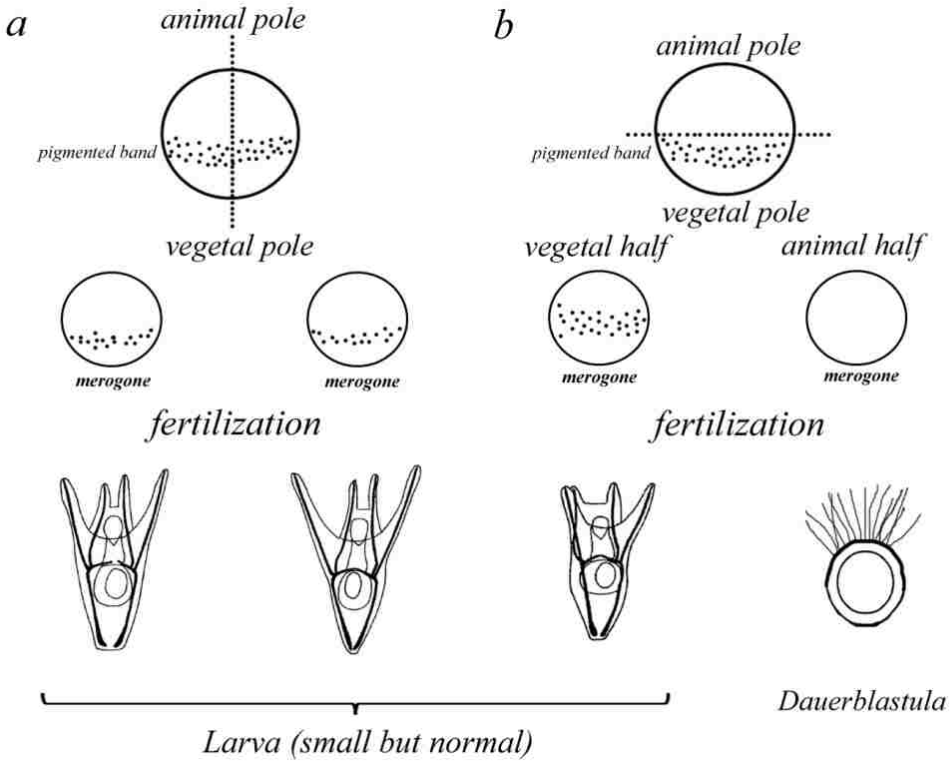

Figure 1.4 Experimental evidence for localized maternal determinants at the vegetal pole. Sven Horstadius demonstrated the unequal developmental potential in the sea urchin egg (*Paracentrotus lividus*) by carrying out a simple experiment. **a,** When he bisected unfertilized eggs meridionally through the AV axis into two equal halves and fertilized each half, both halves developed into smaller but relatively normal pluteus larvae. **b,** However, when he bisected unfertilized eggs equatorially through the equator into two equal halves and fertilized each half, he noted that the animal half gave rise to a hollow ball of epithelial cells, the *dauerblastula*, while the vegetal half gave rise to a relatively normal pluteus larva with derivatives of endomesoderm and ectoderm. Figure adapted from Horstadius, 1920.

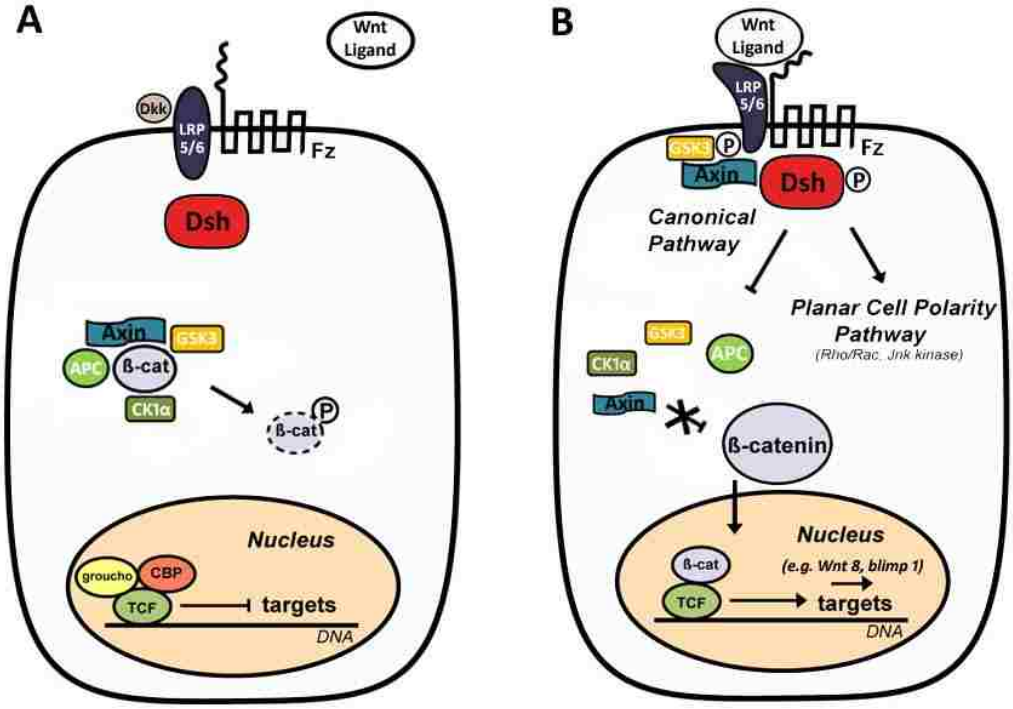

Figure 1.5 The Wnt/β-catenin pathway. A simplified version of the β-catenin dependent Wnt pathway. **a,** The destruction complex is composed of three major proteins, adenomatous polyposis coli protein (APC), glycogen synthase kinase-3β (GSK3), and the axis inhibition protein (Axin). In the absence of Wnt ligands, β-catenin is continuously targeted for degradation by the destruction complex. **b,** In the presence of Wnt ligands, the destruction complex is disassembled, causing β-catenin accumulation in the cytoplasm and this protein eventually translocates into the nucleus and acts as a transcriptional co-activator. The disassembling of the destruction complex is achieved by activation of Dishevelled (Dsh) protein by phosphorylation, which is caused by the Wnt ligand binding to the receptors, LRP and frizzled (Fz). Figure adapted from Christine Byrum.

Chapter II: Specification of the Animal-Vegetal Axis in the Sea Urchin Egg by the Dishevelled Protein

BACKGROUND

The Dishevelled (Dsh) protein

The *dishevelled* (dsh; dvl in vertebrates) gene was first identified in *Drosophila* mutants characterized by disruptions of hair and bristle polarity (Fahmy and Fahmy, 1959). However, it was not until the 1980's that Dsh gained attention for playing a key role in segment polarity in the early *Drosophila* embryo (Perrimon and Mahowald, 1987). Dsh was then placed in the Wnt/β-catenin signaling pathway. It is now known that Dsh protein is activated by interaction of specific Wnt ligands with cell surface receptors that leads to activation of distinct Wnt pathways (Komiya and Habas, 2008). Currently, three major Wnt pathways have been described. These are the Wnt/β-catenin pathway, the planar cell polarity pathway (PCP) and the Wnt/calcium-dependent pathway (reviewed in (Wallingford and Habas, 2005). Dsh contains multiple protein-protein interaction domains (Figure 2.1) including the DIX (named after Dishevelled and axin), DEP (named after Dishevelled, Egl-10 and plekstrin) and PDZ (named after post synaptic density protein (PSD95), Drosophila disc large tumor suppressor (Dlg1), and zonula occludens-1 protein (zo-1))domains (reviewed in (Wallingford and Habas, 2005). Although the protein contains no apparent enzymatic function, previous work has shown that Dsh protein is hyperphosphorylated upon activation of the Wnt signaling pathways (Yanagawa et al., 1995; Semenov and Snyder, 1997; Rothbacher et al., 2000). In addition, it is worth noting two specific regions surrounding the PDZ domain. Preceding the amino terminal of the PDZ domain is a cluster of positive charged (basic) residues. A

proline-rich region is found right after the PDZ domain. With three domains and two specific sites, Dsh protein serves as a hub of Wnt signaling by the dynamic interaction of specific binding partners at the right place and the right time (Gao and Chen, 2009).

Several lines of evidence indicate that localized "activation" of the Dsh protein is required for activation of the endomesodermal gene regulatory network (EGRN) during early sea urchin embryogenesis. First, overexpression of Dsh::GFP leads to accumulation of the protein at the vegetal pole as early as the zygote stage, even though Dsh mRNA is uniformly expressed during early embryogenesis, this indicates that post-translational localization targets Dsh to the vegetal cortex (Weitzel et al., 2004; Leonard and Ettensohn, 2007). Next, overexpression of a dominant-negative that blocks Dsh signaling in the Wnt/β-catenin pathway blocks β-catenin nuclearization and EGRN activation (Weitzel et al., 2004). Finally, while overexpression of activated β-catenin in animal half blastomeres can induce endomesodermal cells in these ectoderm precursors, overexpression of wild-type Dsh in animal half blastomeres does not induce ectopic endomesoderm in these cells (Weitzel et al., 2004). In sum, these observations support the hypothesis that Dsh protein is selectively localized and activated at the vegetal pole where it mediates EGRN activation. A better understanding of how the endogenous Dsh protein is regulated in sea urchin eggs and embryos will likely provide insight into how the AV axis is specified, and how this polarity selectively activates β-catenin signaling in the endomesoderm. To gain insight into the spatiotemporal expression of endogenous Dsh I have used affinity purified anti-Dsh polyclonal antibodies to carry out a detailed analysis of Dsh localization and modification using immunofluorescence and protein analysis by Western blot. I hypothesize that endogenous Dsh protein is localized to and

activated at the vegetal pole to mediate endomesoderm specification in vegetal blastomeres.

MATERIALS AND METHODS

Animal handling and embryo manipulations

Adult sea urchins, *Strongylocentrotus purpuratus* and *Lytechinus pictus* were obtained from Marinus, Garden Grove, CA, and maintained in seawater aquaria at 12°C. Spawning was induced by intracoelomic injection of 0.5M KCl. Embryos were cultured at 15°C in filtered artificial sea water (ASW) in temperature-controlled incubators. Local Hawaiian sea urchins, *Echinometra mathaei*, *Tripneustes gratilla*, and *Colobocentrotus atratus* were collected from the low tide zone around Ala Moana Park, Honolulu, HI, and maintained in sea water aquaria at room temperature, spawned with the same method, and embryos from these species were cultured at 25°C. Fertilization envelopes were removed prior to analysis by passing the embryos through a cell strainer (BD Falcon) with the addition of 0.25 μM 3-amino-1, 2, 4-triazole (ATA) (Sigma) dissolved in ASW.

Preparation of anti-Dsh polyclonal antibodies

The *S. purpuratus* Dsh (SpDsh) protein has 723 amino acids in length, and the molecular size is estimated to be approximately 81 kDa. To investigate the spatiotemporal expression pattern of the Dsh protein, three affinity-purified anti-Dsh polyclonal rabbit antibodies were made against three distinct epitopes on the sea urchin Dsh protein. The selected epitopes were the C-terminus (NH_2-CMVPMMPRQLGSVPEDLSGS-COOH) and N-terminus (NH_2-CASVTTDTRGDSQLPPERTG-COOH) of Dsh protein, and the

entire amino-terminus domain of the Dsh protein up to the end of the DIX domain (pET30a/SpDIXG) (Figure 2.1). Antibodies were generated and affinity-purified using the immunizing antigens by Bethyl Labs (Montgomery, TX). To test the specificity of the antibodies, a preadsorption assay was performed by incubating the Dsh antibodies with the peptides (synthesized by Bethyl labs) or with the Dsh-DIX fusion protein at a 10x molar excess for one hour at room temperature prior to incubating with the samples either for immunostaining or Western blot analysis.

Western blot analysis

Egg and embryo samples were collected and centrifuged for one minute at 86x G. After removing as much seawater as possible, the embryos were lysed in 100 µl of solubilizing solution (40 mM Tris base, 2% SDS, 100 mM DTT) and protein concentrations were determined using the Bradford assay (Bio-Rad). Samples were then mixed with Laemmli sample buffer (Laemmli, 1970) and boiled for 5 minutes. A total of 30 µg of protein from each sample was run on a 10% SDS-PAGE and transferred onto Trans-Blot nitrocellulose membranes (Bio-Rad). Immunoblots were probed with rabbit anti-Dsh SpDsh DIX antibody (1:1000) and mouse anti-tubulin (1:10,000) (Developmental Studies Hybridoma Bank, E7). Blots were developed by chemiluminescence (Pierce) or detected by IRDye 680 (1:15,000) and IRDye 800 (1:15,000) secondary antibodies (LI-COR, Odyssey) respectively.

Immunostaining and image analysis

Embryos, eggs and oocytes were fixed with 4% PFA in PBS for 20 minutes, post fixed with 100% ice cold acetone for 10 minutes and processed for indirect immunofluorescence. Sperm were attached to poly-lysine-coated slides and fixed with 4% PFA in PBS for 10 minutes and washed three times with PBS (10 minutes each) before proceeding to staining. Samples were incubated with primary antibodies for an hour at room temperature using the following dilutions: rabbit anti-SpDsh DIX antibody (1:400), rabbit anti-LvDsh C antibody (1:400), rabbit anti-LvDsh N antibody (1:200), mouse anti-γ-tubulin antibody (1:50, Abcam, ab11321-100), monoclonal anti-acetylated-tubulin antibody (1:1,000, Sigma). Following this the samples were rinsed and incubated in secondary antibodies conjugated to the AlexaFluor series (Invitrogen, Molecular Probes) for 45 minutes at room temperature. DAPI (1:1,000, Invitrogen) and fluorescein phalloidin (3:100, Invitrogen) were added at the end of 45 minutes and incubated for another 15 minutes before wash. Stained eggs and embryos were observed using a Zeiss Axiovert 200 inverted microscope and a Leica SP5 confocal microscope. Captured images were analyzed with ImageJ (NIH) and Volocity (PerkinElmer Inc.) and the figures were prepared using Adobe Photoshop (Adobe Systems Inc.).

Staining the jelly canal with Japanese ink

Unfertilized eggs were collected "dry" to prevent the expansion of the jelly coat, and immersed directly into the Japanese ink for observation in a 60x15mm style tissue culture dish (Falcon). Images of stained jelly canals were captured using a Zeiss Discovery.V8 Stereo microscope.

RESULTS

Dishevelled (Dsh) is broadly expressed during early embryogenesis, but the protein is highly enriched at the vegetal cortex.

It is known that *Dsh* transcripts are expressed throughout the early embryos (Weitzel et al., 2004). To examine when and where Dsh protein is expressed, I performed Western blot analysis to look at the protein expression and localization during embryogenesis. Western blot analysis of developmental stages of sea urchin embryos and the unfertilized egg suggest that the Dsh protein is expressed throughout embryogenesis (Figure 2.2, see control in Supplementary figure 2.1a). Previous studies had shown that when Dsh::GFP is overexpressed by mRNA injection, the fusion protein accumulated at the vegetal cortex as early as the uncleaved zygote stage (Weitzel et al., 2004). However, using mRNA injections it was not possible to determine if the Dsh protein is localized in the unfertilized egg. Moreover, this approach could not definitively identify the endogenous pattern of expression of Dsh in the egg and early embryo. Hence, to determine if endogenous Dsh protein is also asymmetrically expressed along the AV axis, I carried out immunolocalization studies using three different affinity-purified anti-sea urchin Dsh polyclonal antibodies. Staining of unfertilized eggs revealed a striking enrichment of Dsh at the vegetal cortex (Figure 2.3, see control in Supplementary figure 2.1b). Immunolocalization of Dsh following fertilization and during the early cleavage stages showed that the enrichment at the vegetal cortex persisted until the late cleavage stage. By the 32- and 60-cell stages, the cortically enriched domain of Dsh correlated well with the domain of nuclear β-catenin in vegetal blastomeres (Logan et al., 1999). Moreover, Dsh localization is conserved in six other sea urchin species, including a west coast

species, *L. pictus*; an east coast species, *Lytechinus variegatus*; three Hawaiian sea urchin species, *E. mathaei*, *T. gratilla*, and *C. atratus* (Supplementary figure 2.3), and a European species, *P. lividus* (Croce et al., 2011). Scanning confocal microscopic analysis of Dsh in animal pole blastomeres indicated that the Dsh protein is expressed in dispersed puncta throughout the cytoplasm of these cells (Fig 2.3). To confirm that Dsh protein is present in animal pole blastomeres, Western blot analysis on isolated mesomeres and macromere/micromere pairs collected from 16-cell stage embryos was performed in the lab. This analysis showed that the Dsh protein is clearly present in animal pole blastomeres (Supplementary figure 2.2, work done by Joanna Kobayashi and Athula Wikramanayake). I conclude that the Dsh protein has broad distribution in the unfertilized egg and early embryos, but the protein accumulates at relatively high levels at the vegetal pole. This region has previously been described as the vegetal cortical domain (VCD) (Kumburegama and Wikramanayake, 2007).

The recent sequencing of the *S. purpuratus* genome showed that there are eleven *Wnt* ligands, four *Frizzled* receptors and one *LRP* 6 receptor in this species (Croce et al., 2006; Sodergren et al., 2006). Subsequent studies have shown that none of the maternally expressed ligands or receptors are enriched at the vegetal pole of the egg or early embryo (Stamateris et al., 2009; Croce et al., 2011; Lhomond et al., 2012). Hence, the maternal Dsh protein is the only known molecule in the Wnt/β-catenin pathway that is highly concentrated at the vegetal cortex of sea urchin eggs. These data and previous Dsh functional studies together, raise the possibility that the cortical Dsh might play a key role in localized activation of the EGRN.

The female pronucleus does not mark the animal pole in *S. purpuratus* and *L. pictus* eggs

The finding of the VCD raised a discrepancy from previous research. In metazoans, animal pole is defined by where the polar bodies are released during meiotic maturation. Full-grown oocytes complete meiosis with the large germinal vesicle moving asymmetrically to the cell periphery, and then during meiotic reduction two polar bodies are released to produce a haploid mature egg. In *P. lividus*, a European sea urchin species, it has been shown that the female pronucleus remains at the location where germinal vesicle breaks down, and thus is located at the animal pole of the egg (Di Carlo et al., 1996). This was further confirmed by cutting the unfertilized egg into two halves, one containing the pronucleus and the other one without, and both fertilized to assay the phenotype. While most of the nucleated halves developed into a classic "animalized" phenotype, the non-nucleated halves mostly developed normally, suggesting the female pronucleus can serve as an animal pole indicator (Di Carlo et al., 1996). However, in my Dsh staining in unfertilized eggs of two different sea urchin species, *S. purpuratus* and *L. pictus*, the female pronucleus is rarely located across from the VCD (Note: no centrifugation is involved in any step during immunostaining). To resolve this discrepancy, I used another animal pole marker to examine the location of the female pronucleus in *S. purpuratus* and *L. pictus* eggs. In sea urchins and sand dollars, the animal pole can be traced by the jelly canal, a structure that marks where the oocyte was attached to the germinal epithelium (Schroeder, 1980b; Schroeder, 1980a). Studies have shown that the release of polar bodies corresponds to the location of the jelly canal (Schroeder, 1980b). The jelly canal can be revealed by immersing unfertilized eggs in

India ink (Schroeder, 1980b). I immersed *S. purpuratus* and *L. pictus* eggs in Japanese ink (similar to India ink) and assayed for the location of the pronucleus. It is clear that in these two species, the pronucleus is positioned randomly relative to the jelly canal (Figure 2.4). Only 2% (1 out of 50 eggs counted) and 8% (4 out of 50 eggs counted) of the female pronuclei are located directly below the jelly canal in *S. purpuratus* and *L. pictus* respectively. This result suggests that after oocyte maturation in these species, the female pronucleus moves randomly in the egg and thus is not found located across the VCD in the immunostained eggs.

Dsh protein accumulation during oogenesis indicates that the AV polarity is initially established in early oocytes

In the sea urchin, it has been well established that the AV axis is specified during oogenesis. However, the lack of clear molecular markers for the AV axis has made it difficult to determine when this maternal anisotropy is initially established. The VCD clearly plays a key role in specification of the AV axis, and the Dsh protein appears to be a useful marker for identifying the appearance of this scaffold. To determine when the Dsh protein begins to accumulate in the vegetal cortex during oogenesis, I carried out immunolocalization of Dsh in oocytes at different developmental stages from excised ovaries. I noted that the smallest oocytes showed low levels of Dsh expression, and these oocytes did not have the microtubule organizing center (MTOC) that forms at the animal pole prior to meiosis and polar body formation (Egana et al., 2007)(Figure 2.5). I first noted that Dsh protein accumulates asymmetrically in the cortex of small oocytes, and this pole was identified as the vegetal pole by the presence of an MTOC at the opposite

pole of the cell (Figure 2.5c). MTOC staining by phalloidin was further confirmed by anti-γ-tubulin antibody (Boyle and Ernst, 1989) (Figure 2.6) . It is striking that cortical Dsh protein accumulation is strongly correlated with the appearance of the MTOC, suggesting that Dsh domain formation might be linked with MTOC formation in the oocyte. Furthermore, in mid-stage oocytes, Dsh is concentrated in punctate structures within the cytoplasm at the vegetal pole (Figure 2.5d). These puncta may indicate that Dsh is transported to the vegetal pole in a larger protein complex, or that the puncta represent polyribosomes translating *Dsh* mRNA, which might suggest that Dsh protein is synthesized at the vegetal pole. Further studies are needed to distinguish between these possibilities. It is also worth noting that Dsh staining is seen at the animal pole where Dsh co-localizes with the MTOC (Figure 2.5d). This observation adds to the many studies that have localized Wnt pathway components to the centrosomes and/or basal bodies in various cell types (Park et al., 2008; Mitchell et al., 2009; Hirota et al., 2010). However, the MTOC staining of Dsh is only seen when anti-DIX-antibody is used. We conclude that the VCD is formed very early during oogenesis, and accumulation of Dsh on this scaffold marks the vegetal pole for endomesoderm specification later in development.

Dsh protein and γ-tubulin co-localizes at the base of sea urchin sperm head

The observation that Dsh co-localizes with the MTOC in the sea urchin oocytes raised the possibility that Dsh is also expressed in the MTOC in sea urchin sperm. Moreover, it has been demonstrated that Dsh plays pivotal roles during mouse spermiogenesis by regulating actin cytoskeleton reorganization (Park et al., 2008). To test if Dsh is present

in the sperm MTOC, sperm were attached to a poly-lysine-coated slide and fixed for immunostaining by anti-Dsh antibodies. Similar to the oocytes, out of the three antibodies produced to detect Dsh, only the antibody against the DIX region showed a signal at the base of the sperm head (Figure 2.7a). Moreover, the signal partially overlaps with the anti-γ-tubulin antibody (Figure 2.7c-e). When examined closely by scanning confocal microscopy, both staining patterns are not at the location of the MTOC but at the location where the sperm mitochondria is located (Figure 2.6e). The giant sperm mitochondria are generated by the fusion of several mitochondia during spermiogenesis (Lindsley, 1980; Fuller, 1993). The co-localization of Dsh and centrosomal proteins to these sperm mitocondria suggest that they may play a role in giant mitochondria formation or in some structural function, but more work is needed to elucidate these processes. Future work is needed to confirm the result with other MTOC antibodies and to confirm the Dsh expression by Western blot analysis.

DISCUSSION

Immunofluorescence studies of Dsh protein localization during oogenesis and embryogenesis together suggest that the vegetal cortex provides a platform for the accumulation of maternal Dsh during oogenesis, and this platform is inherited and maintained by the most vegetal blastomeres during early development, thus localizing the activation of the endomesoderm gene regulatory net work (EGRN) at the vegetal pole. The spatiotemporal expression of Dsh protein and MTOC during sea urchin oogenesis provides an additional step in understanding the timing and mechanisms involved in generating the AV egg polarity.

The vegetal cortical domain (VCD) recruits Dsh protein for localized activation of endomesoderm specification

Several pieces of evidence from recent studies support the idea that the VCD recruits Dsh protein for localized activation of endomesoderm specification. First, the accumulation of Dsh at the vegetal cortex during oogenesis suggests that the VCD recruits Dsh protein. Second, although the Dsh mRNA is ubiquitously expressed throughout the embryo, the protein is highly concentrated at the vegetal cortex. Moreover, when Dsh::GFP is overexpressed by mRNA injection, a pool of the fusion protein accumulates as cytoplasmic puncta localized to the vegetal cortex of the embryo starting from the zygote stage and is maintained until the 60-cell stage embryo (Weitzel et al., 2004; Leonard and Ettensohn, 2007). Furthermore, overexpressing Dsh in animal pole blastomeres does not lead to ectopic expression of endomesoderm as seen when β-catenin is overexpressed in embryos (Weitzel et al., 2004). This suggests that Dsh is only functional in the Wnt/β-catenin pathway in vegetal pole blastomeres. Last, when Dsh function in the Wnt/β-catenin pathway is blocked by overexpressing the DIX domain of Dsh, endomesoderm specification does not occur. Together, these data suggest that one of the functions of the vegetal cortex is to recruit newly synthesized Dsh to the vegetal pole for endomesoderm specification.

Dishevelled protein accumulation at the vegetal cortex during oogenesis suggests the early establishment of a molecular polarity along the AV axis

In 1901, Theodor Boveri postulated that the AV axis in sea urchin eggs is preset before germinal vesicle breakdown in the oocytes (Boveri, 1901a; Boveri, 1901b). This

hypothesis was reintroduced in the 1980s by studying the echinoderms. All echinoderm oocytes exhibit an AV polarity which is established during oogenesis (Frick and Ruppert, 1996). Holothurian oocytes display the most dramatic polarization: the animal pole can be identified based on the apical protuberance, apically displaced nucleus (Smiley and Cloney, 1985; Smiley, 1988; Frick and Ruppert, 1996), an apical centriole (Smiley, 1988) or a flagellum (Frick and Ruppert, 1996). Similarly, asteroid (starfish) oocytes express an AV polarity that can be identified by apical centrioles (Schroeder, 1985; Schroeder and Otto, 1991), apically displaced nucleus, an absence of large vacuoles and actin-filled spikes at the animal pole (Schroeder and Battaglia, 1985). In several species of echinoids (sea urchins and sand dollars), the animal pole can be traced by the jelly canal, polar body extrusion (Schroeder, 1980a; Schroeder, 1980b), and a cortical microtubule-organizing center (MTOC) (Egana et al., 2007). The strong polarization of the echinoderm oocyte indicates the early establishment of the AV axis in the embryo in some unknown way (Schroeder, 1980b). Although much has been discovered about AV axis specification and patterning, the molecular mechanisms that set up the initial polarity in most metazoan ova is still far from clear. In this study, I showed that Dsh protein localization is detected in small oocytes, which suggests a molecular polarity is established along the AV axis before the germinal vesicle breakdown. The data here also provides the first molecular evidence of how the AV polarity in the sea urchin oocyte can affect the future embryonic patterning in sea urchin embryos. Elucidating the mechanisms that govern the localization of Dsh in developing sea urchin oocytes should shed light on the process through which an oocyte develops into a specialized egg capable of directing the patterning of an embryo.

The observation that cortical Dsh protein accumulation is strongly correlated with the appearance of the MTOC is interesting. This raised the question if VCD is formed at the same time as the MTOC, or if the VCD is already present and the cortical Dsh is accumulated at the time MTOC forms. Due to limited oogonia samples, I was not to be able to determine the exact timing of the appearance of MTOC and the VCD. A recent study by our collaborator on Dsh localization in sea stars shows that Dsh cortical localization is not seen until fertilization (Masato Kiyomoto, unpublished). In addition, MTOC is never observed in mature eggs. This result would suggest that the VCD is established before cortical Dsh accumulation.

In the Dsh staining in sea urchin oocytes, besides the vegetal cortex localization, I also see Dsh labeling in the MTOC. While the cortical Dsh staining pattern is consistent for all three anti-Dsh antibodies, the MTOC labeling by Dsh antibody can only be detected when using the anti-Dsh DIX domain antibody. Although Dsh is shown to be essential for both docking and planar polarization of basal bodies and knock down of Dsh causes defects in ciliogenesis (Park et al., 2008), it is also shown that the DIXDC1 protein, a Dishevelled-Axin (DIX) domain-containing protein involved in Wnt pathway, co-localizes and interacts with γ-tubulin, a marker of the MTOC (Wu et al., 2009). Therefore, it is possible that the anti-DIX antibody is detecting DIXDC1 by the DIX domains, but confirmation of this will necessitate additional studies.

Conclusions and outlook

In the work reported in this chapter, I found that a key scaffolding protein, Dsh, concentrates to the vegetal cortex during sea urchin oogenesis and embryogenesis. This

finding suggests that the key mechanism for selective activation of the EGRN in vegetal blastomeres is the recruitment and possibly localized activation of Dsh at the vegetal cortex. The Dsh protein dynamics in oocytes also provide further understanding the establishment of the AV axis during oogenesis. Moreover, Dsh localization itself provides a perfect marker of the vegetal pole for addressing many interesting questions. First, the identity of other vegetal maternal factors remains to be found. Those include RNAs and proteins that play a role in either establishing the AV axis during oogenesis (e.g. the signal that recruits Dsh to the cortex) or the ligands for the initiation of the Wnt/β-catenin pathway. Second, the mechanisms for accumulating Dsh protein at the vegetal cortex remain to be investigated. This can either be localized translation of Dsh mRNA or a mechanism that involves protein transportation to the vegetal cortex by the cytoskeleton. Furthermore, in most animals, including cnidarians (Momose and Schmid, 2006; Fritzenwanker et al., 2007; Lee et al., 2007; Momose and Houliston, 2007; Momose et al., 2008), *Drosophila* (Rau and Kalthoff, 1980), annelids (Lillie, 1909a; Lillie, 1909b), echinoderms (Boveri, 1901a; Boveri, 1901b; Horstadius, 1973; Schroeder, 1980a; Maruyama et al., 1986), lancelet (Frick and Ruppert, 1997), and *Xenopus* (Scharf and Gerhart, 1983), the primary egg polarity is established during oogenesis before fertilization, however, the mechanisms that establish this primary polarity in other metazoans remain largely unknown. It would be interesting to see if the VCD is conserved in other invertebrate species, including species from the ecdysozoans and lophotrochozoans. Last, the cytoarchitecture of the VCD and the biochemistry of the cortical Dsh should be very interesting. In the next chapter, I examined the Dsh protein on the vegetal cortex and the role of the cytoskeleton in anchoring cortical Dsh.

FIGURES

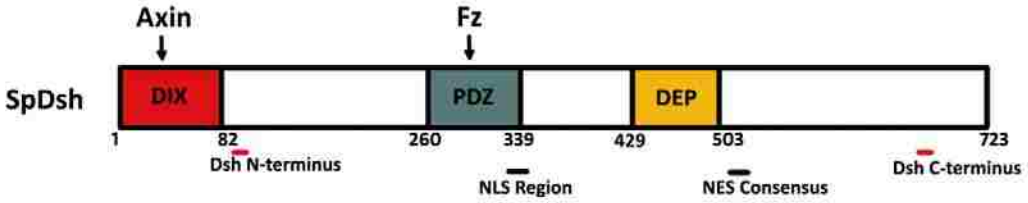

Figure 2.1 The domain structure of the *S. purpuratus* (SpDsh) Protein. The SpDsh protein is a multidomain scaffold protein that contains 723 amino acids, harboring three structural domains DIX, PDZ and DEP. Residue numbers underneath domains denote the domain boundaries. The red bars indicate the sequence locations where anti-Dsh antibodies were designed. The black bars indicate the sequence regions of the leucine-rich nuclear export signal (NES) (M/LxxLxL) and the nuclear localization signal (NLS).

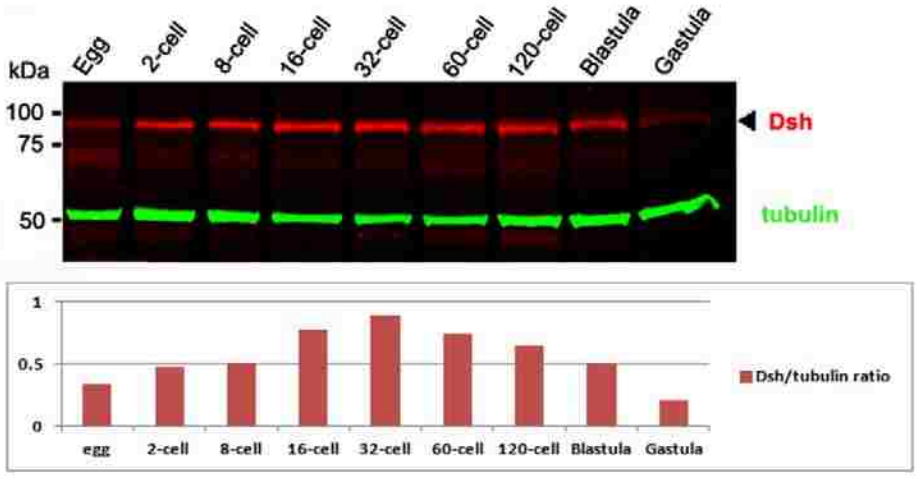

Figure 2.2 Dishevelled (Dsh) protein is expressed throughout embryogenesis. Different stage embryos were collected from *S. purpuratus* to run a Western blot analysis to examine Dsh protein expression. Dsh protein (red) is expressed at different developmental stages. Graph below shows quantified Dsh protein expression normalized by tubulin expression (Dsh/tubulin). Tubulin (green) serves as the loading control.

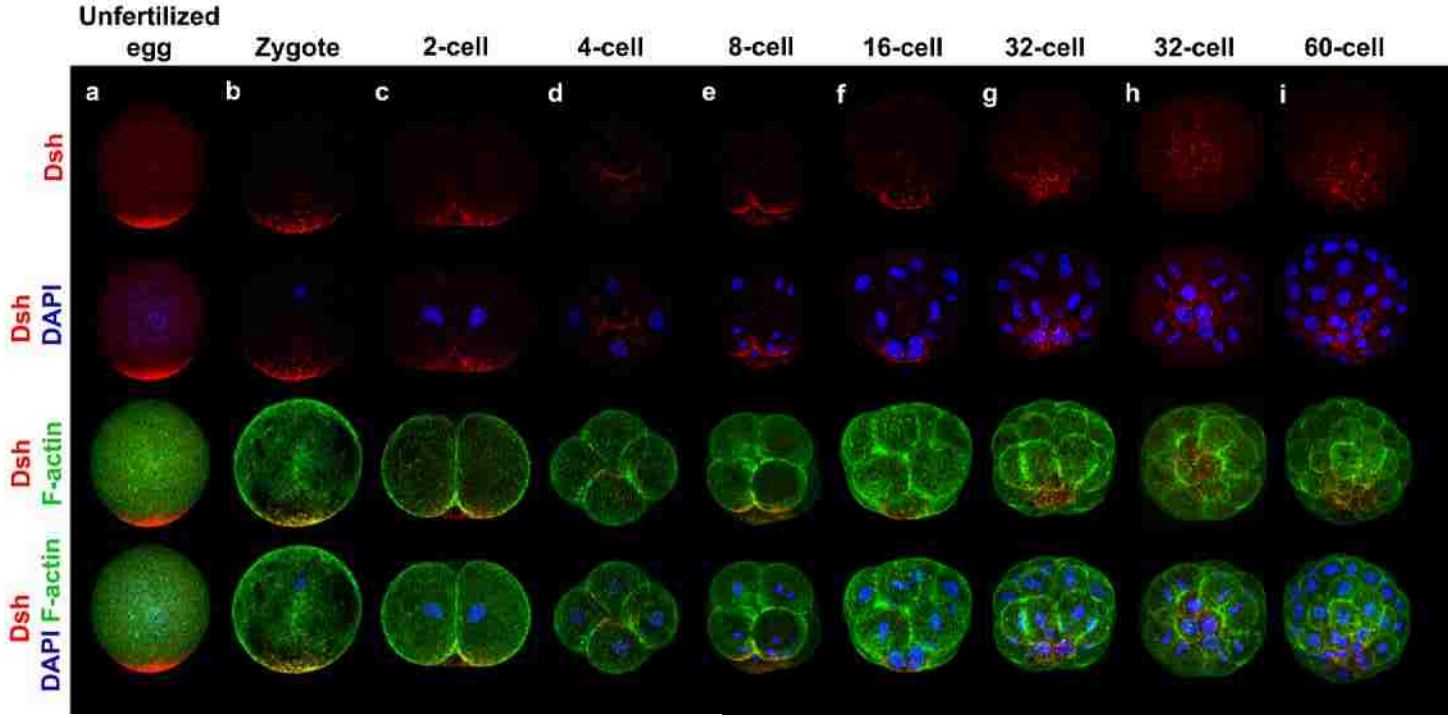

Figure 2.3 Dishevelled (Dsh) protein is highly enriched in the vegetal pole during early embryogenesis. Egg and embryo samples were collected from *S. purpuratus*, stained by anti-Dsh antibodies and viewed with a confocal microscope. **a-i,** Early embryogenesis from an unfertilized egg to 60-cell stage embryo stained by anti-Dsh antibody (red), Filamentous actin is visualized with fluorescein phalloidin (green) and nuclei are visualized with DAPI staining (blue). All images are oriented with the animal pole towards the top and the vegetal pole towards the bottom. **a,** An unfertilized egg showing concentrated maternal Dsh on the vegetal cortex. Notice that the Dsh puncta staining pattern is smooth. **b,** After fertilization, the smooth Dsh pattern becomes more pronounced. **c,** 2-cell stage embryo. **d,** 4-cell stage embryo, Dsh is seen in the vegetal pole of all four cells. **e,** 8-cell stage embryo. Dsh is seen in the four vegetal cells. **f,** 16-cell stage embryo. Dsh is observed in the cortex of micromeres and macromeres. **g,** 32-cell stage embryo. Dsh is seen in the cortex of vegetal tier cells. **h,** Vegetal view of a 32-cell stage embryo. **i,** 60-cell stage embryo. Dsh is expressed maternally and expression is maintained throughout early embryogenesis.

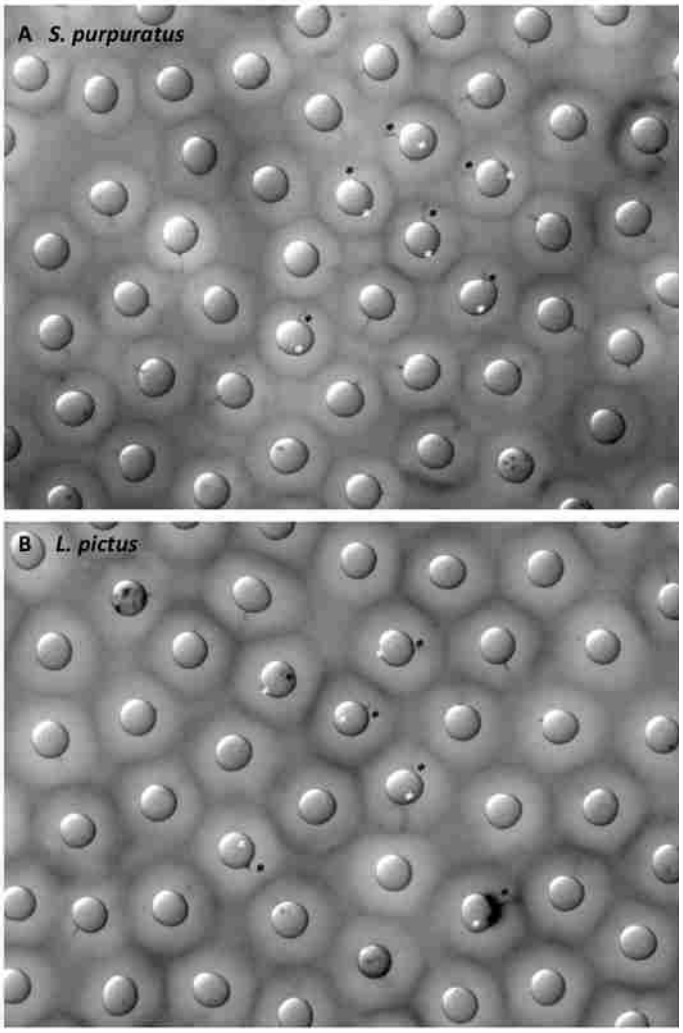

Figure 2.4 Female pronucleus is not at the animal pole in *S. purpuratus* and *L. pictus* eggs. Unfertilized eggs were collected and immersed directly into the Japanese ink to visualize the jelly canal in (A) *S. purpuratus* and (B) *L. pictus* eggs to examine if the female pronucleus (white *) is at the animal pole as indicated by the stained jelly canal (black *). Only 2 % (1 out of 50 eggs counted) and 8% (4 out of 50 eggs counted) of the female pronuclei are located directly below the jelly canal in *S. purpuratus* and *L. pictus* respectively.

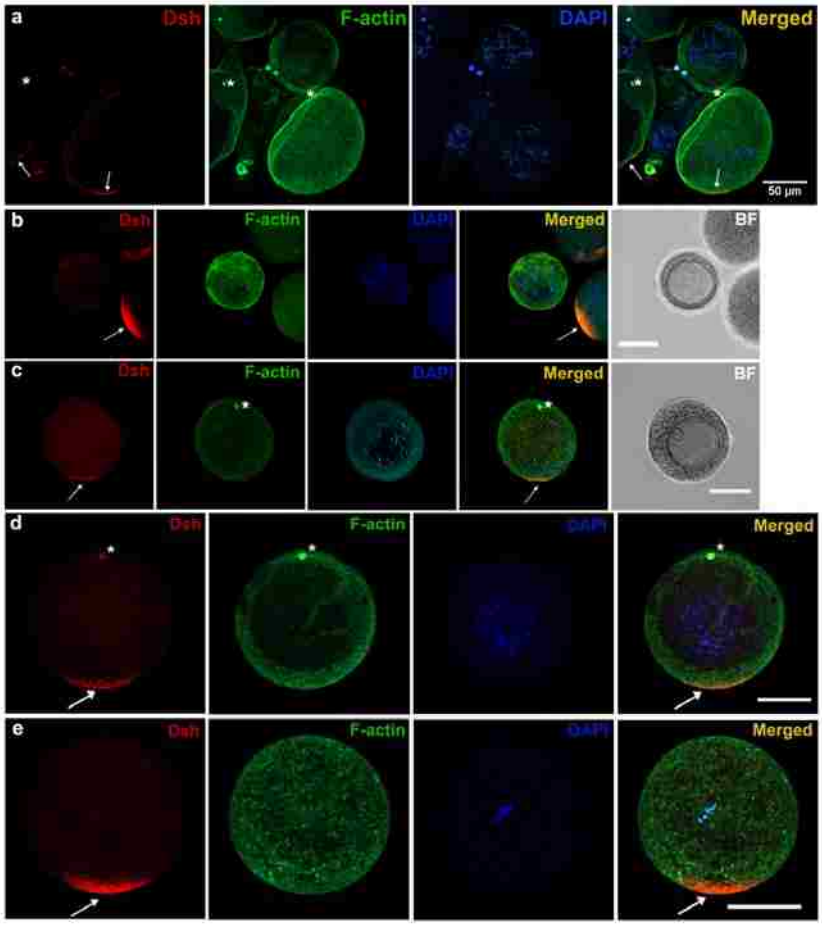

Figure 2.5 Spatiotemporal expression of Dishevelled (Dsh) during oogenesis. These samples were collected from *L. pictus*, immunostained with anti-Dsh antibodies and viewed with a scanning confocal microscope. **a-e,** Expression of the maternal vegetal Dsh protein are in red. Filamentous actin is visualized with fluorescein phalloidin (green) and nuclei are visualized with DAPI staining (blue). Arrows are pointing to Dsh staining and the asterisks (*) indicate the microtubule-organizing center (MTOC). **a,** Oocytes are attached to the somatic cells of the ovary. **b,** No Dsh protein is detected in the primary oocyte. Cortical Dsh localization is detected in the mature eggs on the right of the primary oocyte. **c,** Midsize oocytes showing the first appearance of Dsh and the MTOC, indicating an early establishment of the primary axis. **d,** Full grown oocytes are shown by a large germinal vesicle. Notice that Dsh protein is also found in the MTOC. **e,** A haploid mature egg is packing its DNA into a pronucleus after going through the last phase of meiosis. Also notice that the MTOC is disassembled in the mature egg.

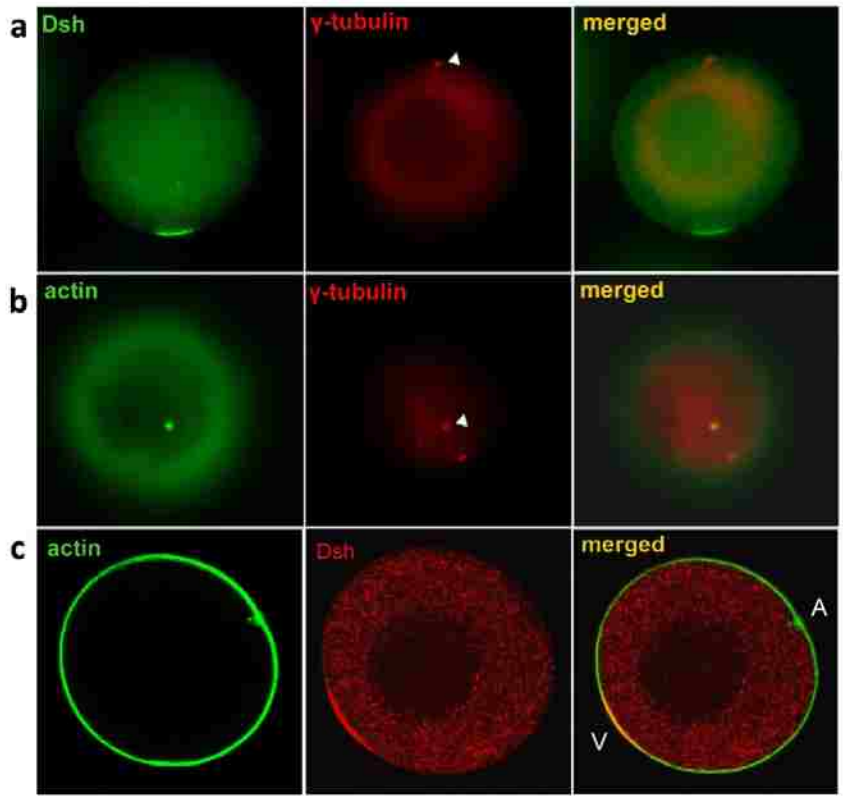

Figure 2.6 Cortical Dishevelled (Dsh) domain is positioned directly across from the cortical microtubule-organizing center (MTOC). These samples were collected from *S. purpuratus*, immunostained with anti-Dsh antibodies and viewed with a fluorescent microscope and a scanning confocal microscope. γ-tubulin is a typical protein found in the centrosome. **a,** Mid-stage oocyte double labeled with anti-Dsh antibody (green) and γ-tubulin antibody (red, indicated by an arrowhead), showing Dsh protein is localized across from the MTOC. **b,** Midstage oocyte double labeled with fluorescein phalloidin (green) and γ-tubulin antibody (red, indicated by an arrowhead), showing that the F-actin enriched structure is the MTOC. **c,** Optic sections collected using a scanning confocal microscope showing that Dsh protein (red) is positioned directly across from the F-actin enriched MTOC. A: animal pole, V: vegetal pole.

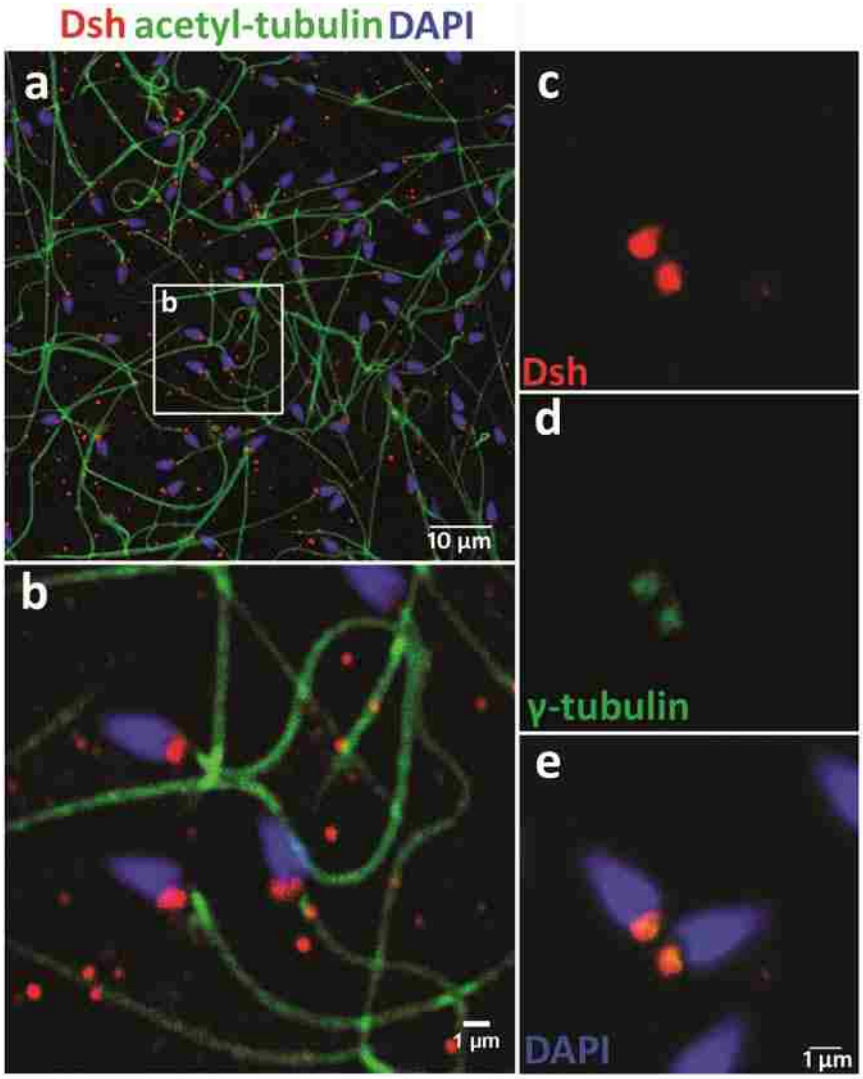

Figure 2.7 Dishevelled (Dsh) protein and γ-tubulin co-localizes at the base of sea urchin sperm head. The sperm samples were collected from *S. purpuratus*, immunostained with anti-DshDIX antibody and viewed with a scanning confocal microscope. **a,** Sea urchin sperm showing Dsh (red) staining at the base of the sperm head. Acetylated tubulin (green) staining the sperm tail, DNA (blue) stained by DAPI. Inset box showing the location where image **b** is taken. **c- e,** Dsh (red) and γ-tubulin (green) co-localizes at the base of sea urchin sperm head, where the giant mitochondria is located.

SUPPLEMENTARY FIGURES

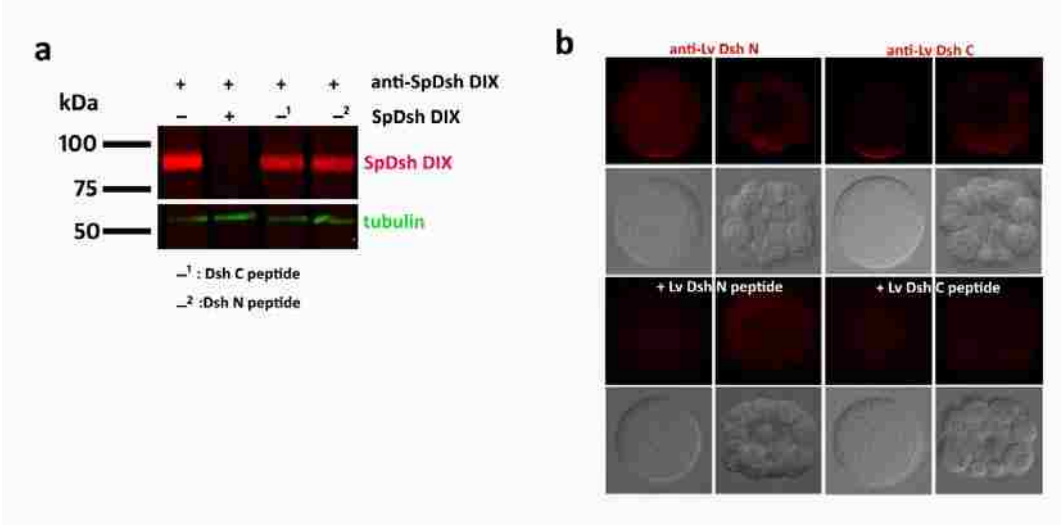

Supplementary figure 2.1 Preadsorption assay confirms the specificity of anti-Dishevelled (Dsh) antibodies. a, Western blot: Tenfold molecular excess of the SpDsh DIX protein that was used as the antigen for the affinity-purified anti-SpDsh DIX polyclonal antibody resulted in elimination of the Dsh band observed in the control lanes either without the antigen, or with Dsh C and N terminal peptides. **b,** Immunostaining: Tenfold molecular excess of the Lv Dsh C or N peptide that were used as the antigen for the affinity purified anti-LvDsh C or N polyclonal antibody resulted in elimination of both vegetal cortex staining in eggs and vegetal blastomeres staining in 32-cell stage embryos.

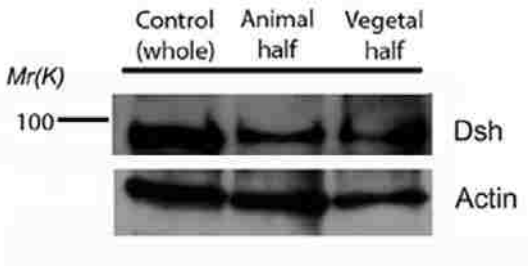

Supplementary figure 2.2 Dishevelled (Dsh) is expressed in both poles of the embryo. Western blot analysis of isolated animal and vegetal halves of the 16-cell stage *S. purpuratus* embryo shows Dsh is expressed in both halves. Actin serves as the loading control. (Work done by Joanna Kobayashi and Athula H. Wikramanayake)

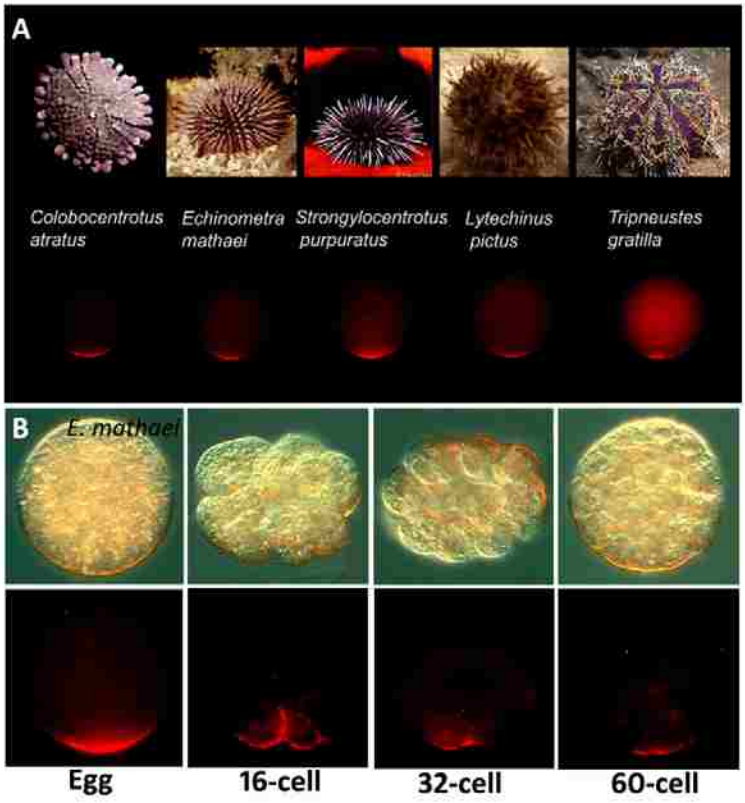

Supplementary figure 2.3 Dishevelled (Dsh) localization is conserved among five different sea urchin species. These samples were collected from various sea urchin species, immunostained with anti-Dsh antibodies and viewed with a fluorescent microscope. **A,** Dsh (red) staining in sea urchins eggs of *C. atratus*, *E. mathaei*, *S. purpuratus*, *L. pictus*, *T. gratilla* show similar enriched cortical staining in the unfertilized eggs. **B,** Dsh (red) protein is highly enriched in the vegetal cortex in early embryos of *E. mathaei*.

Chapter III: The Regulation of Dishevelled Localization and Post-translational Modification in the Egg and Early Embryo

BACKGROUND

Early studies by Horstadius suggested that factors that were crucial for germ layer segregation and gastrulation are tightly bound to the vegetal cortex of the unfertilized sea urchin egg (Horstadius, 1939; Horstadius et al., 1950). For example, when Horstadius removed portions of the egg cytoplasm using a micro-syringe and fertilized these eggs, he noted that the embryos developed into smaller larvae, but they never lost the ability to gastrulate (Horstadius et al., 1950). This result suggested that the maternal determinants for endomesoderm specification are not distributed in the cytoplasm but are attached to the vegetal cortex. This idea has recently been corroborated by the work of Croce et al. (2011), who demonstrated in a series of elegant experiments that the sea urchin vegetal cortex is required for the activation of the EGRN. For example, when the vegetal cortex of the sea urchin egg is removed and these eggs are fertilized, the developing embryos lose the ability to specify endomesoderm (Croce et al., 2011). Furthermore, when the vegetal cortex is transplanted onto the animal pole of a host egg and these eggs are fertilized, these embryos develop sites of ectopic endoderm formation suggesting that the vegetal cortex is sufficient for the activation of endoderm. In sum, a number of studies have indicated that the vegetal cortex of the sea urchin has a cytoarchitectural specialization that enables the activation of the Wnt/β-catenin pathway and endomesoderm specification, but the molecular basis for this scaffold has remained poorly defined. The anti-Dsh polyclonal antibodies that we developed gave me an opportunity to begin to investigate the structural basis for the vegetal cortical domain

(VCD). Furthermore, one-dimensional SDS-PAGE analysis does not provide enough resolution of the post-translationally modified forms of Dsh protein during embryonic development. To address this problem, two-dimensional (2D) SDS-PAGE analysis and Western blot analysis was performed on eggs and embryos.

In this chapter, I found concentrated maternal Dsh is anchored to the vegetal cortex. Moreover, the Dsh puncta are embedded between the microfilaments. By disrupting the microfilaments, I demonstrated that this vegetal cortical domain (VCD) is maintained by an actin-based cortical cytoskeleton. Furthermore, by the use of 2D gel electrophoresis to analyze Dsh on isolated cortices and micromeres, I found that the cortical pool of Dsh is distinct from the rest of the embryo. Together, these results suggest a possible mechanism for the localized activation of endomesoderm specification.

MATERIALS AND METHODS

Isolation of egg cortices and blastomeres

Cortex fragments were isolated from eggs and zygotes following the procedure of Vacquier (1975). Briefly, dejellied unfertilized eggs or zygotes were attached to poly-lysine-coated slides, and then the attached cells were subjected to a stream of cortical lawn isolation buffer (0.8 M mannitol, 50 mM HEPES, 50 mM PIPES, 5 mM EGTA, 2.5 mM $MgCl_2 \cdot 6H_2O$, pH 6.5) squirted from a rinse bottle. This procedure left large circular cortical fragments that were relatively devoid of cytoplasmic material attached to the glass. The samples for immunostaining were then fixed with 4% PFA, immunostained and observed using scanning confocal microscopy as described above. The cortex sample for Western blot analysis was collected on poly-lysine-coated 60x15mm Petri

dishes with the method described above. Cortical fragments were then directly lysed by solubilizing solution (40 mM Tris base, 2% SDS, 100 mM DTT) containing a protease inhibitor cocktail (Roche).

Purified micromeres were collected following the procedure as previously described by Wilt et al. (2004) with modifications of the linear sucrose gradient. The embryos were dissociated at the 16-cell stage into single cells, then separated on a discontinuous sucrose gradient of 4 %(w/v) and 16 %(w/v) in calcium-free seawater on ice. The different size cells were then separated by sedimentation at 1x g for 1 hr. The micromeres were retained in the 4 % sucrose while the larger size blastomeres sedimented between the interface of 4% and 16% sucrose. Micromeres in the 4% sucrose were collected and spun for one minute at 86x g to remove the 4% sucrose before adding the solubilizing solution.

Two-Dimensional (2D) gel electrophoresis and Western blot analysis

Unfertilized eggs, 16-cell stage embryos, and micromeres were collected in a 1.5 ml Eppendorf tube, centrifuged at 86x g for 30 seconds to collect a tight pellet and to remove as much sea water as possible. The cell pellets were then lysed in 100 µl of solubilizing solution. Protein concentration was determined using the Bradford assay (Quick Start Bradford Dye Reagent, BIO-RAD), then desalted with ReadyPrep 2D cleanup kit (BIO-RAD). For 2D gel electrophoresis, 40 µg of total protein of each sample were solubilized in 125 µl of 2D electrophoresis buffer (ReadyPrep 2D Rehydration/Sample Buffer 1; 7 M urea, 2 M thiourea, 1% (w/v), ASB-14, 40mM Tris, 0.001% Bromophenol Blue, BIO-RAD) with the addition of 25 mM DTT, 4% (w/v) CHAPS, and 0.2%Bio-Lyte

pH3-10/4-7(2:1)(BIO-RAD). Samples were loaded on an immobilized pH gradient (IPG) ReadyStrips 4-7(BIO-RAD), isoelectrofocused with the Protean IEF cell (BIO-RAD) by applying a total of 10,000 V-hr, according to the ReadyStrip IPG Instruction Manual (BIO-RAD). The IPG strips were then equilibrated in SDS-PAGE equilibration Buffer (6 M urea, 0.375 M Tris-HCl, pH 8.8, 2% SDS, 20% glycerol, 2% (w/v) DTT) two times (20 minutes each) and transferred to a 10% Tris-Glycine Polyacrylamide Gel. SDS-PAGE was performed and transferred onto Trans-Blot nitrocellulose membranes (Bio-Rad). Immunoblots were probed as previously described. Based on the *S. purpuratus* Dsh protein sequence, the charge of Dsh protein is estimated to be at pI 6.01 (isoelectric point)

Nuclear export inhibition study

To determine if the nuclear transport function of Dsh protein is conserved in sea urchin embryos, a nuclear export inhibitor leptomycin B (Sigma, stock of 5 mg/ml, dissolved in 70% ethanol) was used on sea urchin embryos. The controls included molecular grade ethanol at the same concentrations expected in the diluted inhibitors used in the assay (ethanol to ASW ratio is at 1:200,000 so toxicity of ethanol is limited). Eggs were dejellied before applying the drug at a final concentration of 25 ng/ml. Samples were collected for immunostaining at egg, 2-cell, 4-cell, 8-cell, 16-cell, and 32-cell stage embryos.

RNA Injections

For SpDsh::GFP mRNA injections, cDNAs were subcloned into the pCS2+ vector. The plasmid was linearized with NotI and used as templates to generate 5′ capped mRNA using the SP6 mMessage mMachine Transcription Kit (Ambion). The average mRNA yield was 1.5 ug/ul from 2 μg of DNA template. Injection solutions consisted of 40% glycerol and 0.8 ug/ul SpDsh::GFP mRNA in RNAse-free, sterile water. Fertilized *L. pictus* eggs were injected as described (Bince and Wikramanayake, 2008).

Cytoskeleton disruption studies

To determine if specific components of the cytoskeleton are involved in localizing Dsh to the vegetal cortex of the egg, specific cytoskeletal components were disrupted using the following chemicals: cytochalasin B (Sigma), 10 μg/ml; cytochalasin D (Sigma), 10 μg/ml; colchicines (Sigma), 100 μM; cisplatin (Sigma), 100 μM; 2,3-Butanedione monoxime (BDM) (Sigma), 10 mM; blebbistatin (Sigma), 100 μM. All the inhibitor stock solutions used dimethyl sulfoxide (DMSO) as the solution vehicle, and controls included DMSO at the same concentrations expected in the diluted inhibitors used in the assays. Eggs were dejellied before applying the respective drugs. Samples were collected for immunostaining and Western blot analysis after 2 hr incubation at 15˚C. Recovery experiments was done by incubating the egg in the drugs for 20 minutes, removing the drugs using three changes in ASW, and then incubating the treated eggs for an additional 100 minutes at 15˚C. To follow the expression of Dsh following disruption of microfilaments, unfertilized eggs were treated with cytochalasin B or D for 5 minutes,

washed three times in ASW, and collected for immunostaining and Western blot analysis at different time points.

Artificial activation of cortical granules in F-actin and tubulin inhibited eggs

To test if the reorganization of Dsh cytoplasmic puncta following fertilization is mediated by the reorganization of the actin-based cortical cytoskeleton, F-actin and microtubules in eggs were inhibited by cytochalasin B (Sigma), 10 µg/ml; cytochalasin D (Sigma), 10 µg/ml; colchicine (Sigma), 100 µM, 10 minutes prior to artificial activation of cortical granules. Eggs were dejellied before applying the respective drugs. Since the acrosome reaction is affected by the cytoskeletal inhibitors, calcium ionophore (Calcimycin A23187, Sigma) was used at a final concentration of 2 µg/ml to artificially activate the eggs. Eggs were collected at 5 minutes after calcium ionophore addition and processed for immunostaining as previously described.

RESULTS

A pool of Dsh protein concentrates in a domain at the vegetal cortex

To determine if the Dsh protein was accumulating in a localized domain that was attached to the egg cortex, I immunolocalized the protein in isolated egg cortices. Cortical lawns were fixed and stained using the anti-Dsh antibodies, and analyzed using light microscopy and scanning confocal microscopy. This analysis showed that there is a striking localization of the Dsh protein in the isolated cortical fragments (Figure 3.1a-f). Immunostaining of cortices isolated from zygotes also showed the localized domain of Dsh indicating that the vegetal cortical domain (VCD) is retained after fertilization

(Figure 3.1g-i). While I cannot isolate cell cortices from later blastomeres, the continued accumulation of Dsh in the cortex of vegetal cells indicates that the VCD is inherited by the micromeres and the macromeres, and retained in these cells at least through the 120-cell stage of development (Figure 2.3).

Dsh immunolocalization in isolated cortices also revealed some other interesting features of the VCD. In the immunolocalization experiments, the cortices were also stained with phalloidin to localize filamentous actin. Superimposing the Dsh localization pattern with F-actin staining revealed that in many cases, the Dsh puncta appeared to be embedded between actin microfilaments, most likely short microvilli (Figure 3.1j-l). I also noted that the VCD, as defined by Dsh localization, is a circular domain and that there appears to be a concentration gradient of Dsh puncta, with the highest concentration of puncta in the center of the VCD, which decreased as the domain extended towards the animal pole (Figure 3.1d-f and g-i). This observation suggests that the egg cortex may embed polarity information that is used during early development of the sea urchin embryo.

Several lines of evidence indicate that the "cortical" Dsh is key for the localized activation of the EGRN. First, Dsh protein is highly concentrated on the VCD but broadly expressed in the egg at lower levels. Second, unlike overexpressed β-catenin, which induces ectopic endomesoderm, overexpressing Dsh in the animal half blastomeres does not have an effect, indicating that Dsh is not sufficient for the activation of the EGRN (Weitzel et al., 2004). Third, transplanting the Dsh-containing VCD to the animal pole of a host egg is sufficient to induce ectopic endoderm at the animal pole (Croce et al., 2011). These observations raise the possibility that the VCD-localized Dsh that is

subsequently inherited by vegetal blastomeres is differentially modified to mediate its localization and/or activation in this domain. To investigate this possibility, I carried out two dimensional (2D) gel electrophoresis and SDS-PAGE followed by Western blot analysis on the isolated egg cortices. These results showed a strikingly different pattern of Dsh post-translational modification compared to the pattern seen in whole egg extracts (Figure 3.2). This analysis revealed Dsh isoforms in the whole egg and embryo extract displayed over a wide range of isoelectric points (pI) that stretches from a pH range of 4.2 to 6.6 (Figure 3.1a, c, e, and f). I also carried out 2D SDS-PAGE on micromeres isolated from 16-cell stage embryos. Compared to the whole egg extract, Dsh isoforms in the cortical fragments extract and the micromeres look similar and both are much more condensed at the acidic pI range, between pH 4 and 5 (Figure 3.1b and d). In sum, I conclude that Dsh protein is highly concentrated at the VCD and is differently modified by post-translational modification within this domain. The molecular basis for this modification is not known, but may likely involve phosphorylation since many studies have identified phosphorylated residues on Dsh homologs from various species (Gao and Chen, 2009). In the sea urchin embryo, these modifications may regulate Dsh localization and/or selective activation of Wnt/β-catenin signaling in vegetal blastomeres. This result demonstrated that *endogenous* Dsh is differentially post-translationally modified in different cellular compartments, and provides insight into the regulation of the Wnt pathway during endomesoderm specification in the sea urchin embryo.

Dsh protein shuttles between the nucleus and the cytoplasm in all blastomeres

Nuclear import and export of Dsh protein has been demonstrated to play a role in Wnt/β-catenin signaling during *Xenopus* development (Itoh et al., 2005). This result was led by the finding of a leucine-rich nuclear export signal (NES) (M/LxxLxL) and a nuclear localization signal (NLS) (Figure 2.1), both conserved from *Drosophila* to humans (Itoh et al., 2005). In addition, both signals are conserved in sea urchin Dsh protein sequences (Leonard and Ettensohn, 2007). To determine if endogenous Dsh shuttles between the nucleus and the cytoplasm during early sea urchin embryo development, I treated the developing embryos with a nuclear export inhibitor, leptomycin B, and assayed the spatiotemporal expression of Dsh protein at early developing stage embryos. The rationale for this experiment is that since endogenous Dsh protein is not detected in the nucleus under normal development due to the dynamic movement of the protein shuttling in and out of the nucleus, then inhibiting nuclear export should lead to the accumulation of enough Dsh protein to be detected by immunostaining. The results showed that early cleavage stage (2-cell to 8-cell stages) embryos had no detectable Dsh staining within the nuclei (data not shown). However, by the 16-cell stage, nuclear accumulation of Dsh was visible in the micromere nuclei, but not in the overlying macromeres and mesomeres (Figure 3.3b, e). By the 32-cell stage embryo, nuclear accumulation is seen throughout the embryo when examined by confocal microscopy (Figure 3.3c, f, and h). The leptomycin B treated embryos did not show any defects at the pluteus stage compared to controls (data not shown). It is also worth noting that when overexpressing wild type Dsh::GFP, the GFP signal accumulates in the nuclei throughout the embryo starting at the blastula stage, but no phenotype was observed (data not shown). Moreover, the results

reported above are consistent with the investigation of nuclear import and export of Dsh by overexpression in the sea urchin *L. variegatus* by Leonard et al., (2007). The results reported here suggest that the conserved NLS and NES protein sequences are functional in *endogenous* Dsh. In addition, these data also confirmed that endogenous Dsh is present in animal blastomeres but has no effect on activating the Wnt/β-catenin pathway.

Dsh puncta aggregation after fertilization is not microfilament or microtubule dependent.

The observation that Dsh staining forms cytoplasmic puncta that aggregate after fertilization (Figure 3.4A, a and b) raised the question if this reorganization is caused by cortical cytoskeleton rearrangements. Immediately following the binding of the sperm to the egg, an extensive remodeling of egg surface occurs by the fusion and exocytosis of thousands of cortical granules activated by a transient rise of calcium. This further leads to more extensive changes in cell shape and topology by the underlying dynamic reorganization of an actin-based cortical cytoskeleton (Bonder and Fishkind, 1995). To test if the formation of Dsh cytoplasmic puncta is related to this event, I applied cytochalasin B and D to inhibit the reorganization of the cortical F-actin. Unfertilized eggs were than activated by adding calcium ionophore to overcome the inhibition of acrosomal reaction in sperm by cytoskeletal inhibitors. Calcium ionophore treated eggs were able to form the Dsh cytoplasmic puncta (Figure 3.4B, c). Inhibiting the F-actin or the microtubules in the eggs by cytochalasin and cholchicine prior to introducing calcium ionophore did not abolish puncta formation (Figure 3.4B, d-f). This result suggests that

the formation of Dsh cytoplasmic puncta aggregates is not microfilament or microtubule dependent.

Dsh localization and stability are affected by disruption of microfilaments

The localized accumulation of Dsh in the VCD raises many interesting questions about the mechanism regulating this novel polarity in sea urchin eggs. One relevant question relates to the molecular mechanisms underlying the anchoring of Dsh to the VCD. Several observations made in the current study and in previous studies raised the possibility that Dsh is anchored on the vegetal cortex by components of the cytoskeleton. First, immunostaining of the cortices showed that Dsh puncta are embedded between the actin filaments, which suggested that the Dsh protein might be anchored on the cortex by cortical actin. In addition, Dsh contains known microtubule and microfilament binding domains, and has been shown to interact with these components of the cytoskeleton (Torres and Nelson, 2000). Moreover, extensive arrays of microfilaments, microtubules and cytokeratin-type intermediate filaments and concentrated myosin II have been shown to be present in the cortex of unfertilized eggs, although none of these molecules have been shown to be expressed asymmetrically in the egg cortex (Boyle and Ernst, 1989; Asano and Mabuchi, 2001; Stack et al., 2006). To determine if specific cytoskeletal elements are involved in anchoring Dsh to the vegetal cortex, dejellied eggs were treated with inhibitors that selectively disrupt actin filaments, microtubules, intermediate filaments, myosin or myosin II. The cytochalasins B and D are known to disrupt filamentous actin and induce reorganization of cortical actin filaments into actin patches

or short rods (Foissner and Wasteneys, 2007). While cytochalasin B is irreversible, cytochalasin D was used for its fast and reversible inhibition of F-actin.

Phalloidin staining indicated that the microfilaments in sea urchin eggs are disrupted within 20 min of cytochalasin B or D treatment. However, morphological changes in the eggs within minutes after addition of the chemicals indicated that microfilament disruption took place very rapidly (data not shown). Immunolocalization of Dsh in cytochalasin treated eggs showed that Dsh accumulation in the VCD was unaffected even after 1 or 1.5 hours of incubation in the drugs. However, after approximately 2 hrs of incubation in either form of cytochalasin, we noted the loss of Dsh from the VCD. We also noted that these eggs also appeared to lose Dsh in the cytoplasm (compare figures 3.5). This raised the possibility that disruption of microfilaments was not only causing delocalization of Dsh from the VCD, but this treatment was also leading to the destabilization of Dsh found throughout the egg. To evaluate this possibility, I performed Western blot analysis of eggs treated with cytochalasin B and D at different times following the addition of the drugs. This analysis showed that there was a striking downregulation of Dsh protein in eggs treated with the cytochalasins after approximately 2 hrs following the addition of the microfilament disruptors (Figure 3.6A).

Dsh protein localization and expression was not affected by disruption of microtubules with colchicine (Wessel et al., 2002), intermediate filaments with cisplatin, a general phosphatase inhibitor (Evans and Simpkins, 1998), non-muscle myosin with BDM (Asano and Mabuchi, 2001; Forer and Fabian, 2005) or myosin II with blebbistatin (Stack et al., 2006) (Figure 3.5; data not shown). Unfortunately, besides F-actin, which can be visualized by phalloidin staining, I was limited in my ability to test the effect of

the drugs on microtubules, intermediate filaments, myosin and myosin II. Nevertheless, the concentration of the drugs was chosen based on previous sea urchin studies, except for cisplatin, which is based on a cell line study (Boyle and Ernst, 1989; Evans and Simpkins, 1998; Asano and Mabuchi, 2001; Stack et al., 2006). It is worth noting that when the eggs treated with cytochalasin B or D pulse treatment are fertilized, the embryos failed to develop a gut (with the presence of pigment cells). This observation suggests that the loss of VCD led to the failure of gastrulation, but the survival of these embryos is extremely low. Moreover, without specific rescue experiments I cannot conclude that loss of Dsh is causal for the inhibition of gastrulation in these embryos. In all other treatments, when the eggs were fertilized, they all developed a gut (data not shown). It is important to note that the samples for immunolocalization of Dsh, Western blot analysis, and the phenotype assay came from the same tube. I conclude that the cortical microfilaments are necessary for the localization of Dsh to the VCD, and also that the stability of the Dsh protein in the entire egg is affected by microfilament disruption. However, the timing for the disruption of cortical Dsh by reorganizing microfilaments suggests that this is more of a global effect on the integrity of the cortex. The VCD is affected by the integrity of the cortex, and this further led to the release of cortical Dsh for degradation.

DISCUSSION

In this chapter, an immunofluorescence study of concentrated maternal Dsh in isolated cortical fragments revealed a cytoarchitectural polarity of the sea urchin egg cortex, and this further refined the vegetal cortical domain to a more circular domain. In addition, by

using 2D gel electrophoresis to analyze Dsh in isolated egg cortices and micromeres, I demonstrated that the concentrated cortical pool of Dsh has isoforms that are distinct from the cytoplasmic pool. Last, by disrupting the microfilaments, I demonstrated that the Dsh-enriched vegetal cortical domain (VCD) is maintained by the actin-based cortical cytoskeleton and the stability of Dsh in the egg relies on microfilaments.

The developmental biology of the Dsh protein in the sea urchin embryo

Previous work in our lab has demonstrated that Dsh is ubiquitously expressed in the sea urchin embryo. For example, Dsh protein shows no apparent difference in expression level between the isolated animal pole and vegetal pole blastomeres demonstrated by Western blot (Supplementary figure 2.2). In addition, the cytoplasmic pool of Dsh shuttles in and out of the nucleus in all blastomeres. Although the function of the cytoplasmic pool of Dsh is unknown, several lines of evidence suggest that localized activation of cortical Dsh is required for the activation of the EGRN. First, unlike overexpression of β-catenin, overexpression of Dsh in the animal pole blastomeres does not induce ectopic endomesoderm specification, suggesting Dsh can only be activated at the vegetal pole (Weitzel et al., 2004; Leonard and Ettensohn, 2007). Furthermore, I demonstrated that distinct Dsh isoforms are enriched at the VCD compared to the entire embryo. Most importantly, when the vegetal cortex is stripped from the egg, the embryo fails to specify endomesoderm. When the vegetal cortex is transplanted to a host egg, the embryo develops ectopic endoderm. This suggests that the vegetal cortex is both necessary and sufficient for the activation of the Wnt/β-catenin pathway (Croce et al., 2011). Together, these data suggest that the subcellular localization of Dsh at the vegetal

cortex is essential for the activation of the EGRN. In addition, these results suggest that *endogenous* Dsh is differentially post-translationally modified in different cellular compartments, and provides insight into the regulation of the Wnt pathway during endomesoderm specification in the sea urchin embryo.

Dsh isoforms in the sea urchin embryo

The Dsh isoforms deserve some discussion because of the complexity of the spot pattern shown on 2D protein analysis. According to 2D gel electrophoresis, where the protein is first separated by charge, Dsh protein spots in the whole egg and embryo displayed over a wide range of isoelectric points that stretched from a pH range of 4.2 to 6.6, suggesting the endogenous Dsh has many isoforms. According to the Dsh gene annotation and GLEAN prediction by Gbrowser v3.1 (SpBase: http://www.spbase.org/SpBase/), no splice variants are found. However, four isoforms have been identified from transcriptome data collected from the egg (Data collected by Lingyu Wang). While the net charge of SpDsh is estimated to be 6.03, the spots seem to be more modified towards the acidic pH. This strongly suggests the protein is post-translationally modified by phosphorylation, and even being hyperphosphorylated in the samples collected from the cortices and the micromeres. It is well established that Wnt stimulation induces Dsh phosphorylation (reviewed in (Wallingford and Habas, 2005)). Although the role of phosphorylation remains incompletely understood, it is known that Dsh is phosphorylated via the serine residues mostly scattered in the PDZ and DEP domains of Dsh (Gao and Chen, 2009). Three possible kinase candidates have also been identified, including casein kinase 1 (CK1), casein kinase 2 (CK2) and PAR-1 (Gao and Chen, 2009). The

Dsh isoforms seen by 2D Western blot analysis could be a combination of splice variants and different levels of phosphorylation. However, I was limited in my ability to test Dsh phosphorylation and confirm that the isoforms in 2D analysis are different phosphorylated forms.

Dsh is an enigmatic protein

The subcellular localization of endogenous Dsh in sea urchin development share several characteristics with the vertebrate Dvl (Dsh). Those include translocation of Dsh to the membrane, formation of the Dsh puncta, and shuttling between the cytoplasm and the nucleus. However, the role of subcellular localization of Dsh during vertebrate development remains poorly understood, and can be different from the Dsh location during sea urchin development. For example, first of all, in vertebrate culture cells and in *Xenopus* animal caps, the membrane translocation of Dsh is commonly a consequence of activation of the Wnt/β-catenin signaling (Park et al., 2005). In addition, the formation of Dsh puncta, whether it is intracellular vesicle or protein complex aggregate, is found required for Wnt/β-catenin signaling (reviewed in (Wallingford and Habas, 2005)). Conversely, in human embryonic kidney cells (HEK293), punctate localization of Dsh correlates with decreasing Wnt/β-catenin signaling (Choi and Han, 2005). In sea urchins, however, the subcellular localization of cortical Dsh is preset before the activation of the Wnt pathways, and the cytoplasmic puncta appears right after fertilization while the Wnt/β-catenin pathway is known to be activated several hours later at the 16-cell stage. Secondly, it has been shown that Wnt1 induces Dsh accumulation in and around the nucleus in embryonic mouse kidney cells (Torres and Nelson, 2000). Furthermore, the

nuclearization of Dsh is required for the activation of the Wnt/β-catenin pathway during *Xenopus* development (Itoh et al., 2005). My study confirms that the nuclear signals of Dsh are conserved in sea urchins, but the role for this phenomenon during development remains unclear. Last, it has been shown that the activation of the PCP pathway simultaneously downregulates the Wnt/β-catenin pathway and vice-versa (reviewed in (Wallingford and Habas, 2005)). By contrast, in sea urchin embryos, blocking Dsh function by DIX blocks both endomesoderm specification and morphogenesis. The function of Dsh in sea urchins is well studied, the next step is to understand how it is regulated, however, it is beyond the scope of this study.

The VCD provides a platform for AV axis specification and endomesoderm specification in the sea urchin

The VCD provides a platform for several crucial functions regarding AV axis specification and endomesoderm specification. First, the VCD recruits Dsh protein for AV axis specification during oogenesis and early embryogenesis. Secondly, the VCD maintains Dsh during early development. Third, the VCD activates Dsh for endomesoderm specification. Several lines of evidence support these three functions. First of all, Dsh accumulates at the vegetal cortex during oogenesis. Secondly, when overexpressing Dsh::GFP in the egg, GFP signals are seen at the vegetal cortex, suggesting that the VCD has the ability to recruit Dsh. Third, when the VCD is abolished after the disruption of the actin-rich cortical cytoskeleton, cortical Dsh is lost and is targeted for degradation in the cytoplasm. Interestingly, it has been demonstrated that the membrane targeted Dsh is protected from proteosome-mediated degradation (Simons et

al., 2005). Fourth, overexpressing Dsh at the animal pole cannot induce ectopic endomesoderm formation. However, transplanting the vegetal cortex to the animal pole induces ectopic endoderm, suggesting that the vegetal cortex has the required components to activate the Wnt/β-catenin pathway via Dsh (Croce et al., 2011). Furthermore, my research has shown that the cortical Dsh is distinct from the cytoplasmic pool, suggesting the VCD has the ability to modify Dsh at via other maternal factors localized at the VCD. Together, these data suggest that the VCD provides a platform for the accumulation of maternal factors during oogenesis, and this platform is inherited and maintained by the most vegetal blastomeres during early development by an actin-rich cortical cytoskeleton, thus localizing the activation of the EGRN at the vegetal pole.

The VCD might be an evolutionarily conserved mechanism for the AV axis specification

Since the AV axis is found in nearly all metazoan eggs, the finding of the VCD suggests that it might be an evolutionarily conserved mechanism for the establishment of the AV axis in metazoans. The AV axis is specified in the oocyte in most metazoans studied to date, those includes species from bilaterian and non-bilaterian clades (Boveri, 1901a; Lillie, 1909b; Scharf and Gerhart, 1983; Schroeder and Stricker, 1983; Houliston et al., 1993; Frick and Ruppert, 1997). In some well studied model systems, such as frogs, *Drosophila* and ascidians, it has been shown that mRNA determinants are localized in the oocyte cortex, which is the key event in the establishment of embryonic axes (van Eeden and St Johnston, 1999; Houston and King, 2000; Nishida and Sawada, 2001). Especially in *Xenopus* and ascidians, where there is evidence for strong physical tethering of mRNA

to the vegetal cortical scaffold (Alarcon and Elinson, 2001; Prodon et al., 2005; Sardet et al., 2005). Many cortical mRNAs remain attached to the vegetal cortex once it is isolated, just like the cortical Dsh protein in the VCD found in the sea urchin egg. The mechanisms for the localization of mRNA to the vegetal cortex of oocytes have been well described in *Xenopus* (reviewed in (King et al., 2005)), where it recruits mRNAs at different stages during oogenesis to the vegetal cortex, suggesting that a VCD is present in this species. Using the egg cortex as the repository for spatiotemporal development is a common theme in metazoan embryos (reviewed by (Sardet et al., 2004)). It would be interesting to see if the VCD is conserved in the protostomes to specify the AV axis.

Conclusions and outlook

Cortical Dsh plays a central role in axis specification and in selective activation of endomesoderm specification during sea urchin development. Although the underlying mechanisms remain far from clear, the studies here demonstrated the importance of the subcellular localization of a scaffold protein in the context of development, particularly in endomesoderm specification and gastrulation, events shown to be crucial for the evolution of diverse body plans. My study also provides a stage for asking several questions, including the signals that recruit Dsh to the VCD, the mechanisms that "activate" Dsh protein at the VCD, and the factors that anchor Dsh to the VCD. The isolated cortical fragments provide a useful starting material for looking at enriched RNAs and proteins at the cortex by RNA-Seq next generation sequencing and immunopreciptation. Anti-Dsh antibodies provide reagents for identifying the localization of the candidates along the AV axis. In addition, given that Dsh is a scaffold

protein and is known to associate with more than fifty binding partners (reviewed in (Wallingford and Habas, 2005)), it is an excellent probe to be used to fish the proteins that either play a role in the establishment of the VCD or novel proteins in the Wnt pathways. Finally, it would be interesting to examine the ultrastructure of the VCD domain by either TEM or SEM by using the cortical Dsh as a marker. In sum, these answers will help us understand the mechanisms of specifying the AV axis during early development in metazoans.

FIGURES

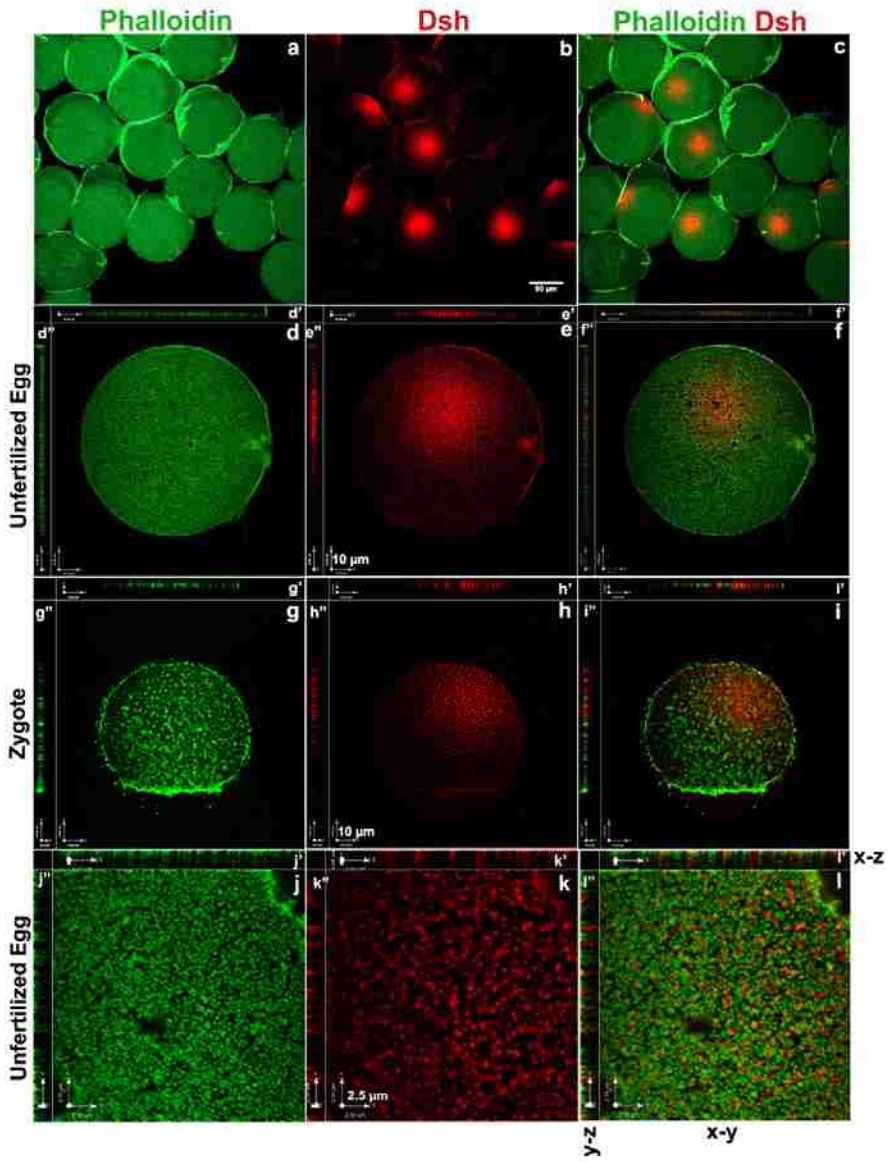

Figure 3.1 Maternal Dishevelled (Dsh) protein accumulation reveals a cytoarchitectural polarity in the sea urchin egg cortex. Egg cortices were collected from *S. purpuratus* eggs and zygotes, stained with anti-Dsh antibodies and viewed with a scanning confocal microscope. **a-c,** Wide field view of unfertilized egg cortices labeled by Dsh (red) and phalloidin (green) shows the asymmetric localization of Dsh protein (Bar=50µm). **d-f,** A closer view of a single cortex labeled by anti-Dsh antibodies and phalloidin shows a uniform F-actin distribution and concentrated Dsh in one domain, (Bar= 10µm). **g-i,** an isolated zygote cortex labeled by anti-Dsh antibodies and

phalloidin shows that Dsh remains localized to the cortex following fertilization, (Bar= 10µm). **j-l,** A higher magnification of concentrated Dsh location shows Dsh is embedded between short actin filaments, (Bar= 2.5µm). There is a low to high concentration gradient of Dsh from left to right. **d'-I' and d"-I",** 90˚ rotation of the 3D confocal dataset shown in d-l (x-y) allows the same image to be viewed in cross sections n' (x-z) and n" (z-y), showing Dsh is embedded between short actin filaments.

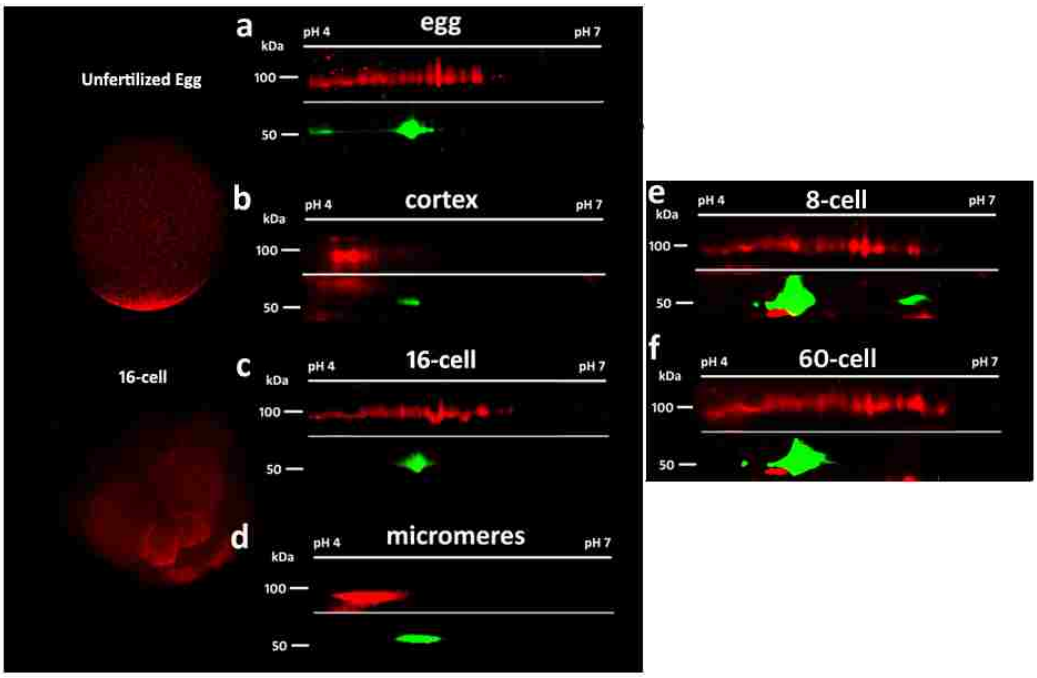

Figure 3.2 A distinct pool of post-translationally modified Dishevelled (Dsh) protein concentrates at the vegetal cortical domain. 40 µg of total protein from each sample were collected from *S. purpuratus* eggs (**a**), isolated cortical fragments (**b**), 8-cell (**e**), 16-cell (**c**), 60-cell (**f**) stage embryos and micromeres (**d**) then analyzed by 2D gel electrophoresis, separating the proteins first by charge (on a pH 4 to pH 7 IPG strip) then by size, and then subjected to Western blot analysis using anti-Dsh antibodies. Dsh (red) isoforms in isolated cortex samples and micromere samples are enriched near the acidic (left) side of the gel, while whole embryo samples showing the Dsh protein spots stretched across the tubulin (green) spot. Tubulin (green) serves as control.

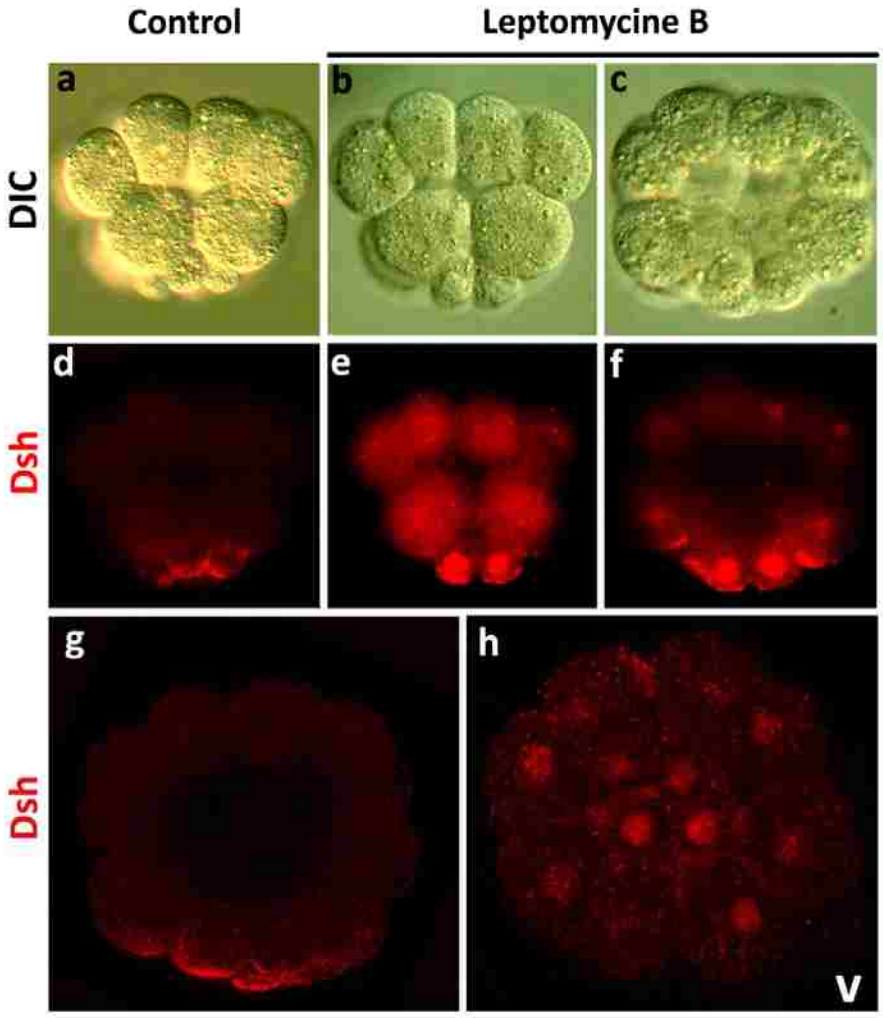

Figure 3.3 Dishevelled (Dsh) protein accumulates in the nuclei in all blastomeres after leptomycine B treatment. The eggs were collected from *S. purpuratus*, treated with the nuclear export inhibitor, stained with anti-Dsh antibodies and viewed with a fluorescent microscope (a-f) and a scanning confocal microscope (g, h). **a and d,** The control (ethanol was used as the carrier for leptomycine B) shows cortical Dsh (Red) localization at the vegetal pole. **b and e,** Staining of leptomycine B treated 16-cell stage embryos shows Dsh staining in the nuclei and cortex of the micromeres. **c and f,** Dsh nuclei localization is seen at the animal blastomeres of a 32-cell stage embryo. **g,** 32-cell stage control embryo showing Dsh concentrated at the vegetal cortex. **h,** Leptomycine treated 32-cell stage embryos viewed from vegetal pole (v). Z-stack collected from scanning confocal microscopy shows Dsh accumulating in all blastomeres.

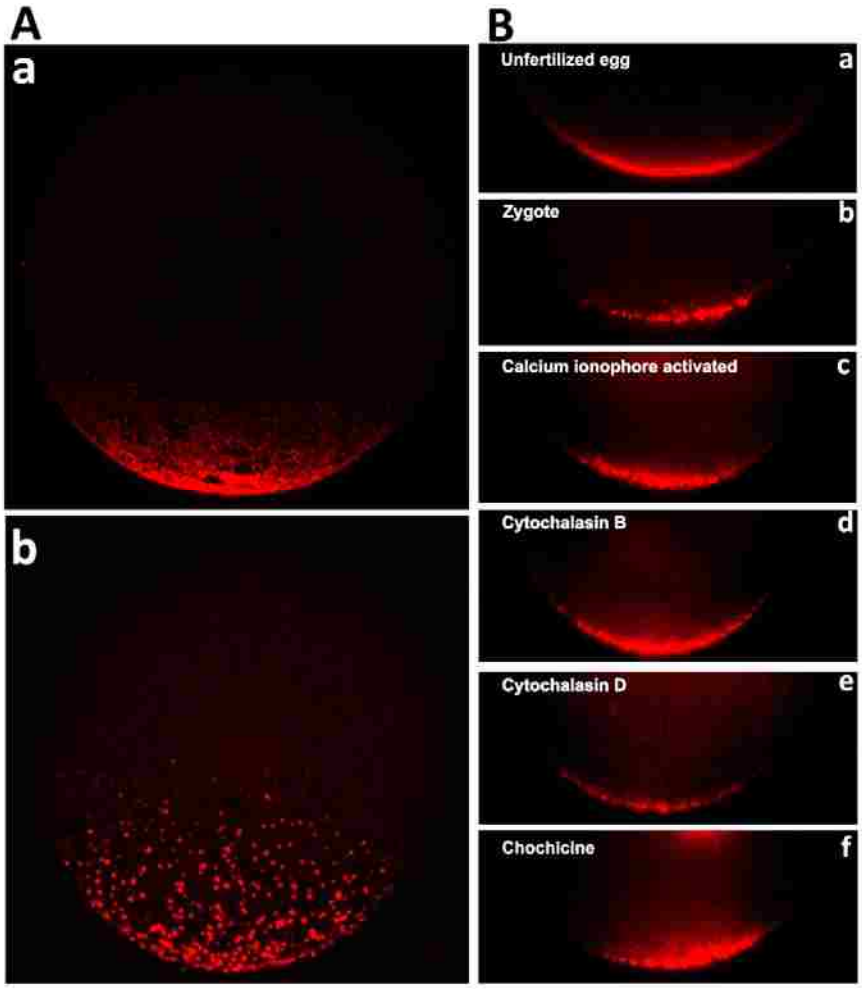

Figure 3.4 Dishevelled (Dsh) puncta formation after fertilization is not microfilament and microtubule dependent. The eggs were collected from *S. purpuratus*, stained with anti-DshC antibody (red) and viewed with a fluorescent microscope. **A**, Confocal images of anti-Dsh antibody stained unfertilized egg (**a**) and 5 minute post fertilized egg (**b**), showing the drastic change of staining pattern from smooth to puncta. **B**, **a-b,** After fertilization, endogenous Dsh pattern in the zygote drastically changes into puncta compared to the smooth cortical stain in the unfertilized egg under a fluorescent microscope. **c,** A similar punctate staining can be induced with artificial activation of the cortical granules by calcium ionophore (Calcimycin A23187). **d and e,** Inhibiting F-actin reorganization with cytochalasin does not block Dsh puncta formation after cortical granule activation. **f,** Inhibiting microtubules polymerization with chochicine has no effect on Dsh puncta formation.

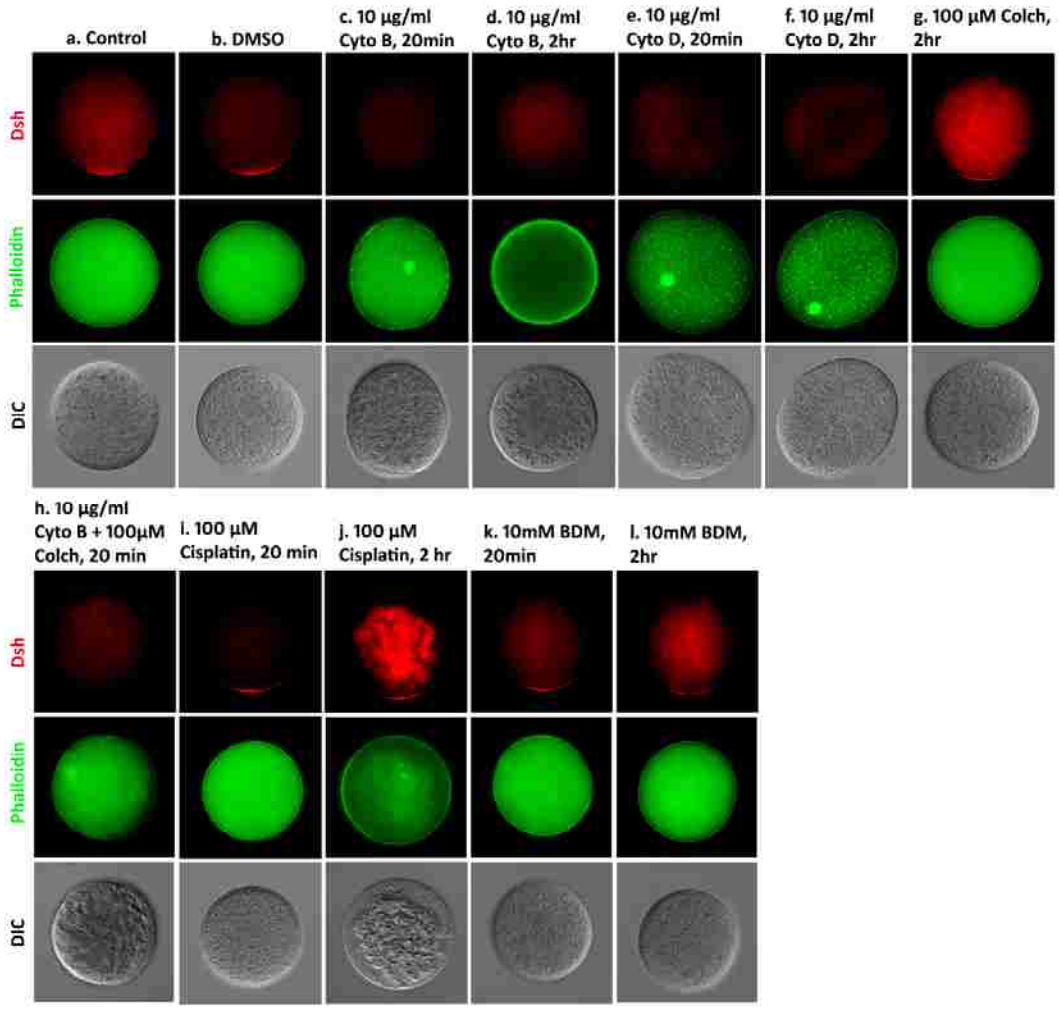

Figure 3.5 Dishevelled protein is indirectly anchored to the cortex by microfilaments. The eggs were collected from *S. purpuratus*, immunostained with anti-Dsh antibodies and viewed with a fluorescent microscope. **a,** The control shows Dsh (Red) localization at one pole of the egg. **b,** DMSO was used as the carrier for all drugs. Staining of Dsh shows DMSO does not affect Dsh localization. **c and e,** Dsh localization was abolished in eggs treated with 10 µg/ml cytochalasin B or D for 20 minutes, washed and incubated in FSW for 2 hours, showing Dsh localization cannot be recovered. **d and f,** Dsh localization was abolished in eggs treated with 10 µg/ml cytochalasin B or D for 2 hours. **g,** Eggs treated with 100 µM colchicine for 2 hours showed no effect on Dsh localization. **h,** Dsh localization was abolished in a recovery experiment. Eggs were treated with both 10 µg/ml Cyto B and 100 µM Colchicine for 20 minutes, washed and incubated for 2 hours. Dsh localization was not recovered. **i and k,** Eggs were treated

with either 100 µM cisplatin or 10 mM BDM for 20 minutes then washed away and incubated for 2 hours. Dsh localization was not affected. **j and l**, Eggs were treated with either 100 µM cisplatin or 10 mM BDM for for 2 hours. Dsh localization was not affected. Phalloidin was used to stain F-actin as control to examine the effect of cytochalasin.

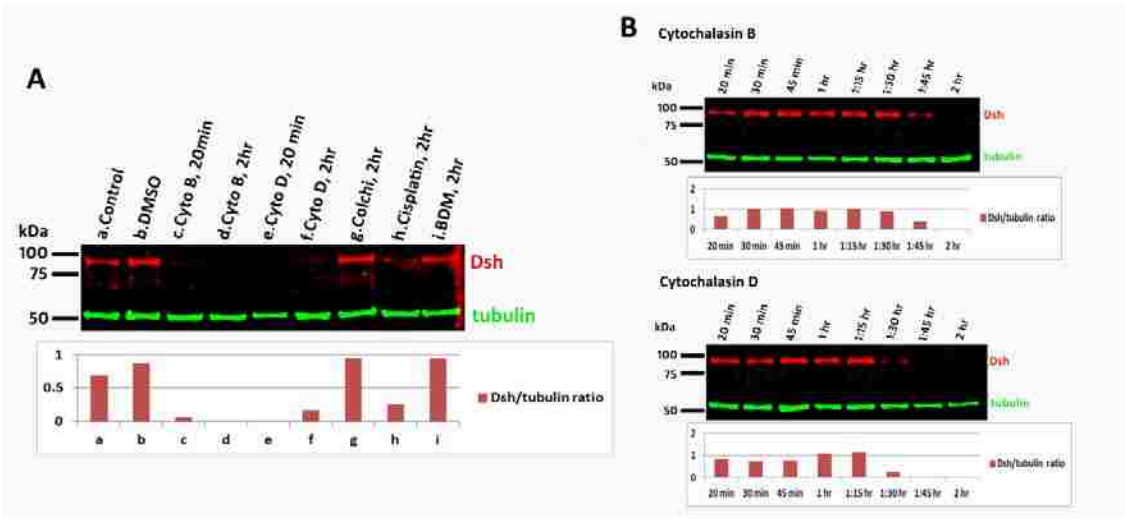

Figure 3.6 Dishevelled (Dsh) protein degrades after cytochalasin treatment. The protein samples were collected from *S. purpuratus* eggs and examined by Western blot analysis. **A. a,** The control shows the primary Dsh (red) band around 90 kDa. **b,** DMSO was used as the carrier for all drugs. DMSO does not affect Dsh. **c and e,** Dsh expression was abolished in eggs treated with 10 µg/ml cytochalasin B or D for 20 minutes, washed and incubated in FSW for 2 hours, showing Dsh cannot be recovered. **d-f,** Dsh protein was degraded in eggs treated with 10 µg/ml cytochalasin B or D for 2 hours. **g,** Eggs treated with 100 µM colchicine for 2 hours showed no effect on Dsh expression. **h and i,** Eggs treated with 100 µM cisplatin or 10 mM BDM had no effect on Dsh protein. Tubulin (green) was used as a loading control. **B.** Eggs were either treated with cytochalasin B or D for 5 minutes then washed away. Dsh protein degradation was monitored by Western blot analysis. Dsh protein degradation can be observed starting at 1:45 hr in cytochalasin B treated eggs. In cytochalasin D treated eggs, Dsh protein degradation can be observed starting at 1:30 hr. Graphs below the Western blot reflect Dsh protein quantity normalized by tubulin.

Chapter IV: The Role of Axis Inhibition Protein (Axin) in Animal-Vegetal Axis Patterning in Sea Urchin Embryos

BACKGROUND

It is known that the cell fates along the AV axis in a sea urchin embryo are first established by the Wnt/β-catenin pathway (Wikramanayake et al., 1998; Logan et al., 1999). One of the most interesting questions in understanding the localized activation of the endomesodermal gene regulatory network at the vegetal pole is: What is the maternal mechanism that regulates entry of β-catenin into the nuclei of vegetal pole blastomeres? In 2004, Weitzel, et al., showed that ß-catenin::GFP protein is nuclearized throughout the embryo initially, but over time, nuclear β-catenin is degraded in animal blastomeres and stabilized in vegetal blastomeres. Alternatively, the question can be asked: what are the maternal factors that stabilize β-catenin at the vegetal pole and the maternal factors that negatively regulate β-catenin in the animal pole blastomeres? A key regulatory mechanism of the Wnt/β-catenin pathway is the regulated proteolysis of the transcriptional co-activator β-catenin via the GSK-3β destruction complex. The main components of this destruction complex includes three major proteins: a β-catenin degradation enhancing protein, adenomatous polyposis coli (APC); an enzyme that phosphorylates β-catenin to target it for degradation, glycogen synthase kinase 3β (GSK-3β); and a multidomain scaffold protein that assembles the destruction complex, axis inhibition protein (Axin) (reviewed in (Wallingford and Habas, 2005)). In the absence of the Wnt ligand, cytosolic β-catenin is constitutively phosphorylated by GSK-3β and targeted for degradation (Figure 1.5a). Upon Wnt stimulation through the LRP and Frizzled receptors, Dsh disassociates the GSK-3β destruction complex through the

recruitment of Axin, leading to the cytosolic accumulation of β-catenin and causing it to translocate into the nucleus to activate downstream target genes (Figure 1.5b). In the previous chapters, my work on Dsh revealed a novel cortical domain that locally activates endomesoderm specification at the vegetal pole in the sea urchin embryos. Thus, an outstanding remaining question is: What are the negative factor(s) that actively regulates β-catenin at the animal pole?

Several lines of evidence suggest that Axin plays a key role in mediating the stability of the β-catenin molecule. First of all, in the vertebrate systems, the inhibition of the GSK-3β complex critically depends on the interaction between Axin and Dsh proteins via the DIX domain in both proteins (Schwarz-Romond et al., 2007; Zeng et al., 2008; Fiedler et al., 2011). Overexpressing Dsh in cells inhibits the GSK-3β complex and thus activates the Wnt/β-catenin pathway (He et al., 1995). Secondly, APC requires Axin to downregulate β-catenin. APC without the Axin binding site is inactive (Kawahara et al., 2000). In contrast, Axin mutants lacking the APC binding domain (RGS) are still able to regulate β-catenin when overexpressed (Itoh et al., 1998; Yamamoto et al., 1998). Moreover, increasing the expression of Axin in cancer cells that lack APC restores the activity of the destruction complex, suggesting that APC is only essential when Axin levels are limiting (Lee et al., 2003). These data suggests that Axin plays a crucial role in the destruction complex. Third, GSK-3β is sufficient and required for the normal development of the sea urchin embryo (Emily-Fenouil et al., 1998). Overexpressing GSK-3β in sea urchin embryo blocks endomesoderm formation, giving an “animalized phenotype”. Blocking GSK-3β function by injecting a dominant negative construct produces a “vegetalized” phenotype. Moreover, a recent study by Weitzel et al. (2004)

showed that GSK-3β is important for regulating nuclear β-catenin. When overexpressing dominant negative GSK3β with β-catenin::GFP, the GFP signal is seen in the nuclei of all blastomeres. These data together suggest that the GSK3β destruction complex plays a role in regulating the AV axis in early sea urchin embryos. Interestingly, overexpressing Dsh in the animal half of the embryo does not induce ectopic gut, suggesting that Dsh cannot disrupt the GSK3β destruction complex at the animal pole (Weitzel et al., 2004). Thus, how the AV axis is specified by the GSK-3β destruction complex in the sea urchin embryo is still unclear, and studying Axin might shed light into this mystery. While the role of Axin in specifying the dorsal-ventral axis in the zebrafish and frog is well understood (Heisenberg et al., 2001; Kofron et al., 2001; Jho et al., 2002; Luo and Lin, 2004; Clevers, 2006), the role of Axin in patterning the embryo along the AV axis has not been studied. Functional studies are needed to establish whether Axin is required for AV axis patterning in sea urchin embryos, and to test when and where in the embryo it carries out its function.

The axis inhibition protein (Axin)

Axin was first identified as a product of the mouse *Fused* (*Fu*) gene (Zeng et al., 1997). The disruption of Axin leads to duplication of the dorsal-ventral axis and embryonic lethality (Zeng et al., 1997). This phenotype, was the clue that led to the suggestion that *Fu* may play a role in the specification of the embryonic axis 60 years ago (Gluecksohn-Schoenheimer and Dunn, 1948). To date, Axin is very well characterized in vertebrates (Luo and Lin, 2004). Axin protein contains four domains that are critical for its function in regulating Wnt/β-catenin pathway (Figure 4.1): an RGS (Regulators of G protein

signaling) domain that binds the APC protein, a GSK3β interacting domain (GID), a β-catenin binding site, and a carboxy-terminus DIX domain that regulates the heterodimerization of Axin and Dsh (the DIX domain in Axin is named DAX to differentiate this DIX domain from the Dsh DIX domain). It is also worth noting that the RGS domain in Axin is too divergent to be recognized by Gα subunits (Luo and Lin, 2004) and DAX domain is too divergent to be recognized by the anti-Dsh-DIX antibody made against Dsh. Moreover, a recent study in cells suggests that Axin is a concentration-limiting component of the destruction complex, and stabilizing Axin by a drug (XAV939) stimulates β-catenin degradation (Lee et al., 2003; Huang et al., 2009).

In this chapter, my studies demonstrated that Axin plays a key regulatory role in patterning the AV axis in the early sea urchin embryo. Combining reverse genetics, molecular and cell biological approaches I show that Axin is both required and sufficient for endomesoderm specification. Knockdown of Axin by a translational blocking morpholino antisense oligonucleotide expands endoderm specification, giving rise to a "vegetalized" phenotype. Conversely, overexpression of Axin blocks endomesoderm formation producing a classic "animalized" phenotype. Moreover, I found *Axin* mRNA and a specific form of the protein are both removed from the most vegetal cells where the Wnt pathway is activated. These results provided new evidence to show that Axin, a multidomain scaffold protein, is a crucial regulatory component that antagonizes Wnt/β-catenin signaling, hence playing a key role in AV axis patterning in the early embryo.

MATERIALS AND METHODS

Phylogenetic analysis and Axin protein sequences

The Axin protein sequences of various species were collected from National Center for Biotechnology Information (NCBI) genomic resources (http://blast.ncbi.nlm.nih.gov/Blast.cgi) to construct a phylogenetic tree. Accession numbers of all sequences used for constructing the tree are as follow: CePry1, *Caenorhabditis elegans* PRY-1 protein (ref_NP_493474.2); Dm, *Drosophila melanogaster* (gi_4582984); Am, *Apis mellifera* (western honey bee) (gi_328784528); Aq, *Amphimedon queenslandica* (sponge)(gi_308194285); Nv, *Nematostella vectensis* (sea anemone)(gi_156395049); Ch, *Clytia hemisphaerica* (hydroid)(gi_170517034); Hm, *Hydra magnipapillata* (gi_221132423); Sk, *Saccoglossus kowalevskii* (Acorn worm, hemichordate)(ref_NP_001158475.1); Lv, *Lytechinus variegates* (sea urchin) (gi_48391468); Sp, *Strongylocentrotus purpuratus* (gi_72016153); Bf, *Branchiostoma floridae* (lancelet, chordate)(ref_XP_002603590.1); Dr, *Danio rerio* Axin 1 (gi_7229078), DrAxin 2 (gi_18858325); Hs, *Homo sapiens* Axin1 (gi_2252820), Axin 2 (gi_195927059); Mm, *Mus musculus* axin 1 (gi_2252816), axin 2 (gi_6653586); Xl, *Xenopus laevis* Axin 1 (gi_147906051), XlConductin, Axin2 (gi_147900983); SpDsh, *S. purpuratus* Dishevelled (unpublished, kindly provided by Gary Wessel, Brown University).

Protein alignments were carried out using ClustalX and saved as nexus files. Phylogenetic trees were generated using MrBayes v.3.1.2 with the mixed method, a convenient way of estimating the fixed-rate model for the amino acid sequence data instead of specifying it prior to the analysis. The analysis was run for 100,000

generations and node probability was calculated after a burn-in of 2,500 generations. The final trees were displayed with TreeView X and saved as gif files and colored by Adobe Photoshop (Adobe Systems Inc.).

Embryonic expression and RT-PCR

S. purpuratus Axin (SpAxin) was obtained by RT-PCR using oligonucleotides designed against the SpAxin sequence (gi_72016153, also available on SpBase (http://www.spbase.org/SpBase/index.php)) from cDNA of mixed stage embryos. The primer sets used for RT-PCR, and *in situ hybridization* probes were:

SpAxin01-F: TAATACGACTCACTATAGGGAGCGTCAAGAGTGGTAAGC

SpAxin01-R: AATTAACCCTCACTAAAGGGTCGGTTGGAGGTAG

The final SpAxin product was 1017 bps. No alternatively spliced forms are found in the sea urchin.

Axin is degraded by Tankyrase after the activation of the Wnt/β-catenin pathway (Huang et al., 2009). To investigate if Tankyrase is expressed in the early sea urchin embryo, Tankyrase sequence (XP_001186587) was obtained and the expression investigated using the primers listed below:

SpTNK01-F: TAATACGACTCACTATAGGGCAATCCGTGAGCATCGTG

SpTNK01-R: AATTAACCCTCACTAAAGGGCGCTTGTATCCGTCTTCC

The final SpTNK product was 1013 bps.

In situ hybridization

Different stage embryos were collected as previously described (Ref?). Fixation was carried out overnight at 4°C in a mixture of 4% (w/v) paraformaldehyde (PFA), 32.5% (v/v) filtered ASW, 32.5mM MOPS pH 7.0, 162.5 mM NaCl, and stored at -20°C. The sense and anti-sense Axin probes were used at a final concentration of 0.1 ng/μL. A direct target of the Wnt/β-catenin pathway in sea urchin development, *Blimp 1* (Accession number: HQ322502) probe was used to assay the overexpression and knockdown effects of Axin at a final concentration of 0.5 ng/μL. *In situ* hybridization using digoxigenin-labeled probes was performed as previously described (Bince et al., 2008).

Preparation of anti-axin polyclonal antibody

To investigate the spatiotemporal expression pattern of the Axin protein, affinity-purified anti-axin polyclonal rabbit antibodies were made against a short sequence in the RGS domain (NH_2-CMVPMMPRQLGSVPEDLSGS-COOH) of Axin protein (Figure 4.1). Antibodies were synthesized by Bethyl Labs (Montgomery, TX). To test the specificity of the antibodies, a preadsorption assay was performed by incubating the antibody with the peptide (provided by Bethyl labs) at a 10 fold molar excess for one hour at room temperature prior to incubating with the samples either for immunostaining or Western blot analysis. The *S. purpuratus* axin (SpAxin) protein is predicted to be 855 amino acids in length, and the molecular size is estimated to be approximately 96 kDa.

Western blot analysis

Samples were collected and treated as previously described. Immunoblots were probed with rabbit anti-SpAxin antibody (1:750) and mouse anti-tubulin (1:10,000) (Developmental Studies Hybridoma Bank, E7). Blots were detected by IRDye 680 (1:15,000) and IRDye 800 (1:15,000) secondary antibodies (LI-COR, Odyssey) respectively.

Immunostaining and image analysis

Embryos were fixed and stained as previously described (Wilt and Benson, 2004). Samples were incubated with rabbit anti-SpAxin antibody (1:500) for an hour at room temperature. Following this the samples were rinsed and incubated in secondary antibodies conjugated to AlexaFluor 568 (Invitrogen) for 45 minutes at room temperature. DAPI (1:1,000, Invitrogen) and fluorescent phalloidin (3:100, Invitrogen) were added at the end of 45 minutes and incubated for another 15 minutes before rinsing in buffer. Stained eggs and embryos were observed using a Leica SP5 scanning confocal microscope. Captured images were analyzed with Fiji (Image J, NIH) and the figures were prepared using Adobe Photoshop (Adobe Systems Inc.).

Cytochalasin D treatment

Studies in sea urchin embryos have shown that the cytoskeletal microfilaments are retracted from the micromeres at the 16-cell stage (Schroeder, 1980a), and Axin is known to bind to microfilaments (Luo and Lin, 2004). To test if the removal of Axin is

regulated by the cortical microfilaments, 8-cell stage embryos were stripped of the fertilization envelope and treated with 1 μg/μl of cytochalasin D at 15°C for 30 minutes (Cytochalasin D is reversible). To remove the cytochalasin D, the embryos were then washed three times in ASW, each time for five minutes, and left in the incubator for further development. Embryos at the 16- and 32-cell stages were collected for immunostaining by anti-Axin antibody and Alexa Fluor fluorescein phalloidin (Invitrogen).

Lithium chloride (LiCl) treatment

It is well known that lithium induces nuclearization of β-catenin by inhibiting GSK-3β activity (Phiel and Klein, 2001). Moreover, the stability of Axin protein decreases in cells treated with LiCl (Yamamoto et al., 1999). To examine if the stability of Axin protein in sea urchin embryos is affected by lithium, 1 M LiCl was added to a final concentration of 30 mM. Embryos were stripped of the fertilization envelope and cultured for collection at 8-cell, 16-cell, 60-cell, hatching blastula stages for Western blot analysis. Phenotypes were observed and recorded at 24 hours post fertilization (hpf), 48 hpf, and 5 day post fertilization using a Zeiss Axiovert 200 inverted microscope mounted with a AxioCam ICc1 or AxioCam MRm camera.

XAV939 treatment

Recent reports suggest that Axin is the concentration-limiting factor in regulating the efficiency of the GSK-3β destruction complex of β-catenin (Lee et al., 2003). To test if the endogenous pool of Axin is sufficient for β-catenin degradation, XAV939, a drug that

stabilizes Axin by inhibiting tankyrase was used (Huang et al., 2009). Stock solution was made to 20 mM in DMSO. Final concentrations of 10, 20, 25, 30, 40 μM were tested. Among all tested concentrations, 25 μM was the best final concentration tested that gave an animalized phenotype with a good survival rate. Concentrations below 20 μM did not produce any animalized phenotypes. Embryos were collected and recorded at 24 and 48 hpf by a Zeiss Axiovert 200 microscope mounted with a AxioCam ICc1 or AxioCam MRm camera.

mRNA synthesis and microinjection

For preparing mRNA for microinjection experiments, cDNAs were subcloned into the pCS2+ vector, including SpAxin::GFP, SpAxinΔRGS::GFP, SpAxinΔGID::GFP, SpAxinΔCAT::GFP (CAT: β-catein binding site), SpAxinΔDAX::GFP (Supplementary figure 4.1). The constructs Axin L396Q mutant (*masterblind*, mutant in zebrafish), CAAX-GID, CAAX-GID-LP were kindly provided by Xi He (Harvard Medical School, MA) (Zeng et al., 2008). GFP mRNA was used as the control. All plasmids was linearized with NotI and served as templates to generate 5′ capped mRNA using the SP6 mMessage mMachine Transcription Kit (Ambion, Austin, TX). The average mRNA yield was 1.5 μg/μl from 2 μg of DNA template. Injection solutions consisted of 40% glycerol and RNase-free, sterile water at the final concentrations: 0.1-0.5 μg/μl SpAxin::GFP mRNA, 0.25 μg/μl SpAxinΔRGS::GFP mRNA, 0.25 μg/μl SpAxinΔGID::GFP mRNA, 0.25 μg/μl SpAxinΔCAT::GFP mRNA, 0.25 μg/μl SpAxinΔDAX::GFP mRNA, 0.25 μg/μl Axin L396Q mRNA, 0.25 μg/μl CAAX-GID mRNA, 0.25 μg/μl CAAX-GID-LP mRNA, 0.3 μg/μl Xl-activated-β-catenin and 0.25

µg/µl GFP mRNA. Fertilized *S.purpuratus* and *L. pictus* eggs were injected as described (Bince and Wikramanayake, 2008) . For each experiment, more than 250 embryos were injected per construct, and the experiments were repeated at least three times. No phenotype difference was observed between *S. purpuratus* and *L. pictus* embryos. The majority of the experiments were performed in *S. purpuratus* for consistency of analyses.

Morpholino injection

Morpholino antisense oligonucleotides (MASO) were obtained from Gene Tools, LLC (Philomath, OR, http://www.gene-tools.com/). The sequence of the morpholino oligonucleotide was directed against the 5' end of the *Axin* transcript oligonucleotides. SpAxin MO: 5'-TATACACTTCTAGACTCATGATGGC-3'. The oligonucleotide sequence spans the start codon from the 5'UTR. The morpholino oligonucleotides were dissolved in nuclease-free water (Ambion) at the stock concentration of 1 mM and used at a range of final concentrations from 100-500 µM SpAxin MO mixed with 40% glycerol and 0.5 µg/µl fluorescein dextran. The negative control was a standard control of random morpholino oligonucleotide sequence (5'-CCTCTTACCTCAGTTACAATTTATA-3') provided by Gene Tools and injected at the same concentration range. Injection of the control oligonucleotide at the concentrations used did not affect sea urchin embryo development. For each experiment, more than 250 embryos were injected per construct, and the experiments were repeated at least three times. To examine the effect of the Axin MASO on Axin protein levels, 750 uninjected embryos, control morpholino injected embryos, and Axin MASO were collected for Western blot analysis respectively.

RESULTS

Phylogenetic analysis of sea urchin Axin

The *Axin* gene was first identified from the characterization of the *Fused* locus in mouse. The loss-of-function of this gene leads to a dramatic axis duplication phenotype (Zeng et al., 1997). Since then, Axin has been extensively studied in animals from chordates (human, mouse, zebrafish, frog) to protostomes (fruit fly (*Daxin*), nematodes (*CePry1*)) (Hamada et al., 1999; Hedgepeth et al., 1999a; Hedgepeth et al., 1999b; Heisenberg et al., 2001; Kofron et al., 2001; Korswagen et al., 2002). Studies from the chordates identified two vertebrate Axin genes, Axin 1 and Axin 2. Although both act as negative regulators, and are functionally equivalent in vivo, Axin 1 is found to be constitutively expressed, while Axin 2 (also called Conductin, or Axil) is induced by Wnt/β-catenin signaling and acts in a negative feedback loop (Yan et al., 2001; Jho et al., 2002; Lustig et al., 2002). Protein sequence analysis of 15 species from Human to sponge by SMART program (http://smart.embl-heidelberg.de/) suggests that the protostome Axins are mostly missing the β-catenin binding site. Those include three Axin sequences from Cnidarians, *Nematostella vectensis*, *Hydra magnipapillata*, *Clytia hemisphaerica*; one sponge, *Amphimedon queenslandica*, and a nematode, *C. elegans*. Axin sequence from *Ciona intestinalis* is incomplete and is highly diverged when compared to the other Axin sequences, thus was omitted from the final analysis. The *S. purpuratus* Dsh sequence was used as an outlier to root the phylogenetic output because of a shared DIX domain.

My analysis shows that, the deuterostome Axins are clustered together, and the vertebrate isoforms Axin 1 and Axin 2 are further separated into different clusters (Figure 4.2). Moreover, with *B. floridae* Axin at the base of the chordate Axin, it suggests that

the duplication of the Axin occurred in the evolution of chordates, before the lancelet lineage diverged from the vertebrates. Interestingly, in *C. elegans*, although the Axin-like protein (PRY-1) contains RGS and DAX domains and lacks a β-catenin binding domain, expressing *pry-1* rescues the zebrafish Axin1 mutation masterblind (Korswagen et al., 2002). This result suggests that *pry-1* can functionally interact with vertebrate destruction complex components without a direct interaction with β-catenin. Furthermore, when overexpressing the sea urchin *Axin*, SpAxin::GFP, in sea anemone embryos (*N. vectensis*), endoderm specification is blocked (unlike bilaterians, non-bilaterians lack mesoderm). This result suggests that the function of Axin in the Wnt/β-catenin pathway is evolutionarily conserved (Kumburegama et al., 2011).

Axin is expressed maternally and dynamically throughout embryogenesis

RT-PCR analysis indicated that *Axin* is maternally expressed and is expressed throughout embryogenesis (Figure 4.3A). To examine the spatial distribution of Axin mRNA, I performed whole mount *in situ* hybridization (Figure 4.4B). Axin transcripts are expressed ubiquitously in the egg and 2-cell stage embryos. However, according to transcriptome data collected by our lab, Axin transcripts are 3.32 fold enriched in the cortex compared to the entire egg (Unpublished, collected by Lingyu Wang). Interestingly, at 16 and 32-cell stages embryos, *Axin* mRNA is expressed at low levels in the micromeres compared to the rest of the embryo, suggesting that *Axin* might be actively removed from the cells where the Wnt/β-catenin pathway is activated (Figure 4.4B, c and d). Moreover, *Axin* mRNA is expressed in the vegetal plate at early and late gastrula (Figure 4.4B, e and f).

To further investigate the function of Axin during early sea urchin development, an anti-Axin antibody was made to investigate the spatiotemporal localization of the protein. The timing of changes in Axin protein expression during development should be suggestive of its early role in development. Using the affinity purified Axin antibodies on Western blot analysis showed that two protein bands are expressed throughout embryogenesis, and the top band at 100 kDa is missing from the micromeres (Figure 4.4A). Pre-adsorption tests show that both bands (Between 75 and 100 kDa) can be competed by pre-incubation with the peptide used as the antigen indicating that the staining pattern is specific. The Axin antibodies were also used to immunostain embryos to examine where the protein functions. First, Axin protein is found in the cortex of unfertilized eggs with no distinct localization pattern (Figure 4.4B, a). Moreover, an optical section of a 2-cell stage embryo suggests that the protein is enriched at the membrane (Figure 4.4B, b). Most interestingly, at the 16 and 32-cell stage, staining results show that the Axin protein is expressed at low levels or is absent from the micromeres (Figure 4.4B,c and d). This result suggests a novel mechanism for Wnt /β-catenin signaling where one critical negative regulator of the pathway is removed from a subset of cells in the embryo to activate this pathway. Classical studies in sea urchin embryos have shown that the cytoskeletal microfilaments are retracted from the micromeres at the 16-cell stage (Schroeder, 1980a). In addition, Axin is known to interact with the microfilaments (Luo and Lin, 2004), and thus it is possible that Axin protein is removed from the micromeres during their formation, thereby removing a negative regulator of β-catenin from these cells. To test this possibility, I inhibited the cortical-actin retraction by treating the embryos with a low dose of a reversible F-actin

inhibitor at 8-cell stage for 30 minutes. The drug was then washed away, and the embryos were allowed to develop until the 16- or 32-cell stage. Results showed a striking enrichment of the cortical filamentous actin in the micromeres, but the Axin protein was still removed from these cells (Figure 4.5). It is also important to note that Wnt stimulation regulates the stability of Axin protein and a decrease in cytoplasmic levels of Axin has been documented (Komiya and Habas, 2008). In sum, the results suggest that the Axin mRNA and one form of Axin protein is removed from the micromeres by a non microfilament-dependent manner to locally activate the Wnt/β-catenin pathway.

Axin is required for negative regulation of Wnt/β-catenin signaling along the AV axis

To assess whether Axin is required for regulation of endomesoderm specification along the AV axis, I carried out loss-of-function studies using morpholino antisense oligonucleotides (MASO). Since Axin is a negative regulator of the Wnt pathway, knocking down Axin should give a phenotype consistent with an expansion of endomesoderm. Strikingly, microinjection of Axin MASO at concentrations ranging from 100-500 μM into *S. purpuratus* eggs gave a "light bulb" phenotype (Figure 4.6A, f). When injecting the morpholino at the lowest concentration, only 50% of the injected embryo gave a phenotype. Injecting at a higher dose of the Axin MASO does not give a more severe phenotype, but a higher percentage of the phenotype is observed. At 48 to 72 hpf, the exogastrulated enlarged gut starts to undergo regionalization into a tripartite structure, and sometimes an even more extensive regionalization is observed (Figure

4.6A, g and h). Moreover, the exogastrulated enlarged gut reflects overdevelopment of the endoderm, probably at the expense of the ectoderm. The animal pole becomes the largest sphere and is decorated with pigment cells and encloses skeletal spicules, which are characteristics of ectoderm. This phenotype is reminiscent of a "vegetalized" phenotype caused by treatment of lithium chloride (LiCl) (Figure 4.6A, i-k). Moreover, endomesoderm cell fate specification in Axin MASO injected phenotype is confirmed with endodermal and mesodermal markers, Endo I and 1d5 (McClay et al., 1983; Wessel and McClay, 1985). Endomesoderm expression in the Axin MASO injected embryos are similar to the vegetalized phenotype previously described (Figure 4.9 e-h) (Nocente-McGrath et al., 1991). This is surprising since I did not expect the knockdown of Axin could produce such strong vegetalized phenotype because of the maternal Axin protein seen in the Western blot analysis and immunostaining. To investigate the knockdown effect at the protein level, Axin expression was monitored by Western blot analysis in morpholino injected embryos and lithium treated embryos. Axin protein level in Axin MASO injected embryos compared to the control (either uninjected embryos or control morpholino injected embryos) showed little or no difference in protein expression levels (Figure 4.6B). In contrast, in LiCl treated embryos collected at various stages, the top band is abolished during development (Figure 4.6C). It has been shown that the stability of Axin protein decreases in cells treated with LiCl (Yamamoto et al., 1999). What this suggests is that the SpAxin MASO is blocking the synthesis of Axin proteins, while lithium treated embryos inhibits GSK-3β and targets one pool of Axin for degradation, both giving a similar phenotype by disrupting the function of the Axin protein. Moreover,

in Axin knockdown experiments, the lower band was never effected suggesting that this form of Axin might not have a function in the Wnt/β-catenin signaling pathway.

To confirm that the vegetalized phenotype is caused by the knockdown of Axin, thus overexpressing the Wnt/β-catenin pathway, I examined the expression of *blimp 1*, a direct target of Wnt/β-catenin signaling. *In situ* hybridization of *blimp 1* in Axin MASO injected embryos showed an expanded expression from the vegetal pole blastomeres to the entire embryo at early blastula, although the transcripts seem to be expressed at a lower level (Figure 4.8). These results suggest that Axin plays a negative role in the Wnt/β-catenin pathway, thus knocking down Axin expression mimics the effect of lithium.

Axin is sufficient for blocking endomesoderm formation

The observation of Axin immunostained 16-cell and 32-cell stage embryos suggest that the Axin protein is removed from the most vegetal micromeres as part of a mechanism to activate Wnt/β-catenin signaling. In addition, it is known that overexpression of Axin in APC knockout cancer cells restores the activity of the destruction complex, indicating that APC is only essential when Axin levels are limiting (Lee et al., 2003). Thus quantitatively, Axin appears to be a limiting factor and may be the key scaffolding molecule that promotes the rapid assembly and disassembly of the destruction complex. To test whether Axin is sufficient to block endomesoderm specification, I carried out overexpression studies by mRNA injection. Axin mRNA was injected at the concentration range from 0.1-0.5 μg/μl. Axin overexpressed embryos gave a range of animalized phenotypes that resembled phenotypes obtained from the depletion of β-

catenin by cadherin, or blocking Dsh function by DIX (Figure 4.7 and Supplementary figure 4.3d). In most cases, the morphology was an epithelium thickened on the animal pole with elongated cilia, indicating a morphological polarity (Figure 4.7d, e, h and j, 60%, n=250). This epithelium then restricts to the animal pole to form the neurogenic ectoderm at the fifth day (Figure 4.7f). In addition, other animalized phenotypes were also observed where the entire embryo develops into a thin epithelium (20%), or sometimes the embryo would develop into a thickened epithelium (5%). However, the epithelium in both animalized phenotypes would still restrict to one pole eventually, suggesting the AV polarity is not lost in those embryos (Figure 4.7 h-j). Surprisingly, overexpressing a zebrafish Axin mutant (*masterblind*, Axin L396Q) also produced animalized phenotype. Although the leucine residue in the GID is conserved in sea urchin Axin, the injection result suggests that the leucine residue crucial for GSK-3β binding in zebrafish does not function the same way in the sea urchin embryo (Figure 4.10e and Supplementary figure 4.2). Last, *Blimp 1* expression was abolished in Axin overexpressed embryos, suggesting that the Wnt/β-catenin pathway was blocked (Figure 4.8). Moreover, immunostaining by endodermal and mesodermal protein markers in 48 hpf embryos confirmed endomesoderm specification is lost (Figure 4.9i-l). Overall, this suggests that Axin is sufficient to block endomesoderm specification, even at low concentrations.

A recent study in cells has shown that Wnt/β-catenin signaling can be antagonized by stabilizing Axin through inhibition of Tankyrase (TNK), a protein that targets Axin for degradation by PARsylation and ubiquitination (Huang et al., 2009). The function of TNK has also been shown to be evolutionarily conserved in *Drosophila* and zebrafish,

where knockdown or depletion of this protein increased β-catenin levels (Huang et al., 2009). Through RT-PCR analysis, TNK is found to be expressed throughout embryogenesis in sea urchin embryos (Supplementary figure 4.1, performed by Sarah Williams and LingYu Wang). To test if endogenous Axin is sufficient for blocking endomesoderm formation, I applied XAV939, a TNK inhibitor to stabilize the endogenous Axin protein in sea urchin embryos. Final concentrations from 10 to 50 μM was tested on the embryos, and I found that 25 μM is the optimal concentration to produce a good number of healthy animalized embryos (Figure 4.7g). Higher concentrations of the drug led to lethality. This result suggests that *endogenous* Axin is sufficient for blocking endomesoderm specification, and moreover that tankyrase may regulate Axin protein stability in the sea urchin embryos during endomesoderm specification.

Axin mRNA can partially rescue Axin knockdown by SpAxin morpholino

To demonstrate the specificity of the morpholino oligonucleotides directed against *Axin*, I performed a rescue experiment in which I co-injected Axin mRNA with the Axin morpholino. This was possible because the morpholino was designed against the SpAxin sequence that spans across the start codon, and the first 6 nucleotides on the 5' end of Axin constructs were excluded on the Axin cDNA. When SpAxin::GFP (0.25 μg/μl) is co-injected with Axin MASO (250 μM), it gave an animalized phenotype (68%, n=100). Similarly, when zebrafish Axin mutant (*masterblind,* 0.25 μg/μl) is co-injected with Axin MASO (250 μM), it also produced an animalized phenotype (86%, n=100). Injected embryos were monitored by the GFP expression, and no vegetalized phenotype was

found in the injected embryos (Figure 4.10 b-d). This partial rescue which gave an animalized phenotype can be possibly explained by the molar ratio of the mRNA and MASO not being equal, thus causing the knockdown of Axin to be overwhelmed by the overexpressed mRNA. This suggests that the vegetalized phenotype by injecting Axin MASO can be rescued by Axin mRNA expression.

Axin domain analysis

Recent studies on the mechanisms regulating the initiation of Wnt/β-catenin signaling proposed an interesting role for the Axin protein. It was proposed that a Wnt ligand induces Fz-Lrp complex formation and promotes initial Lrp6 phosphorylation via the recruitment of the GSK3β-Axin complex by Dsh protein. The recruitment of the GSK-3β-Axin complex promotes further Lrp6 phosphorylation to activate the Wnt/β-catenin pathway, while proteins like β-catenin, CK1, APC are left in the cytoplasm (Zeng et al., 2008) (Figure 1.5b). Thus, while Axin plays a negative role in down regulating β-catenin in the cytoplasm, it plays a positive role in activating the signaling pathway at the membrane. To determine the key domains of Axin in regulating the Wnt/β-catenin pathway in the early sea urchin embryo, I expressed different Axin deletion constructs by mRNA injection. These include SpAxinΔRGS::GFP, SpAxinΔGID::GFP, SpAxinΔCAT::GFP, SpAxinΔDAX::GFP and Axin L396Q (where the point mutation at amino acid position 396 from a Lysine to glutamic acid abolishes the binding of GSK-3β to the Axin protein) (Supplementary figure 4.1, all constructs were made by Ronghui Xu, and preliminary experiments were performed by Joanna Kobayashi). Overall, injection of all deleted constructs produced animalized phenotypes at different levels. For example, deletion of the RGS domain (APC binding site) and GSK binding domain (GID) had a

weak animalizing effect on the injected embryos when overexpressed. Gastrulation in those injected embryos is significantly delayed for at least 24 hpf compared to the GFP injected control. Moreover, the delay of gastrulation is not due to the decay of the injected mRNA since GFP signal is still observed at those stages. This result suggests that an Axin, APC and GSK-3β complex is required for the negative regulation of β-catenin in early sea urchin embryos. Conversely, deletion of the β-catenin binding site and DAX domain gave strong animalized embryos similar to the phenotype produced by overexpressed wild-type Axin. The result of the β-catenin binding domain deletion construct might suggest that the ability of Axin to reduce cytoplasmic β-catenin levels does not depend on direct binding of β-catenin to Axin. Moreover, studies in cells during development have shown that when Wnt ligands bind to its receptors Lrp and frizzled, the destruction complex composed of Axin, Gsk-3β, and APC is taken apart and Axin is then targeted for degradation by TNK at the cell membrane (Huang et al., 2009). This inhibition critically depends on the interaction between Dsh and Axin through the DIX domain on both proteins respectively (Itoh et al., 2000). The result of the DIX deleted domain construct suggests that the interaction between Dsh and Axin might be crucial for the recruitment of the GSK-3β-Axin complex to the cortex, thus Axin is kept in the cytoplasm to down regulate β-catenin. Lastly, to test if Dsh and Axin work in the same signaling pathway, I co-injected Dsh-DIX::GFP and SpAxin MASO. The dominant-negative construct DIX overexpression inhibits the activation of the Wnt/β-catenin pathway. Knocking down Axin in the DIX overexpressed embryos partially rescued animalized phenotypes to produce skeletogenic mesenchyme cells (Supplementary figure

4.3 d and e). This suggests that Axin might work downstream of Dsh to regulate β-catenin signaling.

DISCUSSION

In this chapter, I have characterized sea urchin Axin, a key scaffold protein in the Wnt/β-catenin pathway that regulates endomesoderm specification along the AV axis. By manipulating the level of Axin in the sea urchin embryo, the cell fate of blastomeres shifted to either more towards the ectoderm (animal pole) or the endomesoderm (vegetal pole), thus generating morphological defects ranging from the most extreme animalized phenotype to the most vegetalized phenotype that was described over a hundred years ago (Herbst, 1892). These results suggest that the normal embryonic patterning along the AV axis relies on Axin expression level.

Axin is required for embryonic patterning along the AV axis in the sea urchin embryo.

Axin has been well studied in vertebrates due to its role in axis formation. Mice lacking Axin function have duplicated axes (Zeng et al., 1997). Moreover, depletion of Axin in zebrafish and frog embryos leads to the overexpression of axial structures, with excessive notochord and head structures and reduced tail and ventral components (Heisenberg et al., 2001; Kofron et al., 2001). Furthermore, although maternal Axin is found to be expressed ubiquitously in the early *Xenopus* embryo, and it was found that localized ventral activity of Axin is critical for the patterning of the embryo (Kofron et al., 2001).

In sea urchins, I predict that Axin is required for maintaining ectodermal cell fate by down regulating β-catenin at the presumptive ectoderm in the veg_1 tier blastomeres (Figure 1.2). Several lines of evidence support this hypothesis. First of all, it has been shown that the specification of individual veg_1 cleavage progeny to become endoderm or ectoderm precursors is correlated with its relative proximity to the adjacent cells. Veg_1 can either be influenced by the underlying veg_2 cells or the overlying mesomere progeny (Figure 1.2) (Ransick and Davidson, 1998). In other words, veg_1 progeny remain plastic with respect to cell fate specification throughout the cleavage period. Knockdown of Axin by MASO expanded early *blimp 1* expression from the localized presumptive mesomeres to almost the entire embryo, including the veg_1 progeny, suggesting the EGRN is activated in those progeny by ectopic activation of Wnt/β-catenin signaling. Secondly, it has been well established that, in normal sea urchin development, the veg_1 tier of the sixth cleavage embryo contributes progeny to both ectodermal lineages and portions of the archenteron (endoderm) (Ransick and Davidson, 1998). The veg_1 lineage progeny in lithium treated embryos were respecified as endoderm (Cameron and Davidson, 1997). Moreover, knockdown of Axin produced a vegetalized phenotype similar to lithium treated embryos, suggesting Axin is required for the correct patterning of ectoderm. Together, these findings suggest that Axin play an essential role in maintaining ectodermal cell fate in the veg_1 tier blastomeres.

Axin is the limiting factor regulating β-catenin signaling in sea urchin embryos.

It has been proposed that GSK-3β might be the key component for the regulation of β-catenin stability along the AV axis for several reasons (Emily-Fenouil et al., 1998;

Weitzel et al., 2004; Ettensohn, 2006). First, degradation of β-catenin during early *Xenopus* and sea urchin embryonic development depends on phosphorylation of β-catenin by the serine-threonine kinase, GSK-3β (He et al., 1995; Yost et al., 1996; Weitzel et al., 2004). Moreover, overexpression of GSK-3β animalizes the embryo, and overexpression of a dominant-negative GSK-3β vegetalizes the embryo by stabilizing β-catenin (Emily-Fenouil et al., 1998; Weitzel et al., 2004). Together, these results suggest that GSK-3β level controls the patterning of the sea urchin embryo by regulating β-catenin (Emily-Fenouil et al., 1998). However, functional studies on the scaffold protein Axin suggest that Axin is the key "limiting factor" for regulating β-catenin signaling in sea urchin embryos. First, although Axin contains no enzymatic property, overexpression of Axin blocks endomesoderm specification. Moreover, knocking down Axin induces ectopic endoderm specification at the expense of ectoderm specification. Because of the limited level of endogenous Axin protein knockdown in morpholino injected embryos, but a strong vegetalized phenotype, I suspect that the morpholino is blocking Axin synthesis at the veg_1 tier progeny, thus accumulating β-catenin to activate endoderm specification. Also, knockdown of Axin should not activate β-catenin ectopically, since GSK-3β should still be present at those blastomeres to regulate β-catenin levels. This suggests that GSK-3β alone cannot function to phosphorylate β-catenin. In addition, when endogenous Axin is stabilized by inhibiting TNK, the embryo becomes animalized, suggesting the localized activation of EGRN depends on a mechanism that requires the degradation of the Axin protein and the endogenous level of Axin is sufficient for restricting nuclear β-catenin levels along the AV axis. This data is further strengthened by the immunolocalization of Axin, which shows Axin is abolished in the micromere progeny. Last, *Axin* mRNA is

expressed at the right time and right place in early stage embryos. While *Axin* is missing from the micromeres at early cleavage stages, it is expressed in the presumptive veg_1 cells. Also, *Axin* is expressed at the vegetal plate in early and late gastrula embryos, right at the boundary of endoderm and ectoderm. On the other hand, GSK-3β mRNA is only expressed in the endoderm at the gastrula (Emily-Fenouil et al., 1998). In sum, this suggests that Axin is the key regulator of Wnt/β-catenin signaling to establish embryonic patterning along the AV axis in sea urchins.

Conclusion and outlook

In this chapter, I establish in the sea urchins, the involvement of Axin in regulating a primary axis (AV) by Wnt/β-catenin signaling. The echinoderms diverged shortly after the protostome-deuterostome separation, suggesting a conserved basis for the negative role of Axin for axial patterning and cell fate specification between invertebrate and vertebrate in deuterostomes. Furthermore, the data in sea urchins also raises the possibility that the ancestral role of Axin was to pattern the AV axis in basal deuterostomes before being co-opted to pattern the dorsal-ventral axis in vertebrates. However, the Axin overexpressing and knockdown embryos would need better characterization by investigating gene expression in all three germ layers. These genes include early markers like Wnt 8, a direct target of Wnt/β-catenin signaling in the micromeres (Wikramanayake et al., 2004) , endomesodermal markers (e.g. *Gsm, Hox11/13b, Notch*), and ectodermal markers (e.g. *FoxQ2* and *six3*) (Yaguchi et al., 2008). The examination of these germ layer markers would give a better picture of how Axin regulates the patterning of the early sea urchin embryos.

The sea urchin embryo has been used for over a hundred years to study the basic embryonic patterning in animals. Although much has been discovered, it was not until the last decade when β-catenin was identified to be the crucial maternal factor for endomesoderm specification that lead to the construction of the endomesoderm gene regulatory network, showing the basic mechanisms of cell specification at a systems level (Wikramanayake et al., 1998; Logan et al., 1999; Davidson et al., 2002). One of the most important questions that remain is: how is endomesoderm specification locally activated at one pole of the embryo? When I started graduate school, it was proposed that β-catenin is differentially stabilized along the AV axis by Dsh and GSK-3β, but the mechanisms that established this polarity were still unclear. Based on my results and previous studies, I would like to propose the following model to explain the endomesoderm specification along the AV axis (Figure 4.11): First, a vegetal cortical domain (VCD) is established during early oogenesis along with the appearance of the microtubule organizing center, setting up an early polarity in the developing oocytes. This VCD then recruits activated forms of Dsh and other maternal factors to the egg vegetal cortex during oogenesis. Second, during the first few cleavage stages, the VCD recruits maternal factors including Dsh. Third, the VCD is then inherited by the most vegetal blastomeres, the micromeres and macromeres, at the 16-cell stage for the localized activation of the EGRN. Following Wnt/β-catenin pathway activation by Dsh, Axin at those blastomeres is targeted for degradation. The veg_1 tier progeny that did not inherit the VCD, became specified to ectodermal cell fates.

Over the past few years, Axin has been shown to be a multidomain scaffold protein, and it is involved in many other pathways, including TGF-β, the c-Jun N-terminal kinase,

and p53 signaling pathways (Luo and Lin, 2004). Recently, a β-catenin independent dorsalization pathway activated by Axin/JNK signaling has been demonstrated in zebrafish development (Rui et al., 2007). Interestingly, in the sea urchin, a Wnt/β-catenin signal, still unknown, from the macromere progeny restricts FoxQ2 expression to the animal plate, allowing the nodal to operate in the future oral ectoderm. It would be interesting to see if Axin/JNK is this unknown signal to be involved in the oral-aboral axis specification in sea urchin embryo.

FIGURES

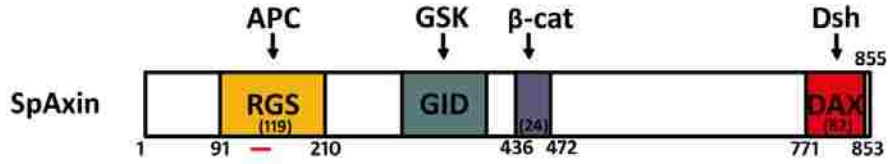

Figure 4.1 The domain structures of the *S. purpuratus* Axin (SpAxin) protein. The SpAxin contains 855 amino acids, harboring structural domains RGS (Regulators of G protein signaling), GID (GSK interacting domain), β-catenin binding domain and DAX (similar to DIX in Dsh protein, but to differentiate DIX domain from the Dsh, DIX domain in Axin is named DAX). Proteins above indicate binding partners to the respective domain. Residue numbers underneath domains denote the domain boundaries. Parentheses in the domains indicate size in amino acids. Red bar indicates the region corresponding to the peptide used as the antigen for generating anti-Axin polyclonal antibodies.

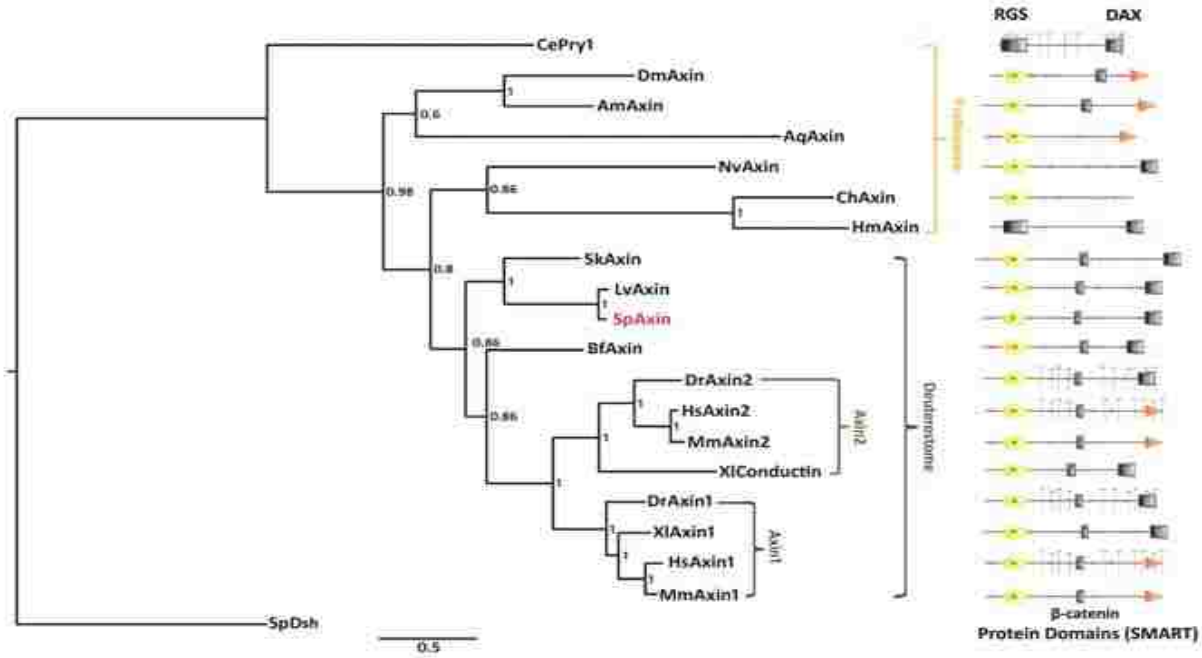

Figure 4.2 Phylogenetic analysis of Axin. Confidence values were calculated using a mixed method. SpDsh, which also contains the DIX domain, is used as an outgroup. Right panel: Protein sequence analyzed by SMART (http://smart.embl-heidelberg.de/) to determine functional domains. From left to right are RGS domain, β-catenin binding domain, and DAX (DIX) domain at the very end. Accession numbers of all the Axin sequences used to generate the tree are indicated in the materials and methods section. CePry1, *Caenorhabditis elegans* PRY-1 protein; Dm, *Drosophila melanogaster*; Am, *Apis mellifera* (western honey bee); Aq, *Amphimedon queenslandica* (sponge); Nv, *Nematostella vectensis* (sea anemone); Ch, *Clytia hemisphaerica* (hydroid); Hm, *Hydra magnipapillata*; Sk, *Saccoglossus kowalevskii* (Acorn worm, hemichordate); Lv, *Lytechinus variegates* (sea urchin); Sp, *Strongylocentrotus purpurartus*; Bf, *Branchiostoma floridae* (lancelet, chordate); Dr, *Danio rerio*; Hs, *Homo sapiens*; Mm, *Mus musculus*; XlConductin, *Xenopus laevis* Axin2; SpDsh, *S. purpurartus* Dishevelled. SpAxin is marked in red.

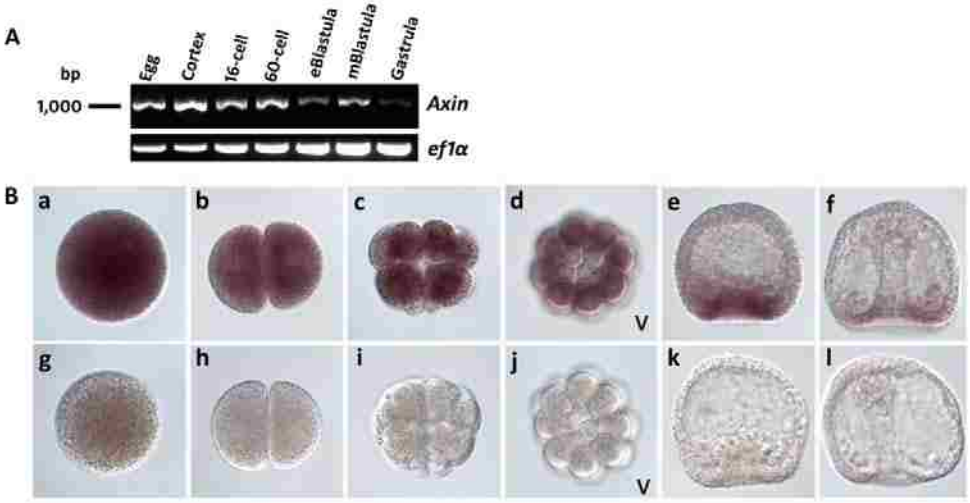

Figure 4.3 SpAxin mRNA is expressed maternally and dynamically throughout embryogenesis. **A,** RT-PCR analysis shows *Axin* is maternally expressed and is expressed throughout embryogenesis. Elongation factor-1 alpha (ef1α) is used as a loading control. **B,** Spatial distribution of Axin mRNA revealed by *in situ* hybridization. **a-f,** anti-sense Axin probe. **a,** Axin is ubiquitously expressed in an egg. **b,** 2-cell stage. **c,** 16-cell stage embryo showing low expression of *Axin* in the micromeres. **d and j,** Vegetal view(v) of a 32-cell stage embryo showing low expression of Axin in the micromeres. **e-f,** Axin mRNA is expressed at the vegetal plate of early and late gastrula embryos. **g-l,** Sense Axin probes are used as the negative control.

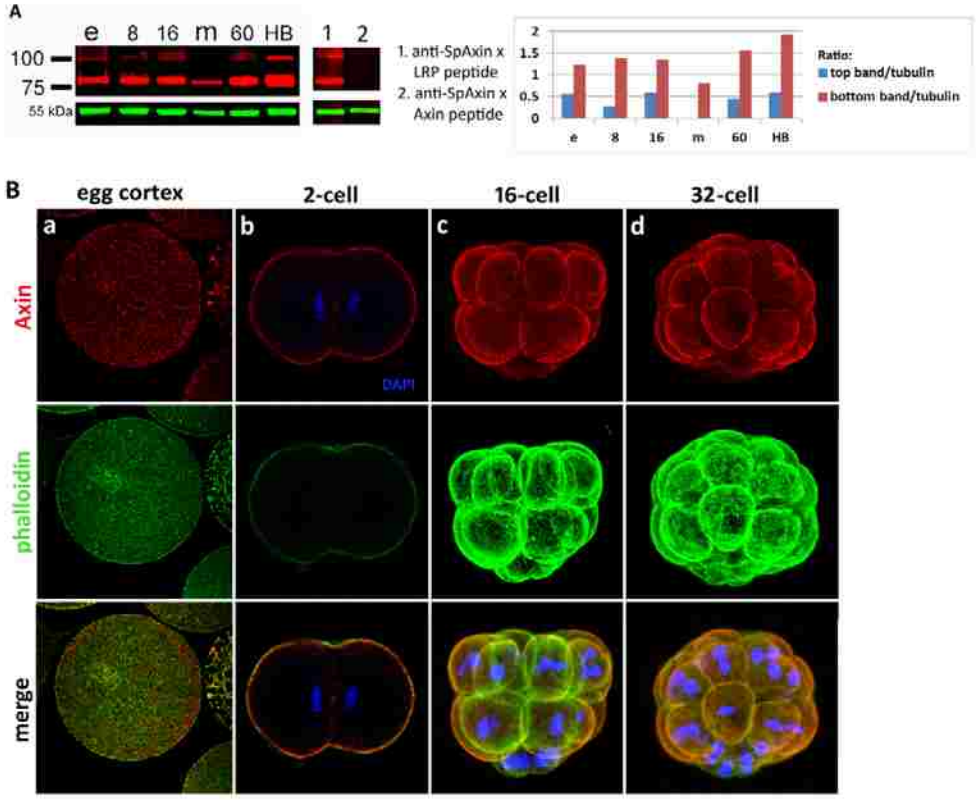

Figure 4.4 Axin protein is expressed maternally and down regulated in the micromeres at the early cleavage stages. A. Western blot analysis shows that there are two major bands of Axin (red), suggesting a possible post-translational modification. The bottom band (~80kDa) is expressed ubiquitously throughout embryogenesis. Top band (~96kDa) is missing from the micromeres (m). Key: e, egg; 8, 8-cell stage; 16, 16-cell stage; m, isolated micromeres; 60, 60-cell stage; HB, hatching blastula. Tubulin (green) is used as a loading control. Pre-adsorption tests: 1. Anti-Axin antibody pre-adsorbed by LRP peptide. 2. Anti-Axin antibody pre-adsorbed by axin peptide. The molecular size of Axin is estimated (according to amino acid sequence) to be approximately 96 kDa. Graph on top right: Quantification of Axin protein expression. Blue: top band (100kDa); Red: bottom band (80kDa). **B.** Confocal images of Axin staining. **a,** Axin protein is localized on the unfertilized egg cortex with no distinct localization pattern. **b,** An optic section of a 2-cell stage embryo showing Axin concentrated on the cell membrane. **c, d,** Axin is cleared from the micromeres in both 16-cell stage and 32-cell stage embryos. Axin (red); F-actin is stained by fluorescein phalloidin (green); DAPI (blue).

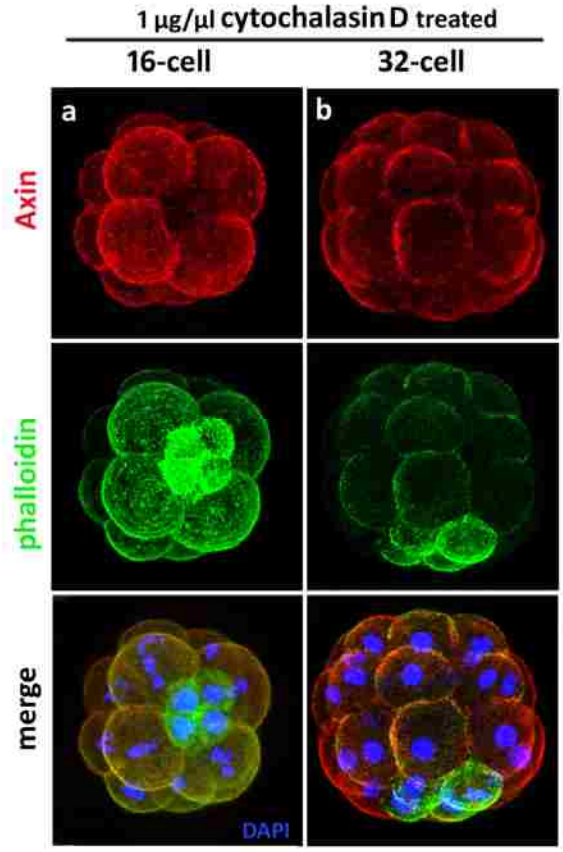

Figure 4.5 Removal of Axin protein in the micromeres is not microfilament-dependent. To test if Axin is removed by cortical-actin retraction in the micromeres, 8-cell stage embryos were stripped of the fertilization envelope and treated with 1 µg/µl of cytochalasin D at 15°C for 30 minutes (Cytochalasin D is reversible). To remove the cytochalasin D, the embryos were than washed 3 times in ASW, each time for 5 minutes, and left in the incubator for further development. 16-cell, 32-cell stage embryos were collected for immunostaining by anti-Axin antibody. **a,** Axin protein expression is still abolished in the micromeres at the 16-cell stage embryo, while cortical-actin failed to retract (F-actin somehow becomes enriched in the micromeres). **b,** Some embryos failed to divide asymmetrically to form macromeres-micromeres pairs at the vegetal pole. As a result, equal size vegetal blastomeres are seen at the vegetal pole and the presumptive micromeres are enriched with F-actin, but no Axin is found in those blastomeres. Axin (Red), Phalloidin (green), DAPI (blue). Controls are collected at the same trial and shown in Figure 4.4.

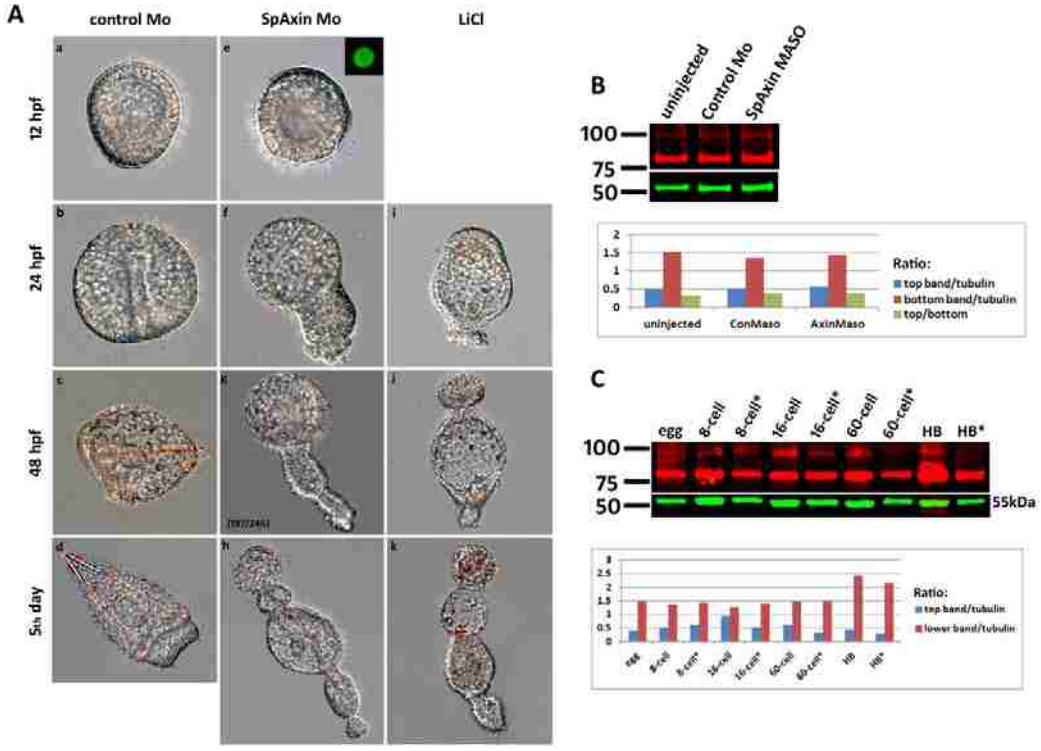

Figure 4.6 Axin is required for negative regulation of Wnt/β-catenin signaling along the AV axis. A, To determine if Axin is required for endomesoderm specification, Axin morpholino antisense oligonucleotides (MASO) were injected to knockdown the protein expression. Randomized morpholino sequence was used as a control (Control Mo). **a-d,** Control embryos developed normally (86/100=86% normal, 14% injection artifact phenotypes, no vegetalized phenotype observed). **e-h,** Axin MASO injected embryos developed a classic "vegetalized" phenotype (187/246=76%, 24% injected artifact phenotypes, no normal embryos observed) regardless of MASO concentration (100-500 μM). Inset figure in **e,** Fluorescein dextran were co-injected with the MASO to trace injection success, all counted embryos display florescence. **i-k,** embryos treated with 25 μM LiCl developed to a classic vegetalized phenotype, displaying a greatly enlarged exogastrulated gut. **B,** Axin protein expression in SpAxin MASO injected embryos was monitored by Western blot at the blastula stage. Axin (Red), Tubulin (green). Result shows no significant difference between the control Mo and SpAxin MASO injected embryos. Graph in B shows quantified protein expression by Axin/tubulin ratio. Blue: 100 kDa band; Red: 80 kDa band; Green: ratio between top band and bottom band are equal between all three samples, suggesting both bands are equally transferred. **C,** To investigate if Axin is degraded after the disruption of the destruction complex by LiCl, 8-cell, 16-cell, 60-cell, and hatching blastula stage embryos were collected to perform an Axin protein analysis by Western blot. Axin in LiCl treated embryos (*) are expressed at lower levels when compared to the controls.

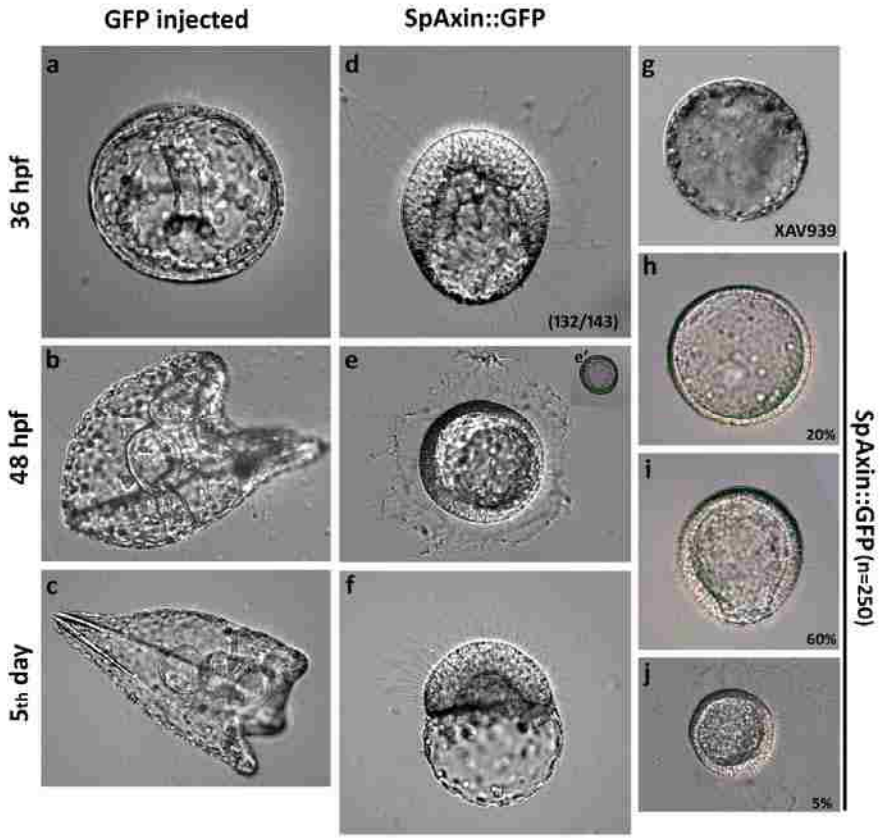

Figure 4.7 Axin is sufficient to block gastrulation. To examine the function of Axin, 0.1-0.5 µg/µl SpAxin::GFP mRNA was injected and assayed for phenotype. **a-c,** GFP mRNA were used as a control for injection, no animalized phenotype were found (176/198=89% normal, 11% injection artifact phenotypes). **d and e,** Axin overexpressed embryos gave a classic "animalized" phenotype (at 0.25 µg/µl, 132/143=92%, the other 8% produced injection artifact phenotypes, all injected embryos were confirmed by GFP expression as in **e'**, a hollow ball of cells which consists almost exclusively animal ectoderm with elongated cilia. **f,** This neurogenic ectoderm restricts to the animal pole as development progresses. **g,** Stabilizing Axin in sea urchin embryos by XAV939 blocks gastrulation, giving a weak animalized phenotype. **h-j,** SpAxin::GFP injected embryos gave a range of phenotypes; A strong animalized phenotype (**h,** 20% of total embryos injected); The most common observed animalized phenotype (**I,** 60% of total embryos injected); A weaker animalized phenotype (**j,** 5% of total embryos injected). n=250.

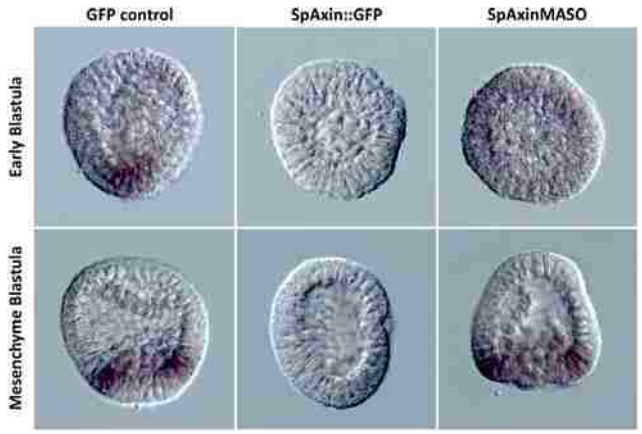

Figure 4.8 *Blimp1* expression is affected by Axin expression. *In situ* hybridization of *Blimp 1* in Axin overexpressing and knockdown embryos. *Blimp 1*, a direct target of the Wnt/β-catenin pathway, is abolished in Axin overexpressed embryos. In contrast, *Blimp1* expression expands in Axin knockdown embryos.

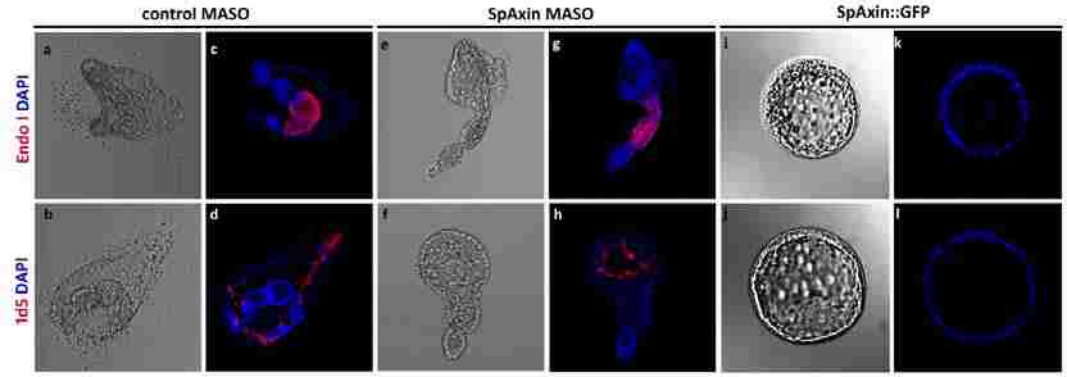

Figure 4.9 Endoderm and mesoderm formation is affected by Axin expression. a-d, Control MASO injected embryos showing the regular endomesoderm specification pattern in the pluteus. **e-f,** In Axin knockdown larvae, vegetalized phenotypes examined by endodermal (Endo I) and mesodermal (1d5) markers show endoderm specification at the enlarged exogastrulated gut, and reduced skeletogenic mesenchyme (mesoderm) inside of the ectoderm. **i-l,** In contrast, in Axin overexpressed embryos, animalized phenotype examined by both markers shows that endomesoderm specification is lost. Endo I (red): midgut and hindgut. 1d5 (red): skeletogenic mesenchyme cells. DAPI (blue).

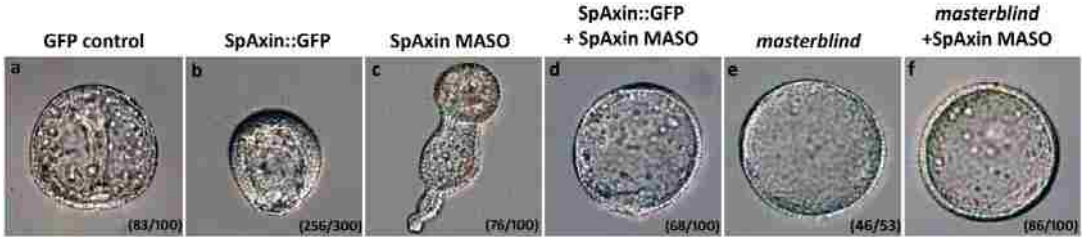

Figure 4.10 SpAxin MASO injected phenotype can be partially rescued by overexpressing Axin mRNA. To determine if the vegetalized phenotype produced by the Axin knockdown is Axin specific, Axin mRNA was co-injected with the SpAxin MASO to perform a rescue experiment. **a,** GFP mRNA is used as an injection control (83/100=83% developed normally). **b and e,** SpAxin::GFP, and *masterblind* (Axin L396Q, zebrafish axin mutant construct) both gave animalized phenotype (256/300=85% and 46/53=86% respectively). **c,** SpAxin MASO gave a vegetalized phenotype (76/100=76%). **d and f,** Both SpAxin::GFP and *masterblind* co-injected with SpAxin MASO produced animalized phenotypes (68/100=68% and 86/100=86% respectively).

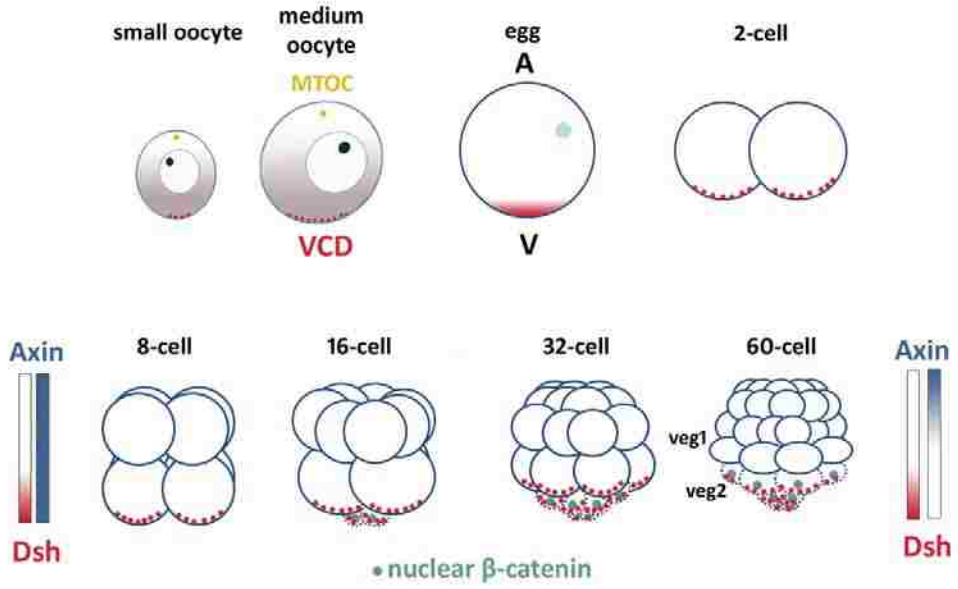

Figure 4.11 Proposed model for patterning the early sea urchin embryo by Dsh and Axin. Dsh (Red) and Axin (Magenta) each play crucial roles in patterning the early embryo along the AV axis by regulating β-catenin. First, a vegetal cortical domain (VCD) is established during early oogenesis along with the appearance of the microtubule organizing center (MTOC, green), setting up an early polarity in the developing oocytes. This VCD then recruits activated forms of Dsh and other maternal factors to the egg vegetal cortex during oogenesis. Secondly, during the first few cleavage stages, the VCD recruits maternal factors including Dsh. Third, the VCD is then inherited by the most vegetal blastomeres, the micromeres and macromeres, at the 16-cell stage for the localized activation of the EGRN. Finally, following the Wnt/β-catenin activation by Dsh (nuclear β-catenin, ocean blue), Axin at those blastomeres are targeted for degradation. The veg_1 tier progeny that did not inherit the VCD, became specified as ectoderm.

SUPPLEMENTARY FIGURES

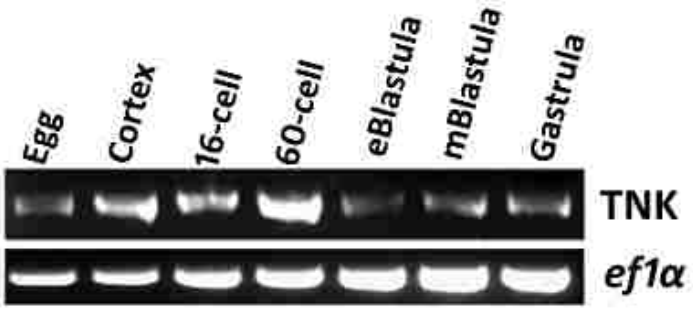

Supplementary figure 4.1 Tankyrase (TNK) mRNA is expressed throughout sea urchin embryogenesis. TNK targets Axin for degradation. Before testing the XAV939, a TNK inhibitor, to stabilize Axin in the sea urchin embryos, RT-PCR was performed to see if Tankyrase is expressed at early development stages in sea urchins. (Experiment performed by Sarah Williams and LingYu Wang).

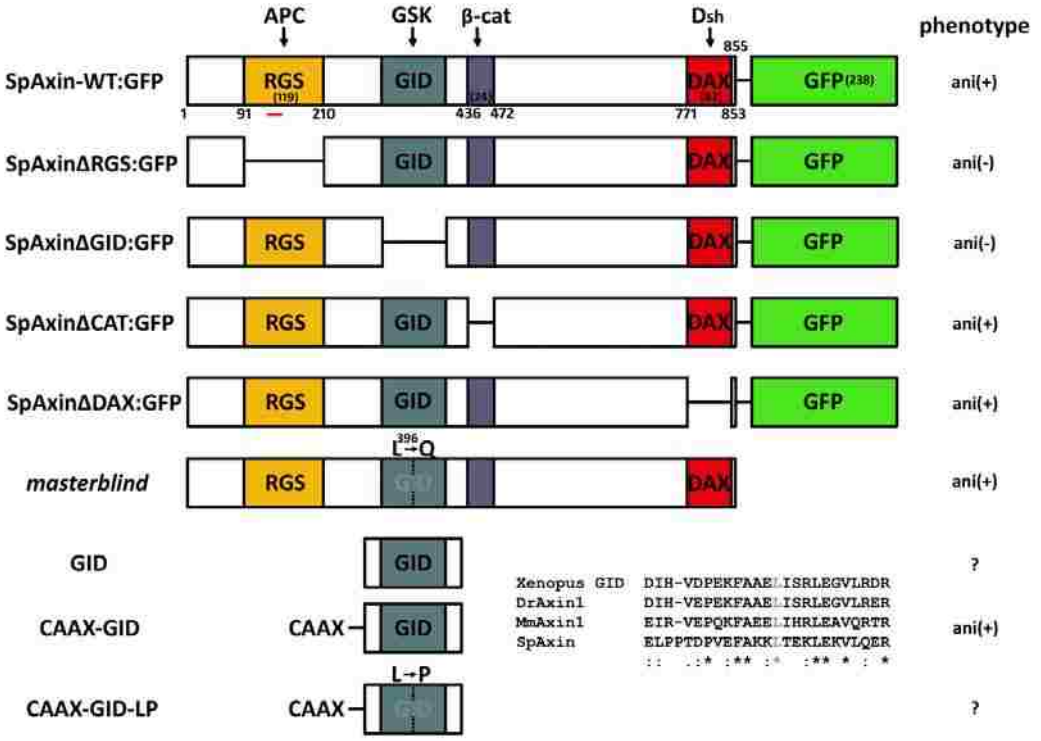

Supplementary figure 4.2 Function of Axin domains. Schematic representations of injected Axin constructs. On top showing Axin associated proteins binding to their known structural domains RGS (Regulators of G protein signaling), GID (GSK-3β interacting domain), β-catenin domain and DAX (similar to DIX in Dsh protein, but to differentiate DIX domain from the Dsh, DIX domain in Axin is named DAX). All constructs were injected at 0.25 µg/µl. All injected constructs, including SpAxin::GFP(WT), SpAxinΔRGS::GFP, SpAxinΔGID::GFP, SpAxinΔCAT::GFP, SpAxinΔDAX::GFP, *masterblind* mutant (Axin L396Q mutant from zebrafish), CAAX-GID, produced animalized phenotypes, either strong (+) or weak (-). Strong animalized phenotype are classic ciliated epithelial balls (*Dauerblastulae*); Weak animalized phenotype are the embryos that eventually develop a gut, but compared to GFP injected controls, the gastrulation process is significantly delayed (24 hr late). Question mark (?) denotes result of injection is inconclusive or not done. Residue numbers underneath domains denote the domain boundaries. Parentheses in the domains indicate size in amino acids. Red bar indicates the region anti-SpAxin antibody is made. Bottom right alignment: protein sequence alignment of GID domain from frog (*Xenopus*), zebrafish (Dr), mouse (Mm) and purple sea urchin (Sp). Highlighted L indicates the amino acid crucial for GSK-3β binding.

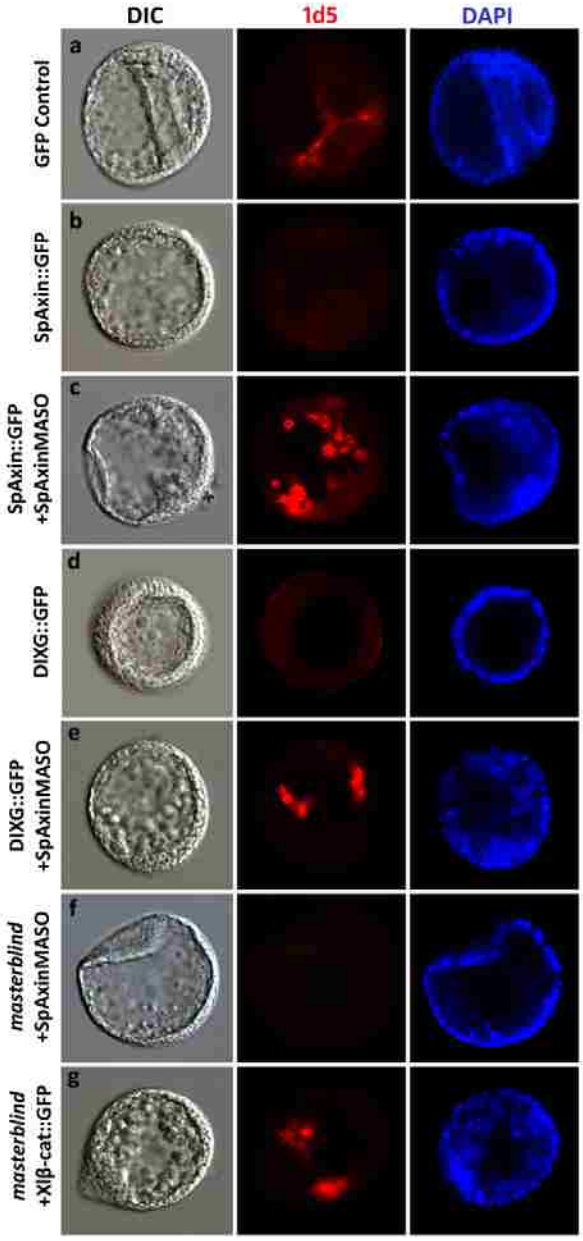

Supplementary figure 4.3 Co-injecting Wnt/β-catenin pathway positive and negative components partially rescues animalized phenotypes caused by blocking the Wnt pathway. To test if the animalized phenotypes caused by overexpression of SpAxin::GFP, masterblind and DIX::GFP is due to the disruption of the Wnt/β-catenin pathway, SpAxin MASO and a constitutively activated β-catenin construct from *Xenopus* (Xlβ-cat::GFP) were co-injected with the above constructs, and analyzed by a mesodermal marker (1d5: skeletogenic mesenchyme cells, red).
a, Control: GFP mRNA. **b and d,** overexpression of SpAxin::GFP and DIXG::GFP blocked endomesoderm specification. Knockdown of Axin by Axin MASO partially rescued mesoderm specification as demonstrated by mesenchymal cells expressing skeletogenic marker (**c and e**). Overexpressing zebrafish axin mutant (*masterblind*) also blocked endomesoderm specification in sea urchin embryos. Knocking-down Axin (**f**), or expressing a constitutively activated β-catenin (Xlβ-cat:GFP, **g**) in those embryos induced cell migration. No skeletogenic markers are detected in **f**. A portion of mesenchymal cells express skeletogenic markers in **g**.

REFERENCES

Alarcon, V. B. and Elinson, R. P. (2001) 'RNA anchoring in the vegetal cortex of the Xenopus oocyte', *J Cell Sci* 114(Pt 9): 1731-41.

Angerer, L. M. and Angerer, R. C. (2000) 'Animal-vegetal axis patterning mechanisms in the early sea urchin embryo', *Dev Biol* 218(1): 1-12.

Asano, Y. and Mabuchi, I. (2001) 'Calyculin-A, an inhibitor for protein phosphatases, induces cortical contraction in unfertilized sea urchin eggs', *Cell Motil Cytoskeleton* 48(4): 245-61.

Bince, J. M., Peng, C. F. and Wikramanayake, A. H. (2008) 'Detecting expression patterns of Wnt pathway components in sea urchin embryos', *Methods Mol Biol* 469: 201-11.

Bince, J. M. and Wikramanayake, A. H. (2008) 'Functional analysis of Wnt signaling in the early sea urchin embryo using mRNA microinjection', *Methods Mol Biol* 469: 213-22.

Bonder, E. M. and Fishkind, D. J. (1995) 'Actin-membrane cytoskeletal dynamics in early sea urchin development', *Curr Top Dev Biol* 31: 101-37.

Boveri, T. (1901a) 'Die Polarität von Oocyte, Ei und Larve des Stronglocentrotus lividus', *Zool. Jb. Abt. Anat. Ont.* 14: 630-635.

Boveri, T. (1901b) 'Über die Polarität des Seeigeleies', *Verh. Phys. Med. Ges. Wurzburg* 34: 145-167.

Boyle, J. A. and Ernst, S. G. (1989) 'Sea urchin oocytes possess elaborate cortical arrays of microfilaments, microtubules, and intermediate filaments', *Dev Biol* 134(1): 72-84.

Cameron, R. A. and Davidson, E. H. (1997) 'LiCl perturbs ectodermal veg1 lineage allocations in Strongylocentrotus purpuratus embryos', *Dev Biol* 187(2): 236-9.

Choi, S. C. and Han, J. K. (2005) 'Rap2 is required for Wnt/beta-catenin signaling pathway in Xenopus early development', *EMBO J* 24(5): 985-96.

Clevers, H. (2006) 'Wnt/beta-catenin signaling in development and disease', *Cell* 127(3): 469-80.

Croce, J., Range, R., Wu, S.-Y., Miranda, E., Lhomond, G., Peng, J. C.-f., Lepage, T. and McClay, D. R. (2011) 'Wnt6 activates endoderm in the sea urchin gene regulatory network', *Development* 138(15): 3297-3306.

Croce, J. C. and McClay, D. R. (2006) 'The canonical Wnt pathway in embryonic axis polarity', *Semin Cell Dev Biol* 17(2): 168-74.

Croce, J. C., Wu, S. Y., Byrum, C., Xu, R., Duloquin, L., Wikramanayake, A. H., Gache, C. and McClay, D. R. (2006) 'A genome-wide survey of the evolutionarily conserved Wnt pathways in the sea urchin Strongylocentrotus purpuratus', *Dev Biol* 300(1): 121-31.

Darras, S., Gerhart, J., Terasaki, M., Kirschner, M. and Lowe, C. J. (2011) 'beta-catenin specifies the endomesoderm and defines the posterior organizer of the hemichordate Saccoglossus kowalevskii', *Development* 138(5): 959-70.

Davidson, E. H., Rast, J. P., Oliveri, P., Ransick, A., Calestani, C., Yuh, C. H., Minokawa, T., Amore, G., Hinman, V., Arenas-Mena, C. et al. (2002) 'A genomic regulatory network for development', *Science* 295(5560): 1669-78.

Di Carlo, M., Romancino, D., Ortolani, G., Montana, G., Giudice, G. and Giudice, G. (1996) 'Molecular mechanism for establishment of the animal-vegetal axis in sea urchin development', *Rendiconti Lincei* 7(1): 45-50.

Egana, A. L., Boyle, J. A. and Ernst, S. G. (2007) 'Strongylocentrotus drobachiensis oocytes maintain a microtubule organizing center throughout oogenesis: implications for the establishment of egg polarity in sea urchins', *Mol Reprod Dev* 74(1): 76-87.

Emily-Fenouil, F., Ghiglione, C., Lhomond, G., Lepage, T. and Gache, C. (1998) 'GSK3beta/shaggy mediates patterning along the animal-vegetal axis of the sea urchin embryo', *Development* 125(13): 2489-98.

Ettensohn, C. A. (2006) 'The emergence of pattern in embryogenesis: regulation of beta-catenin localization during early sea urchin development', *Sci STKE* 2006(361): pe48.

Evans, R. M. and Simpkins, H. (1998) 'Cisplatin induced intermediate filament reorganization and altered mitochondrial function in 3T3 cells and drug-sensitive and -resistant Walker 256 cells', *Exp Cell Res* 245(1): 69-78.

Fahmy, O. G. and Fahmy, M. J. (1959) 'Differential gene response to mutagens in *Drosophila melanogaster*', *Genetics* 44(6): 1149-71.

Fiedler, M., Mendoza-Topaz, C., Rutherford, T. J., Mieszczanek, J. and Bienz, M. (2011) 'Dishevelled interacts with the DIX domain polymerization interface of Axin to interfere with its function in down-regulating beta-catenin', *Proc Natl Acad Sci U S A* 108(5): 1937-42.

Foissner, I. and Wasteneys, G. O. (2007) 'Wide-ranging effects of eight cytochalasins and latrunculin A and B on intracellular motility and actin filament reorganization in characean internodal cells', *Plant Cell Physiol* 48(4): 585-97.

Forer, A. and Fabian, L. (2005) 'Does 2,3-butanedione monoxime inhibit nonmuscle myosin?', *Protoplasma* 225(1-2): 1-4.

Frick, J. E. and Ruppert, E. E. (1996) 'Primordial germ cells of *Synaptula hydriformis* (Holothuroidea; Echinodermata) are epithelial flagellated-collar cells: Their apical-basal polarity becomes primary egg polarity', *Biol Bull* 191(2): 168-177.

Frick, J. E. and Ruppert, E. E. (1997) 'Primordial germ cells and oocytes of Branchiostoma virginiae (Cephalochordata, Acrania) are flagellated epithelial cells: relationship between epithelial and primary egg polarity', *Zygote* 5(2): 139-51.

Fritzenwanker, J. H., Genikhovich, G., Kraus, Y. and Technau, U. (2007) 'Early development and axis specification in the sea anemone Nematostella vectensis', *Dev Biol* 310(2): 264-79.

Fuller, M. T. (1993) *In* the development of *Drosophila melanogaster*. in M. B. a. A. Martinez-Arias (ed.) *Spermatogenesis*. New York: Cold Spring Harbor Laboratory.

Gao, C. and Chen, Y. G. (2009) 'Dishevelled: The hub of Wnt signaling', *Cell Signal*.

Gluecksohn-Schoenheimer, S. and Dunn, L. C. (1948) 'A new type of hereditary harelip in the house mouse', *Anat Rec* 102(3): 279-87.

Hamada, F., Tomoyasu, Y., Takatsu, Y., Nakamura, M., Nagai, S., Suzuki, A., Fujita, F., Shibuya, H., Toyoshima, K., Ueno, N. et al. (1999) 'Negative regulation of Wingless signaling by D-axin, a Drosophila homolog of axin', *Science* 283(5408): 1739-42.

He, X., Saint-Jeannet, J. P., Woodgett, J. R., Varmus, H. E. and Dawid, I. B. (1995) 'Glycogen synthase kinase-3 and dorsoventral patterning in Xenopus embryos', *Nature* 374(6523): 617-22.

Heasman, J. (2006) 'Maternal determinants of embryonic cell fate', *Semin Cell Dev Biol* 17(1): 93-8.

Hedgepeth, C. M., Deardorff, M. A. and Klein, P. S. (1999a) 'Xenopus axin interacts with glycogen synthase kinase-3 beta and is expressed in the anterior midbrain', *Mech Dev* 80(2): 147-51.

Hedgepeth, C. M., Deardorff, M. A., Rankin, K. and Klein, P. S. (1999b) 'Regulation of glycogen synthase kinase 3beta and downstream Wnt signaling by axin', *Mol Cell Biol* 19(10): 7147-57.

Heisenberg, C. P., Houart, C., Take-Uchi, M., Rauch, G. J., Young, N., Coutinho, P., Masai, I., Caneparo, L., Concha, M. L., Geisler, R. et al. (2001) 'A mutation in the Gsk3-binding domain of zebrafish Masterblind/Axin1 leads to a fate transformation of telencephalon and eyes to diencephalon', *Genes Dev* 15(11): 1427-34.

Henry, J. Q., Perry, K. J., Wever, J., Seaver, E. and Martindale, M. Q. (2008) 'Beta-catenin is required for the establishment of vegetal embryonic fates in the nemertean, Cerebratulus lacteus', *Dev Biol* 317(1): 368-79.

Herbst, C. (1892) 'Experimentelle untersuchungen über einfluss der veranderten chemischen zusammensetzung des umgebenden mediums auf die entwicklung der tiere I teil. Versuche an Seeigeleiern.', *Z. Wiss. Zool.* 55: 446-518.

Hirota, Y., Meunier, A., Huang, S., Shimozawa, T., Yamada, O., Kida, Y. S., Inoue, M., Ito, T., Kato, H., Sakaguchi, M. et al. (2010) 'Planar polarity of multiciliated ependymal cells involves the anterior migration of basal bodies regulated by non-muscle myosin II', *Development* 137(18): 3037-46.

Horstadius, S. (1939) 'The mechanism of sea urchin development as studied by operative methods.', *Biol. Rev.* 14: 132-179.

Horstadius, S. (1973) Experimental Embryology of Echinoderms.: Clarendon Press, Oxford.

Horstadius, S., Lorch, I. J. and Danielli, J. F. (1950) 'Differentiation of the sea urchin egg following reduction of the interior cytoplasm in relation to the cortex', *Experimental Cell Research* 1(2): 188-193.

Houliston, E., Carre, D., Johnston, J. A. and Sardet, C. (1993) 'Axis establishment and microtubule-mediated waves prior to first cleavage in Beroe ovata', *Development* 117(1): 75-87.

Houston, D. W. and King, M. L. (2000) 'Germ plasm and molecular determinants of germ cell fate', *Curr Top Dev Biol* 50: 155-81.

Howard-Ashby, M., Materna, S. C., Brown, C. T., Tu, Q., Oliveri, P., Cameron, R. A. and Davidson, E. H. (2006) 'High regulatory gene use in sea urchin embryogenesis: Implications for bilaterian development and evolution', *Dev Biol* 300(1): 27-34.

Huang, S. M., Mishina, Y. M., Liu, S., Cheung, A., Stegmeier, F., Michaud, G. A., Charlat, O., Wiellette, E., Zhang, Y., Wiessner, S. et al. (2009) 'Tankyrase inhibition stabilizes axin and antagonizes Wnt signalling', *Nature* 461(7264): 614-20.

Imai, K., Takada, N., Satoh, N. and Satou, Y. (2000) '(beta)-catenin mediates the specification of endoderm cells in ascidian embryos', *Development* 127(14): 3009-20.

Itoh, K., Antipova, A., Ratcliffe, M. J. and Sokol, S. (2000) 'Interaction of dishevelled and Xenopus axin-related protein is required for wnt signal transduction', *Mol Cell Biol* 20(6): 2228-38.

Itoh, K., Brott, B. K., Bae, G. U., Ratcliffe, M. J. and Sokol, S. Y. (2005) 'Nuclear localization is required for Dishevelled function in Wnt/beta-catenin signaling', *J Biol* 4(1): 3.

Itoh, K., Krupnik, V. E. and Sokol, S. Y. (1998) 'Axis determination in Xenopus involves biochemical interactions of axin, glycogen synthase kinase 3 and beta-catenin', *Curr Biol* 8(10): 591-4.

Jacobs-Cohen, R. J., Spiegelman, M., Cookingham, J. C. and Bennett, D. (1984) 'Knobbly, a new dominant mutation in the mouse that affects embryonic ectoderm organization', *Genet Res* 43(1): 43-50.

Jho, E. H., Zhang, T., Domon, C., Joo, C. K., Freund, J. N. and Costantini, F. (2002) 'Wnt/beta-catenin/Tcf signaling induces the transcription of Axin2, a negative regulator of the signaling pathway', *Mol Cell Biol* 22(4): 1172-83.

Kawahara, K., Morishita, T., Nakamura, T., Hamada, F., Toyoshima, K. and Akiyama, T. (2000) 'Down-regulation of beta-catenin by the colorectal tumor suppressor APC requires association with Axin and beta-catenin', *J Biol Chem* 275(12): 8369-74.

King, M. L., Messitt, T. J. and Mowry, K. L. (2005) 'Putting RNAs in the right place at the right time: RNA localization in the frog oocyte', *Biol Cell* 97(1): 19-33.

Kloc, M., Bilinski, S., Chan, A. P., Allen, L. H., Zearfoss, N. R. and Etkin, L. D. (2001) 'RNA localization and germ cell determination in Xenopus', *Int Rev Cytol* 203: 63-91.

Kofron, M., Klein, P., Zhang, F., Houston, D. W., Schaible, K., Wylie, C. and Heasman, J. (2001) 'The role of maternal axin in patterning the Xenopus embryo', *Dev Biol* 237(1): 183-201.

Komiya, Y. and Habas, R. (2008) 'Wnt signal transduction pathways', *Organogenesis* 4(2): 68-75.

Korswagen, H. C., Coudreuse, D. Y., Betist, M. C., van de Water, S., Zivkovic, D. and Clevers, H. C. (2002) 'The Axin-like protein PRY-1 is a negative regulator of a canonical Wnt pathway in C. elegans', *Genes Dev* 16(10): 1291-302.

Kumburegama, S., Wijesena, N., Xu, R. and Wikramanayake, A. H. (2011) 'Strabismus-mediated primary archenteron invagination is uncoupled from Wnt/beta-catenin-dependent endoderm cell fate specification in Nematostella vectensis (Anthozoa, Cnidaria): Implications for the evolution of gastrulation', *Evodevo* 2(1): 2.

Kumburegama, S. and Wikramanayake, A. H. (2007) 'Specification and patterning of the animal-vegetal axis in sea urchins by the canonical Wnt signaling pathway', *Signal Transduction* 7(2): 164-173.

Laemmli, U. K. (1970) 'Cleavage of Structural Proteins during the Assembly of the Head of Bacteriophage T4', *Nature* 227(5259): 680-685.

Larabell, C. A., Torres, M., Rowning, B. A., Yost, C., Miller, J. R., Wu, M., Kimelman, D. and Moon, R. T. (1997) 'Establishment of the dorso-ventral axis in Xenopus embryos is presaged by early asymmetries in beta-catenin that are modulated by the Wnt signaling pathway', *J Cell Biol* 136(5): 1123-36.

Lee, E., Salic, A., Kruger, R., Heinrich, R. and Kirschner, M. W. (2003) 'The roles of APC and Axin derived from experimental and theoretical analysis of the Wnt pathway', *PLoS Biol* 1(1): E10.

Lee, P. N., Kumburegama, S., Marlow, H. Q., Martindale, M. Q. and Wikramanayake, A. H. (2007) 'Asymmetric developmental potential along the animal-vegetal axis in the anthozoan cnidarian, Nematostella vectensis, is mediated by Dishevelled', *Dev Biol* 310(1): 169-86.

Leonard, J. D. and Ettensohn, C. A. (2007) 'Analysis of dishevelled localization and function in the early sea urchin embryo', *Dev Biol* 306(1): 50-65.

Lhomond, G., McClay, D. R., Gache, C. and Croce, J. C. (2012) 'Frizzled1/2/7 signaling directs beta-catenin nuclearisation and initiates endoderm specification in macromeres during sea urchin embryogenesis', *Development* 139(4): 816-25.

Lillie, F. R. (1909a) 'Karyokinetic figures of centrefuged egg; an experimental teat of the center of force hypothesis', *Biol. Bull.,* 17.

Lillie, F. R. (1909b) 'Polarity and bilaterality of the annelid egg. Experiments with centrifugal force.', *Biol. Bull.,* 16: 54.

Lindsley, D., and K. T. Tokuyasu (1980) *In* Genetics and biology of *Drosophila*. in M. a. W. Ashburner, T. R. F., eds. (ed.) *Spermatogenesis*, vol. 2. New York: Academic Press.

Logan, C. Y., Miller, J. R., Ferkowicz, M. J. and McClay, D. R. (1999) 'Nuclear beta-catenin is required to specify vegetal cell fates in the sea urchin embryo', *Development* 126(2): 345-57.

Luo, W. and Lin, S. C. (2004) 'Axin: a master scaffold for multiple signaling pathways', *Neurosignals* 13(3): 99-113.

Lustig, B., Jerchow, B., Sachs, M., Weiler, S., Pietsch, T., Karsten, U., van de Wetering, M., Clevers, H., Schlag, P. M., Birchmeier, W. et al. (2002) 'Negative feedback loop of Wnt signaling through upregulation of conductin/axin2 in colorectal and liver tumors', *Mol Cell Biol* 22(4): 1184-93.

Martindale, M. Q. and Hejnol, A. (2009) 'A developmental perspective: changes in the position of the blastopore during bilaterian evolution', *Dev Cell* 17(2): 162-74.

Maruyama, Y. K., Yamamoto, K., Mita-Miyazawa, I., Kominami, T. and Nemoto, S. (1986) 'Manipulative methods for analyzing embryogenesis', *Methods Cell Biol* 27: 325-44.

McClay, C. G., Wessel, G. M., Fink, R. D. and Marchase, R. B. (1983) *Patterns of antigenic expression in early sea urchin development*, Liss, N.Y.

McClay, D. R., Peterson, R. E., Range, R. C., Winter-Vann, A. M. and Ferkowicz, M. J. (2000) 'A micromere induction signal is activated by beta-catenin and acts through notch to initiate specification of secondary mesenchyme cells in the sea urchin embryo', *Development* 127(23): 5113-22.

Mitchell, B., Stubbs, J. L., Huisman, F., Taborek, P., Yu, C. and Kintner, C. (2009) 'The PCP pathway instructs the planar orientation of ciliated cells in the Xenopus larval skin', *Curr Biol* 19(11): 924-9.

Miyawaki, K., Yamamoto, M., Saito, K., Saito, S., Kobayashi, N. and Matsuda, S. (2003) 'Nuclear localization of beta-catenin in vegetal pole cells during early embryogenesis of the starfish Asterina pectinifera', *Dev Growth Differ* 45(2): 121-8.

Momose, T., Derelle, R. and Houliston, E. (2008) 'A maternally localised Wnt ligand required for axial patterning in the cnidarian Clytia hemisphaerica', *Development* 135(12): 2105-13.

Momose, T. and Houliston, E. (2007) 'Two oppositely localised frizzled RNAs as axis determinants in a cnidarian embryo', *PLoS Biol* 5(4): e70.

Momose, T. and Schmid, V. (2006) 'Animal pole determinants define oral-aboral axis polarity and endodermal cell-fate in hydrozoan jellyfish Podocoryne carnea', *Dev Biol* 292(2): 371-80.

Nishida, H. and Sawada, K. (2001) 'macho-1 encodes a localized mRNA in ascidian eggs that specifies muscle fate during embryogenesis', *Nature* 409(6821): 724-9.

Nocente-McGrath, C., McIsaac, R. and Ernst, S. G. (1991) 'Altered cell fate in LiCl-treated sea urchin embryos', *Dev Biol* 147(2): 445-50.

Park, T. J., Gray, R. S., Sato, A., Habas, R. and Wallingford, J. B. (2005) 'Subcellular localization and signaling properties of dishevelled in developing vertebrate embryos', *Curr Biol* 15(11): 1039-44.

Park, T. J., Mitchell, B. J., Abitua, P. B., Kintner, C. and Wallingford, J. B. (2008) 'Dishevelled controls apical docking and planar polarization of basal bodies in ciliated epithelial cells', *Nat Genet* 40(7): 871-9.

Perrimon, N. and Mahowald, A. P. (1987) 'Multiple functions of segment polarity genes in Drosophila', *Dev Biol* 119(2): 587-600.

Petersen, C. P. and Reddien, P. W. (2009) 'Wnt signaling and the polarity of the primary body axis', *Cell* 139(6): 1056-68.

Phiel, C. J. and Klein, P. S. (2001) 'Molecular targets of lithium action', *Annu Rev Pharmacol Toxicol* 41: 789-813.

Prodon, F., Dru, P., Roegiers, F. and Sardet, C. (2005) 'Polarity of the ascidian egg cortex and relocalization of cER and mRNAs in the early embryo', *J Cell Sci* 118(Pt 11): 2393-404.

Ransick, A. and Davidson, E. H. (1998) 'Late specification of Veg1 lineages to endodermal fate in the sea urchin embryo', *Dev Biol* 195(1): 38-48.

Rau, K. G. and Kalthoff, K. (1980) 'Complete reversal of antero-posterior polarity in a centrifuged insect embryo', *Nature* 287(5783): 635-7.

Roeser, T., Stein, S. and Kessel, M. (1999) 'Nuclear beta-catenin and the development of bilateral symmetry in normal and LiCl-exposed chick embryos', *Development* 126(13): 2955-65.

Rothbacher, U., Laurent, M. N., Deardorff, M. A., Klein, P. S., Cho, K. W. and Fraser, S. E. (2000) 'Dishevelled phosphorylation, subcellular localization and multimerization regulate its role in early embryogenesis', *EMBO J* 19(5): 1010-22.

Rui, Y., Xu, Z., Xiong, B., Cao, Y., Lin, S., Zhang, M., Chan, S. C., Luo, W., Han, Y., Lu, Z. et al. (2007) 'A beta-catenin-independent dorsalization pathway activated by Axin/JNK signaling and antagonized by aida', *Dev Cell* 13(2): 268-82.

Sardet, C., Dru, P. and Prodon, F. (2005) 'Maternal determinants and mRNAs in the cortex of ascidian oocytes, zygotes and embryos', *Biol Cell* 97(1): 35-49.

Sardet, C., Prodon, F., Pruliere, G. and Chenevert, J. (2004) '[Polarization of eggs and embryos: some common principles]', *Med Sci (Paris)* 20(4): 414-23.

Scharf, S. R. and Gerhart, J. C. (1983) 'Axis determination in eggs of *Xenopus laevis*: a critical period before first cleavage, identified by the common effects of cold, pressure and ultraviolet irradiation', *Dev Biol* 99(1): 75-87.

Schneider, S., Steinbeisser, H., Warga, R. M. and Hausen, P. (1996) 'Beta-catenin translocation into nuclei demarcates the dorsalizing centers in frog and fish embryos', *Mech Dev* 57(2): 191-8.

Schroeder, T. E. (1980a) 'Expressions of the prefertilization polar axis in sea urchin eggs', *Dev Biol* 79(2): 428-43.

Schroeder, T. E. (1980b) 'The jelly canal marker of polarity for sea urchin oocytes, eggs, and embryos', *Exp Cell Res* 128(2): 490-4.

Schroeder, T. E. (1985) 'Cortical Expressions of Polarity in the Starfish Oocyte*', *Development Growth & Differentiation* 27(3): 311-321.

Schroeder, T. E. and Battaglia, D. E. (1985) '"Spiral asters" and cytoplasmic rotation in sea urchin eggs: induction in Strongylocentrotus purpuratus eggs by elevated temperature', *J Cell Biol* 100(4): 1056-62.

Schroeder, T. E. and Otto, J. J. (1991) 'Snoods: a periodic network containing cytokeratin in the cortex of starfish oocytes', *Dev Biol* 144(2): 240-7.

Schroeder, T. E. and Stricker, S. A. (1983) 'Morphological changes during maturation of starfish oocytes: surface ultrastructure and cortical actin', *Dev Biol* 98(2): 373-84.

Schwarz-Romond, T., Metcalfe, C. and Bienz, M. (2007) 'Dynamic recruitment of axin by Dishevelled protein assemblies', *J Cell Sci* 120(Pt 14): 2402-12.

Semenov, M. V. and Snyder, M. (1997) 'Human dishevelled genes constitute a DHR-containing multigene family', *Genomics* 42(2): 302-10.

Simons, M., Gloy, J., Ganner, A., Bullerkotte, A., Bashkurov, M., Kronig, C., Schermer, B., Benzing, T., Cabello, O. A., Jenny, A. et al. (2005) 'Inversin, the gene product mutated in nephronophthisis type II, functions as a molecular switch between Wnt signaling pathways', *Nat Genet* 37(5): 537-43.

Smiley, S. (1988) 'The dynamics of oogenesis and the annual ovarian cycle of *Stichopus californicus* (Echinodermata; Holothuroidea).', *Biol Bull* 175: 79-93.

Smiley, S. (1990) 'A review of echinoderm oogenesis', *J Electron Microsc Tech* 16(2): 93-114.

Smiley, S. and Cloney, R. A. (1985) 'Ovulation and the fine structure of the *Stichopus californicus* (Echinodermata; Holothuroidea) fecund ovarian tubules.', *Biol. Bull.* 169: 342-364.

Sodergren, E. Weinstock, G. M. Davidson, E. H. Cameron, R. A. Gibbs, R. A. Angerer, R. C. Angerer, L. M. Arnone, M. I. Burgess, D. R. Burke, R. D. et al. (2006) 'The genome of the sea urchin Strongylocentrotus purpuratus', *Science* 314(5801): 941-52.

Stack, C., Lucero, A. J. and Shuster, C. B. (2006) 'Calcium-responsive contractility during fertilization in sea urchin eggs', *Dev Dyn* 235(4): 1042-52.

Stamateris, R. E., Rafiq, K. and Ettensohn, C. A. (2009) 'The Expression and Distribution of Wnt and Wnt Receptor mRNAs During Early Sea Urchin Development', *Gene Expr Patterns*.

Tao, Q., Yokota, C., Puck, H., Kofron, M., Birsoy, B., Yan, D., Asashima, M., Wylie, C. C., Lin, X. and Heasman, J. (2005) 'Maternal wnt11 activates the canonical wnt signaling pathway required for axis formation in Xenopus embryos', *Cell* 120(6): 857-71.

Torres, M. A. and Nelson, W. J. (2000) 'Colocalization and redistribution of dishevelled and actin during Wnt-induced mesenchymal morphogenesis', *J Cell Biol* 149(7): 1433-42.

Vacquier, V. D. (1975) 'The isolation of intact cortical granules from sea urchin eggs: calcium lons trigger granule discharge', *Dev Biol* 43(1): 62-74.

van Eeden, F. and St Johnston, D. (1999) 'The polarisation of the anterior-posterior and dorsal-ventral axes during Drosophila oogenesis', *Curr Opin Genet Dev* 9(4): 396-404.

Wallingford, J. B. and Habas, R. (2005) 'The developmental biology of Dishevelled: an enigmatic protein governing cell fate and cell polarity', *Development* 132(20): 4421-36.

Weitzel, H. E., Illies, M. R., Byrum, C. A., Xu, R., Wikramanayake, A. H. and Ettensohn, C. A. (2004) 'Differential stability of beta-catenin along the animal-vegetal axis of the sea urchin embryo mediated by dishevelled', *Development* 131(12): 2947-56.

Wessel, G. M., Conner, S. D. and Berg, L. (2002) 'Cortical granule translocation is microfilament mediated and linked to meiotic maturation in the sea urchin oocyte', *Development* 129(18): 4315-25.

Wessel, G. M. and McClay, D. R. (1985) 'Sequential expression of germ-layer specific molecules in the sea urchin embryo', *Dev Biol* 111(2): 451-63.

Wikramanayake, A. H., Hong, M., Lee, P. N., Pang, K., Byrum, C. A., Bince, J. M., Xu, R. and Martindale, M. Q. (2003) 'An ancient role for nuclear beta-catenin in the evolution of axial polarity and germ layer segregation', *Nature* 426(6965): 446-50.

Wikramanayake, A. H., Huang, L. and Klein, W. H. (1998) 'beta-Catenin is essential for patterning the maternally specified animal-vegetal axis in the sea urchin embryo', *Proc Natl Acad Sci U S A* 95(16): 9343-8.

Wikramanayake, A. H., Peterson, R., Chen, J., Huang, L., Bince, J. M., McClay, D. R. and Klein, W. H. (2004) 'Nuclear beta-catenin-dependent Wnt8 signaling in vegetal cells of the early sea urchin embryo regulates gastrulation and differentiation of endoderm and mesodermal cell lineages', *Genesis* 39(3): 194-205.

Wilt, F. H. and Benson, S. C. (2004) Methods in Cell Biology. in A. C. Ettensohn A. Wray, G., and M. Wessel, G. (eds.) *Development of Sea Urchins, Ascidians, and other Invertebrate Deuterostomes: Experimental Approaches*, vol. 74: Elsevier Academic Press.

Wu, Y., Jing, X., Ma, X., Ding, X., Fan, W. and Fan, M. (2009) 'DIXDC1 co-localizes and interacts with gamma-tubulin in HEK293 cells', *Cell Biol Int* 33(6): 697-701.

Yaguchi, S., Yaguchi, J., Angerer, R. C. and Angerer, L. M. (2008) 'A Wnt-FoxQ2-nodal pathway links primary and secondary axis specification in sea urchin embryos', *Dev Cell* 14(1): 97-107.

Yamamoto, H., Kishida, S., Kishida, M., Ikeda, S., Takada, S. and Kikuchi, A. (1999) 'Phosphorylation of axin, a Wnt signal negative regulator, by glycogen synthase kinase-3beta regulates its stability', *J Biol Chem* 274(16): 10681-4.

Yamamoto, H., Kishida, S., Uochi, T., Ikeda, S., Koyama, S., Asashima, M. and Kikuchi, A. (1998) 'Axil, a member of the Axin family, interacts with both glycogen synthase kinase 3beta and beta-catenin and inhibits axis formation of Xenopus embryos', *Mol Cell Biol* 18(5): 2867-75.

Yan, D., Wiesmann, M., Rohan, M., Chan, V., Jefferson, A. B., Guo, L., Sakamoto, D., Caothien, R. H., Fuller, J. H., Reinhard, C. et al. (2001) 'Elevated expression of axin2 and hnkd mRNA provides evidence that Wnt/beta -catenin signaling is activated in human colon tumors', *Proc Natl Acad Sci U S A* 98(26): 14973-8.

Yanagawa, S., van Leeuwen, F., Wodarz, A., Klingensmith, J. and Nusse, R. (1995) 'The dishevelled protein is modified by wingless signaling in Drosophila', *Genes Dev* 9(9): 1087-97.

Yost, C., Torres, M., Miller, J. R., Huang, E., Kimelman, D. and Moon, R. T. (1996) 'The axis-inducing activity, stability, and subcellular distribution of beta-catenin is regulated in Xenopus embryos by glycogen synthase kinase 3', *Genes Dev* 10(12): 1443-54.

Zeng, L., Fagotto, F., Zhang, T., Hsu, W., Vasicek, T. J., Perry, W. L., 3rd, Lee, J. J., Tilghman, S. M., Gumbiner, B. M. and Costantini, F. (1997) 'The mouse Fused locus encodes Axin, an inhibitor of the Wnt signaling pathway that regulates embryonic axis formation', *Cell* 90(1): 181-92.

Zeng, X., Huang, H., Tamai, K., Zhang, X., Harada, Y., Yokota, C., Almeida, K., Wang, J., Doble, B., Woodgett, J. et al. (2008) 'Initiation of Wnt signaling: control of Wnt coreceptor Lrp6 phosphorylation/activation via frizzled, dishevelled and axin functions', *Development* 135(2): 367-75.